<div align="center">

COMMITTEE No I.1

ENVIRONMENT

</div>

COMMITTEE MANDATE

Concern for descriptions of the ocean environment, especially with respect to wave, current and wind, in deep and shallow waters, and ice, as a basis for the determination of environmental loads for structural design. Attention shall be given to statistical description of these and other related phenomena relevant to the safe design and operation of ships and offshore structures. The committee is encouraged to cooperate with the corresponding ITTC committee.

AUTHORS/COMMITTEE MEMBERS

Chairman: Thomas Fu, *USA*
Alexander Babanin, *Australia*
Abderrahim Bentamy, *France*
Ricardo Campos, *Portugal*
Sheng Dong, *China*
Odin Gramstad, *Norway*
Geert Kapsenberg, *The Netherlands*
Wengang Mao, *Sweden*
Ryuji Miyake, *Japan*
Alan John Murphy, *UK*
Fredhi Prasetyo, *Indonesia*
Wei Qiu, *Canada*
Luis Sagrillo, *Brazil*

KEYWORDS

Environment, ocean, wind, wave, current, sea level, ice, deep water, shallow water, data source, modelling, rogue waves, climate change, design condition, operational condition, uncertainty.

CONTENTS

1.   INTRODUCTION

This report builds upon the work of the previous Technical Committees in charge of Environment. The goal continues to be to review scientific and technological developments in the field since the last report, and to provide context of the developments, in order to give a balanced, accurate and up to date picture about the natural environment as well as data and models which can be used to accurately model it. The content of this report also reflects the interests and subject areas of the Committee membership. Additionally, in accordance with the ISSC I.1 mandate, this Committee has reported on the resources available for design and the operational environment. The Committee has also continued cooperation with the corresponding ITTC Committees initiated in 2010.

The Committee consisted of members from academia, research organizations, research laboratories and classification societies. The Committee formally met as a group in person two times: in Melbourne, Australia (5-6 December 2016) and in Arlington, Virginia, USA (26-27 September 2017), and held a number of regular teleconferences. Additionally, Committee members also met on an ad hoc basis at different scientific conferences and industrial workshops, including the 35th and 36th International Conference on Ocean, Offshore and Arctic Engineering (OMAE 2016 and 2017). With the wide range of subject areas that this report must cover, and the limited space as well as the boundaries presented by the range of specialties and competencies of the Committee members, this Committee report doe s not purport to be exhaustive. However, the Committee believes that the reader will be presented a fair and balanced view of the subjects covered, and we recommend this report for the consideration of the ISSC 2018 Congress.

1.1   Applications

1.1.1   Design

High steep waves and strong winds can create dangerous metocean conditions for ships and offshore engineering activities. This complex load environment results in various responses, stresses, motions etc. Under limited time and geographical region, the loads are described by power spectral densities. Since the densities are changing in time, long-term variability of the environment are described using some spectral parameters, e.g. significant wave height, zero crossing period, wave steepness or average wind speed. The variability of spectral parameters are described by means of uni- or multi-valued long-term distributions. Reliable estimates of the distributions over the oceans are important for safe shipping and offshore engineering activities. Environmental contours derived from the long-term probability density functions are often used. Furthermore, it is also important to clearly specify which type of distribution is relevant, long-term distribution at fixed positions, variability over a region or sea state parameters encountered by a sailing ship.

The long-term distributions of wind and waves for marine design are often employed to determine necessary resistance of ships (offshore structure details) for various material aging processes, where fatigue and crack growth are the most important. The long-term response analysis may be used when specifying design criteria and performing load and response assessment of marine structures. Alternative to full long-term response analysis, the environmental contours are quite often established independently of any structural problem without reference to specific environment design standard. The contour lines correspond to a set of sea states, which may be used to explore design options. Hence, computational intensive response analyses are only required for a limited set of design sea states for each design proposal.

Drago et al. (2015) presents metocean design criteria for the off-shore hydrocarbon extraction activities in very deep waters up to more than 2000 m. For the development of those subsea systems, the metocean design data and criteria to be developed and the applicable methodologies to derive them should be well established, since the system components, e.g., risers,

moorings, etc. can suffer from severe damages due to the occurrence of critical combinations of different variables during a single sea storm due to the surface developments and the connections through the water column. Therefore, this paper considers the joint occurrence of different forcing conditions, and it provides a simplified methodology to perform a sensible multivariate analysis of the contemporary data such as wind, waves and current. Three different cases, i.e., the correlation of extremes of different variables (wind, wave and current), the extreme profiles of current, and the current profile climate, are investigated in the paper. It is concluded that for the wind, wave and current directional extremes correlation, it should be sufficiently enough to provide only the cases which could have relevance in the design analyses, rather than providing the directional correlated extreme of the marginal variable from many different cases.

Bitner-Gregersen (2015) presented a very complex probability density function of the long-term distribution of sea state parameters; mean wind speed; wind direction; main wave direction (sea and swell); current speed; current direction; significant wave height (sea and swell); spectral peak period (sea and swell); sea water level astronomical tides and meteorologically induced surges. The model has been fitted to hind cast data from four locations: Southern North Sea, West Shetland, and Northwest Shelf of Australia and off coast of Nigeria. Presence of wind-sea and swell will affect design and operability of fixed and floating off-shore structures as well as LNG terminals. The presented a joint met-ocean model can be applied for design and operations of marine structures, including LNG platforms. Uncertainties of the proposed fits are examined focusing on location specific features of the wave climate.

The environmental contour concept, commonly applied in marine structural design, allows for the consideration of extreme environmental conditions independently of a particular structure. The idea is to define contours in environmental parameters space (e.g., significant wave height and zero crossing wave period) along which extreme loads and responses with a given return period should lie. In this way, design sea states may be identified along the contour and time consuming long-term load determination and response calculations are only needed for a limited set of design sea states. Alternatively, joint environmental models need to be utilized in full long-term response analysis of marine structures. Vanem and Bitner-Gregersen (2015) compared the recently proposed new approach to estimate environmental contours in the original physical space by direct Monte Carlo simulations with the traditional method employing Rosenblatt transformation. The methods lead to different results, which are compared in a number of case studies. The different results given by these two methods are the practical consequences of the choice of approach. Attention is given to mixed sea systems; in these situations, the two approaches to environmental contours may be very different. Montes-Iturrizaga and Heredia-Zavoni (2016) studied the influence of statistical correlation between significant wave height and peak period on the reliability assessment of mooring lines. This paper proposed to use copulas models to define the joint probability distribution of a set of random variables. It is used to describe the correlation structure of metocean parameters for the reliability analysis of mooring line of a Floating Production, Storage and Offloading vessels (FPSO). The copula models include such as Frank, Gumbel and Gaussian distributions that can be fitted from the hindcast metocean data, in particular significant wave height and peak period. It shows that such correlation structure has big impact on the estimation of the reliability index, while using Gaussian copula will lead to significantly large reliability index in comparison with other copulas models.

Reliability of offshore structures is also dependent on its response to the extreme wave climate. Therefore, an adequate knowledge of the wave climate at a location is a prerequisite. Typically, one is interested in estimates frequency of ultimate failures. Orimolade et al. (2016) investigated the extreme wave climate in the Norwegian Sector of the Barents Sea. Three commonly used methods for the estimation of extreme wave heights, i.e., the initial distribution method, the peak over threshold method, and the annual maxima method, are

used. The estimated 100-year significant wave heights obtained from the three methods differ. While it is difficult to single out the best method among the three, the estimated values give knowledge of the possible range of the extreme significant wave heights at the locations. Generally, the datasets considered in this study suggest that the wave climate is less harsh further north compared to the southern region of the Barents Sea. The datasets do not suggest any temporal trends in the historical significant wave heights at any of the locations.

Most often the sea states are described using long-term distributions of spectral parameters. However in the design responses resulting from interactions of waves (sea elevations) and wind gusts with an offshore structure is needed. Often a linear filtering approach can be applied. However in extreme seas the responses can be hard to determine because of the non-linearity of the interactions. The distributions of responses can be obtained using in situ measurements, model tests or by simulations using dedicated numerical software. In Guo et al. (2016), the various numerically derived extreme responses, e.g. 3 hours extremes, has been compared with results obtained in test tank on ships models. In particular, the influence of forward speed on ship responses in extreme sea is studied.

The long-term distribution changes with geographical location, particularly when one compares open sea and coastal areas. In Bitner-Gregersen (2017), differences between open sea and coastal water wind and wave climate, using hindcast data in the analysis, were investigated. Wind and wave climate is much region and location dependent, affected by local properties of ocean environment. Wind and waves have large impacts on ship design, marine operations and they challenge ability of ships to maintain manoeuvrability in sea states. Recently, it has attracted attention due to the issue of the 2013 Interim Guidelines by IMO, where adverse weather conditions to be used in assessment of ship manoeuvrability have been proposed. Correlations between wind speed and significant wave height as well as significant wave height and spectral peak period are established and compared with the ones suggested by the 2013 Interim.

In Bitner-Gregersen et al. (2016), definition of the severity or adversity of met-ocean conditions under which ships need to maintain manoeuvrability were discussed. Specification of such adverse weather conditions was one of the objectives of the SHOPERA (Energy Efficient Safe SHip OPERAtion) (2013–2016) project, funded by the European Commission in the frame of FP7. Three distinct situations requiring different adverse weather criteria are considered in the project: manoeuvring in the open sea, manoeuvring in coastal waters and low-speed manoeuvring in restricted areas. The purpose of the present study is twofold, first to investigate metocean climate associated with the three selected scenarios and specifying its main properties, second identifying critical metocean characteristics requiring sensitivity studies in numerical simulations and model tests. Both measured and hindcast data are used in the analysis. The North Atlantic deep water metocean environment and three coastal locations are considered. The definitions are basis for formulating power and steering requirements for ships.

From 2015-2017, some research was dedicated to study whether the design criterion should include a possible climate change where the time horizon is the end of 21th century. That is whether the long-term distributions or maximum responses distributions, used in design, may considerably change in future. Weisse et al. (2015) presented the so-called "climate services" for the decision making processes of particular interest in the maritime applications in Europe. A series of examples ranging from naval architecture, offshore wind and more generally renewable energies, shipping emissions, tidal basin water exchange and eutrophication levels, etc., are described covering the generation, transformation and the use of climate information in decision making processes. This paper also investigated the effects of climate change on coastal flood damages and the need for coastal protection is considered. It is concluded that reliable climate information in data sparse regions is urgently needed. For many applications, historical climate information may be as or even more important as future long-term projec-

tions. Aarnes et al. (2017), Bitner-Gregersen and Toffoli (2015), and Vanem (2016) present detailed investigations of possible changes in future distributions of significant wave height, periods and steepness. The fits to historical data are compared with estimates of future wave climates based on several emission scenarios. The results are very uncertain and not yet influencing the present design procedures. In Aarnes et al. (2017), wave model simulations covering the northeast Atlantic have been conducted using 3-hourly near-surface winds obtained from six CMIP5 models. It is found that a decrease in significant wave height in the northeast Atlantic by the end of the 21st century. The study indicates the largest changes in significant wave height near the mean, while the tendency is weaker going into the upper tail of the distribution. Locally, these extremes are approximately one standard deviation higher in the future climate. A similar, but weaker increase is found in the southern coastal areas of Norway.

Wave steepness is an important parameter not only for design and operations of marine structures but also for statistics of surface elevation as well as occurrence of rogue waves. Bitner-Gregersen and Toffoli (2015) investigates potential changes of wave steepness in the future wave climate in the North Atlantic. The Fifth Assessment Report of the Intergovernmental Panel on Climate Change (IPCC) uses four scenarios for future greenhouse gas concentrations in the atmosphere called Representative Concentration Pathways (RCP). Two of these scenarios with radiative forcing of 4.5 and 8.5 W/m2 by the end of the 21st century have been selected to project wave conditions in the North Atlantic. The analysis includes total sea, wind-sea, and swell. Changes of wave steepness for these wave systems are shown and compared with wave steepness derived from historical data. Long-term probability description of wave steepness variations is proposed. Consequences of changes in wave steepness for statistics of surface elevation and generation of rogue waves are demonstrated. Uncertainties associated with wave steepness projections are discussed.

In many marine and coastal engineering applications, the simultaneous distribution of several metocean variables is required for risk assessment and load and response calculations. For example, a joint probabilistic description is needed to construct environmental contours for probabilistic structural reliability analyses. Typically, the joint distribution of significant wave height and wave period is needed as a minimum, but other environmental parameters such as wind, current, surges and tides might also be relevant. Vanem (2016) presents a study on various joint models for the simultaneous distribution of significant wave height and zero-crossing wave period. The alternative models that have been investigated are a conditional model, a bivariate parametric model and several models based on parametric families of copulas. Each of the models is fitted to data generated from a numerical wave model for the current climate and for two future climates consistent with alternative climate scenarios. Additionally, the potential effect of climate change on the simultaneous distribution will be investigated. Initial investigation reveals that straightforward application of some of the most commonly used copulas will not give reasonable joint models. The reason for this is that they are symmetric, whereas the empirical copulas display asymmetric behaviour. However, asymmetric copulas can be constructed based on these families of copula, and this significantly improves the fit. Analyses of the extremal dependence in the data indicate that the variables are asymptotically independent. Furthermore, the results suggest that extreme significant wave height and zero-crossing wave period tend to be more correlated in a future climate compared to the current climate.

1.1.2   Operation

The reduction of emissions of greenhouse gas (GHG) has become an urgent global task for the prevention of global warming. In order to reduce the GHG emissions from the international maritime sector ahead of the other sectors, amendments to MARPOL ANNEX VI making "Energy Efficiency Design Index (EEDI)" and "Ship Efficiency Management Plan (SEEMP)" mandatory were adopted at the 62nd session of Marine Environment Protection Committee

(MEPC 62) held in July 2011, and have entered into force on 1 January 2013. This was the first legally binding climate change treaty to be adopted since the Kyoto Protocol.

Furthermore, at MEPC 70 held in October 2016, amendments to MARPOL Annex VI to make mandatory the data collection system (DCS) for fuel consumption of ships and amendments to the SEEMP guidelines were adopted. Under the amendments to MARPOL Annex VI, on or before 31 December 2018, in the case of a ship of 5,000 gross tonnage and above, the SEEMP shall include a description of the methodology that will be used to collect the data and the processes that will be used to report the data to the ship's flag State.

On the other hand, in June 2013, the European Commission proposed a strategy for progressively integrating maritime emissions into the EU's policy for reducing its domestic GHG emissions. After a two-year legislative process, involving all EU institutions, this strategy was adopted by the European Parliament in April 2015. The Regulation 2015/757 ('Shipping MRV Regulation') came into force on 1 July 2015. The strategy consists of three consecutive steps:

- Monitoring, reporting and verification of carbon emissions from ships
- GHG reduction targets for the maritime transport sector
- Further measures, including Market-Based Measures (MBM)

The first step of the strategy is the design of a robust Monitoring, Reporting and Verification (MRV) system of carbon emissions for ships exceeding 5,000 gross tonnage (GT) on all voyages to, from and between EU ports applicable from 2018.

At the early stage of deliberations on EEDI regulation, since the EEDI regulation requires to reduce EEDI value by 30 % in phase 3, there was concern that ships with excessively small propulsion power would be constructed just for the purpose of improving the EEDI value. Therefore, discussions on minimum propulsion power in adverse weather condition were started. Consequently, it was required that the installed propulsion power shall not be less than the propulsion power needed to maintain the manoeuvrability of the ship in adverse conditions in accordance with "2013 Interim guidelines for determining minimum propulsion power to maintain the manoeuvrability in adverse conditions" (Resolution MEPC.232(65), 2013). The purpose of the interim Guidelines is to verify that ships, complying with the EEDI requirements, have sufficient installed power to maintain the maneuverability in adverse conditions. The interim minimum propulsion power Guidelines are applicable only to bulk carriers, tankers and combination carriers of 20,000DWT or above to which compliance with required EEDI is required during phase 0 (from 2013 to 2014) and phase 1 (from 2015 to 2019) of the EEDI implementation.

In 2014, in order to revise the interim minimum propulsion power Guidelines, a Japan's research project was launched by Japanese maritime societies. For the same purposes at almost the same time, the EU PF7 project "Energy Efficient Safe Ship Operation (SHOPERA)" was also launched by European maritime societies. In 2015, in order to address the challenges of this issue by more in depth research, SHOPERA and the Japan's research project (these projects hereinafter being collectively referred as "the Projects") have worked together through technical and practical considerations and evaluation. At MEPC 71 held in July 2017, in order to revise the interim Guidelines, draft revised Guidelines reflecting the results of the Projects were introduced (MEPC 71/5/13 and MEPC 71/INF.28, 2017).

The Projects developed three realistic scenarios for evaluating ship's handling in adverse conditions (MEPC 71/INF.29, 2017). The specification of the scenarios was based on a series of interviews with ship owners, ship masters and chief engineers, accidents and weather statistics, as well as the analysis of the seakeeping performance of ships in waves.

Based on the evaluation of results of conducted studies for a series of existing eco-ships, the Projects have reached a conclusion that the following scenario "Weather-vaning in coastal

areas under strong gale condition" is always more demanding, in comparison with other scenarios, with respect to the required installed propulsion power for tankers, bulk carriers and combination carriers. Therefore, this scenario is proposed to be considered as the only required scenario for the evaluation of the sufficiency of ship's propulsion power to maintain the manoeuvrability in adverse conditions for bulk carriers, tankers and combination carriers.

Scenario "Weather-vaning in coastal areas under strong gale condition"

Area	Coastal areas
Weather conditions	BF8 (gale) for L_{pp}<200 m to BF9 (strong gale) for L_{pp}>250 m, linear over L_{pp} between 200 m and 250 m
Encountered wave and wind angle	Head seas to 30 degrees off-bow for a situation of weather-vaning
Propulsion ability	Speed through water at least 2 knots
Steering ability	Ability to keep heading into head seas to 30 degrees off-bow

Based on the assessment of results of the seakeeping performance in waves of a series of existing ships, the interviews held with ship owners, ship masters and chief engineers, shipping log data provided by ship operating companies, metocean statistical data, as well as statistics of accidents and corresponding weather conditions (Beaufort strength), the Projects have developed the adverse weather conditions that should be applied in the assessment.

Because of the diversity of the weather and sea conditions, in view of the many parameters affecting them, the Projects share the view that the adverse weather conditions applied in the assessment should be verified based on the results of the assessment of the operability of a big number of existing ships in specified weather conditions (benchmark). Based on these studies and the validation results for a series of representative existing bulk carriers and tankers, the Projects have reached a conclusion that the following conditions are suitable for the specification of the adverse weather conditions of the scenario:

BF8 for L_{pp} < 200 m, BF9 for L_{pp} > 250 m; and linearly interpolated over L_{pp} between 200 m and 250 m.

Based on the results of measurements in coastal areas within 20 nautical miles from the Pacific Coast of Japan and at 20-30 nautical miles from the North Sea coastline of Great Britain regarding the relation between Beaufort number (wind speed) and significant wave height, the Projects determined the significant wave height corresponding to Beaufort number in coastal areas, which should be applied in the assessment of the scenario (coastal areas), considering an additional safety margin.

As a result of the discussion at MEPC 71 held in July 2017, it was agreed to continue discussion at MEPC 72 (will be held in April 2018) due to the fact that different opinions were expressed on the adverse weather condition etc. Furthermore, for the current guidelines, it was agreed to extend the application period towards phase 2 (from 2020 to 2024) of the EEDI implementation.

Present day marine operations use advisory systems that combine weather information, vessel characteristics and criteria to minimize fuel cost, emissions and risk (Simonsen et al., 2012). Optimization of operations requires algorithms to generate and evaluate alternatives and object functions that are used to quantify the result of the operation. Usually constraints are included, such as the ship route should not cross land or shallow water.

Examples of marine operations are ship planning, studies on fatigue damage and the development of warning systems for high sea states and extreme waves. These operations require a more detailed description of sea state variability than the long-term sea-state distributions

used for design purposes. These applications use correlations between sea-state parameters at different locations and moments in time. Such information is often a part of spatio-temporal models of sea state variability. The delimitation treaty between Norway and the Russian Federation, signed in September 2010, has opened new opportunities for the shipping and offshore industry in the Barents Sea and brought the need for further research of metocean and ice conditions in the Arctic regions.

Planning

The shipping industry makes frequent use of planning systems that combine the concepts of weather routing and voyage optimization. The primary objective of planning is to increase ship safety, gain more economic benefit and reduce emissions. Conventional weather routing will determine the minimum distance, duration and fuel consumption of the voyage, but other performance characteristics can be used to optimize the route. For example, Kim et al. (2017) developed a weather routing method to optimize the transport of an offshore structure. The duration of weather systems appeared to be a crucial aspect in the feasibility of the operation. In his study, Kim used the WaveWatch III database. Also minimizing the accumulation of fatigue damage can be used as an object function for planning; Mao et al. (2010a) developed such a model for a small size container ship to be used in a planning system.

Park et al. (2015) proposed a method to use a two-phase approach to weather routing. The first phase optimizes the heading of the ship at each time instant while keeping the speed constant. IMO safety regulations are applied as constraints. The second phase optimizes the speed. They claim that an almost optimal solution is found in a more efficient way than competing methods. Existing density maps of historical ship routes can also be used to plan short to mid-range ship routes, as explained by Azariadis (2017).

De Garcia et al (2016) developed the fatigue damage assessment metodology based on weather routing system by analysing the minimum time route and (MTR) and Great circle route (GCR) of US/Japan route in order to emulate the as real wave load sequences. He used the weather routing planning by several objective, there are maximise safety and crew comfort, minimum fuel consumption and minimum time underway.

Lee et al (2015) proposed a planning path by considering the effects in path planning, a energy efficiency due to maneuverable path. In detail, the plath planner will be analysis based on a realistic energy cost that it determines from loads of vehicle due to tidal current and water depth.

Algorithms

Traditional algorithms used in weather routing simply looked for the shortest route, examples of this are isochrones and isopone methods. More advanced algorithms try to optimize an object function that normally combines several aspects that are combined using weighing factors. Examples of such algorithms are 2D dynamic programming, 3D dynamic programming and Dijkstra's algorithm (Wang et al. 2017). Larsson et al. (2015) presented a Dividing Rectangles (DIRECT) algorithm and also further divide constraints into fuel constraints, generic constraints, and ship-specific constraints.

Grin et al. (2016) used the voyage simulation tool SafeTrans to determine the performance of ferries with respect to comfort, fuel efficiency and schedule. This tool uses Dijskstra's algorithm for weather routing and Monte Carlo simulations for voyage optimization. Different bow flares and routes were compared and optimized to minimize the wave conditions encountered, vibration dose and voyage duration.

Tamaru (2016) proposed an optimization of ship routing plan based on the analyzing isochrones by taking into account ship speed loss, significant wave height and relative heading angle of ship include with spatio temporal seastate information. The optimization solution is

generic algorithm which can decide the minimum time route of spatiotemporal distribution of significant wave height and wave direction.

More detailed and complicated algorithms can be used due to increased computing power. A rational and robust optimization procedure is the key to make the complicated algorithm more trustworty in order to reduce the uncertainties (Vettor and Soares (2016)). However, further improvements are more limited by the quality and time span of weather forecasts than by the complexity of the vessel hydrodynamic models and constraints.

Forecast Data

Commercially available forecast data is typically used in weather routing, but some public sources are documented in literature. Some sources include pilot charts (US National Geospatial-Intelligence Agency), ocean drifter data (US Coast Guard Mariano Global Surface Velocity Analysis, MGSVA), or satellite data (Ocean Surface Current Analyses Real-time, OSCAR). The quality of the database depends on the resolution and number of years available. Lu et al. (2017) conducted benchmarking of the WAVEWATCH III model for the Southern hemisphere by varying spatial and temporal resolution, and validating the results with measured onboard ship motion data. The EC SAFE OFFLOAD project has proposed a procedure utilizing information about wind-sea and swell in the specification of a risk-based approach for the safety of offloading operations from the LNG terminals to shuttle gas tankers. Chang et al. (2015) present a 3D geographic information system (GIS) for the initial planning of routes between Asia and Europe via the Arctic Northeast Passages, including data such as sea ice distribution, shore topology, and water depths. Skoglund et al (2015) conducted the investigation of the use of ensemble weather forecasts. The investigation is conducted because the question of the availibility of forecast data due to re-routing simulation.

Furthermore, if the commercial data forecast is not available, the weather routing systems, could use the numerical prediction based on the location of voyage. For example, Mao and Rychlik proposed the statistic distribution for wind speeds along North Atlantic route.

Constraints

Constraints in weather routing should not only include land avoidance, but also hazards such as ice, and seasonal weather effects. McGonigal et al. (2011) show results of an investigation in the presence of EIFs (Extreme Ice Features) in the area between Ellesmere Island and Prince Patrick Island. The data was collected in August 2008 from satellite images. Roughly 200 EIFs were identified, including 40 ice islands, 93 ice island fragments and 67 multi-year hummock fields. Ice island fragments were defined as less than 1 km in the longer dimension, ice islands had a diameter between 1.6 and 5.2 km, and multi-year hummock fields a diameter between 1.7 and 13.8 km. Mudge et al. (2011) analysed Canadian Ice Service (CIS) records from 1982 to 2010 and studied two passages of Viscount Melville Sound (VMS) by CCGS Amundsen in order to assess feasibility of navigation in the Canadian Arctic region. The authors observed a high degree of spatial and temporal variability in ice conditions in the area of the Northwest Passage with large seasonal variations. The study indicated the importance of timely and accurate ice information in making the Northwest Passage feasible for trade as numerical models are not inaccurate. Erceg et al. (2013) tested the economic feasibility of higher polar classes for LNG transit operations on the route from Rotterdam to Yamal. Reimer et al. (2013) simulate the impact of a Northern Sea route on exhaust gas emission, as well as travelling time. Way et al. (2015) examined the use of speed optimization to determine whether it is potentially more profitable for a container shipping company to ship from Rotterdam to Yokohama through the Suez Canal year round, or to ship through the Northern Sea route during the months it was passable. Monte Carlo simulations were used to calculate the average profit per trip, with the main parameters being the fuel consumption and speed of an ice-class and non-ice-class vessel. The speed in ice-covered water was considered independent of the ice. It was indicated that the variability in schedule might be more suited to bulk shipping than containerized shipping.

Warning and Decision Support Systems

Several authors have studied relations between spectral parameters and occurrence of extreme or rogue waves and the topic is also investigated in the EC EXTREME SEAS project. Clauss et al. (2009) used a short-crested, multi-directional forecast to predict encountering wave trains for alternative cruising velocities and courses. Mori et al. (2011) used Monte Carlo simulations on the Nonlinear Schrodinger equation in two horizontal dimensions and found that increasing directional spread decreases kurtosis, a parameter accepted to be related to higher probability of rogue wave occurrences. On the other hand Tofioli et al. (2011b) found higher kurtosis values when analysing waves in bimodal sea states, with higher occurrences when directional differences were between 20 and 40 degrees.

The distribution of encountered wave slope was used to predict risks for capsizing of vessels, see Leadbetter et al. (2011) and Aberg et al. (2008) for the theoretical background of the method. The development of decision support systems remains in focus. As proposed by Nielsen et al. (2011) and Nielsen and Jensen (2011), they require the collection of relevant data e.g. metocean, ship response, on board. These types of data can also be used for self-learning (see the EC project NavTronic for example). Utne et al. (2017) gave a list of risk-influencing factors for autonomous marine systems, based on the operation and environment parameters, and how those factors can be used proactively (planning) or reactively (decision support). Alford et al. (2016) describe a real-time multi-ship environmental and ship motion forecasting system, using off-the shelf marine radar to give 30s predicted ship motions and identify relevant warning criteria. Reite et al. (2017) present a generic framework that combines onshore analysis of historical data and a tool for real-time decision support onboard to optimize hybrid propulsion of a fishing vessel. This allows for decision support based on measurements rather than mathematical models

Search and Rescue operations require specific decision support systems. Their planning relies on accurate forecasting of the drift of objects under search. The most widely used approach for drift assessment is based on the Leeway method in which Leeway coefficients taking into account combined action of wind and waves are experimentally identified for various classes of objects allowing assessment of drift velocity and direction as a function of wind speed. Breivik et al. (2011) propose a standardised method for assessment of Leeway coefficients from field experiments. Uncertainties in forcing fields (wind and currents) as well as other information such as initial date and location of the drift are accounted for when introducing a stochastic approach based on a Monte Carlo technique for the computation of an ensemble of equally probable perturbed trajectories (Breivik et al., 2008).

Accuracy of drift prediction is highly dependent on the quality of the forecasting of environmental data. It was pointed out during the 4th Int. Workshop on Technologies for Search And Rescue and other Emergency Marine Operations (2011) that the use of HF-radar and Lagrangian oats (SLDMBs) data for assimilation or correction of current can provide efficient improvement of the accuracy of the drift prediction. Iyerusalimskiy et al. (2011) present a state-of-the-art ice load monitoring and alarm system that was installed on a large icebreaking tanker operating between the Barents Sea and Murmansk. The system is designed to measure and record in real time the ice pressure and loads and calculates structural responses in selected locations on the hull.

The scale of the environmental forecast can have an effect on the quality of the warning system. Sasa (2017) describes the optimal routing of short-distance ferries from the evaluation of mooring criteria. For short-distance ferries, ocean wave monitoring systems cause difficulty and confusion because they represent typhoons and depressions that are several hundred kilometers away. Therefore, a different system is devised based on the motions of the ships moored in the harbour, which is more relevant to short-distance ferry services.

Dong et al (2016) proposed the decision support system for a mission by multi performance criteria on ship routing. The criteria aspects considered consist of the expected repair cost, fatigue damage, travel time, and CO2 emission. Furthermore, the risk is also taken into account from the decision maker aspect by integration into the presented approach of utility theory.

Since the encountered metocean conditions will have direct impact on the ship/offshore structural safety, energy efficiency, and emissions during their operation stages, most of ocean-crossing vessels are instrumented with voyage planning or weather routing systems. Such systems can be used to assist ship operation in a more optimal way based on weather forecast information. Furthermore, due to the strict regulation on energy efficiency and air emissions from shipping industry, a large amount of research and innovation within the maritime community have been devoted to develop wind propulsion technologies which utilize wind power to provide auxiliary propulsion forces to ships. Loyd's report (Loyd 2015) and Dagmar et al. (2016) have carried out in-depth analysis on the commercial and technical opportunities and challenges to use wind propulsion technologies in shipping industry. The actual benefits of such technologies pretty much depends on the possible encountered wind and wave conditions a ship may encounter during her service life, as well as the ship's performance in the complex metocean conditions. In Mao and Rychlik (2017), a spatio-temporal wind model is developed based on the transformed Gaussian process using 30 years of environment data from European Centre for Medium-Range Weather Forecasts (ECMWF) and measurements in ships. This model can be used to simulate the wind conditions encountered by a vessel to study the potential wind propulsion energy after the installation of such technologies. Furthermore, similar as the ordinary ship operation in the open sea, to get the best benefit from the wind propulsion technologies will rely even more on the voyage optimization, which helps to choose the best optimal wind conditions for ship navigation (Lu et al.2017). In a preliminary study by Mao et al. (2012), a simple configuration of route planning through change of possible departure time leads to encounter better metocean conditions during a ship's sailing. It is illustrated that using voyage planning has the potential to reduce at least 50% of the fatigue damage accumulation in ship structures when crossing North Atlantic Ocean. In Simonsen et al. (2015), different algorithms used in today's weather routing market have been reviewed. Their cons and pros with respect to optimization capabilities and objectives to enhance ship safety, energy efficiency, and expected time of arrival are also discussed in the paper. In the more recent paper by Wang et al.(2017), a further benchmark study regarding most of the available optimization algorithms in the maritime community has been carried out with its focus on their capability of voyage planning with minimum fuel cost through optimal choice of optimal encountered metocean (wind, wave and current) conditions during sailing. A similar system is also studied by Vettor and Guedes Soares (2016) with a bit focus on the ship's performance when operating at sea and wave spreading.

1.2   Waves

There has been significant progress in both phase-resolved wave modelling and observations of the sea surface over a spatial domain. Again, this is distinct from the more traditional statistical processing of time series collected at a single point in space. Much of the effort in phase-resolved wave measurements has centered on marine RADAR, which can be noncoherent radar (e.g., Qi et al, 2016), or can use coherent Doppler processing (Connell et al. 2015). Other remote sensing approaches include airborne scanning LIDAR (e.g., Reineman et al, 2009), shipboard stereo video (e.g., Schwendeman & Thomson, 2017), and satellite images of sun glitter (Kudryavtsev et al, 2017). Recently, there has also been progress in using arrays of buoys or other point measurements to reconstruct a phase-resolved sea surface (e.g., Takagi et al, 2017).

1.3   Wind

As indicated above, surface wind vectors are vital for operational and scientific issues. For instance, they are routinely used as primary forcing function component for ocean circulation, wave, and current models at global and/or local scales. They have great impact on coastal upwelling, cross shelf transport, deep water formation, and ice transport and variability. They are essential for reliable estimation of momentum (wind stress vector), heat fluxes (latent and sensible), mass flux (e.g. CO_2 and H_2O). They are used to investigate the climate change as well as the storm surge and wave forecasts.

The knowledge of surface wind vectors are requested with various characteristics depending upon the atmospheric, oceanic, and climate application. However, better global spatial and temporal resolutions as well as accuracy are highly needed.

The surface wind vectors are routinely derived from in-situ (mooring buoys, ships) and satellite radar and radiometers measurements, and from numerical weather prediction (NWP) models.

Surface wind speed and/or directions and the related parameters (wind stress, wind divergence, wind curl, and turbulent heat fluxes) are derived from remotely sensed observations. The latter are retrieved from onboard satellite radars and radiometer such as scatterometers, altimeters, radiometers, and SAR. Scatterometer provide, over free land and ice global oceans, both wind speed and direction over a wind vector cell (WVC) of 25km×25km and/or 12.5km×12.5km cross swaths varying between 500km and 1800km width. Altimeters and radiometer provide only wind speed estimates over free and ice global oceans. SAR measurements enable the estimation of wind speed and direction with very high spatial resolution (lower than 1km) at some selected oceanic areas.

The satellite wind products are available with various levels. L2b, L3, and L4 levels are associated with wind retrievals over instrument swath or along track, spatial gridded swath data, and space and time gridded wind fields, respectively. The processing, archiving, and dissemination of satellite products are handled by several space agencies and/or research organizations. Following are some useful links (not exhaustive):

http://cersat.ifremer.fr/

https://podaac.jpl.nasa.gov/OceanWind

http://www.remss.com/

https://sentinels.copernicus.eu/

http://marine.copernicus.eu/

http://www.osi-saf.org/

http://projects.knmi.nl/scatterometer/

In near future, three satellites will be launched in 2018 with onboard scatterometers, radiometers, and/or altimeters. The Chinese-French Ocean Satellite CFOSAT (CNES, NSOAS and CNSA). Two payloads are on-board: the French SWIM (Surface Waves Investigation and Monitoring), a real-aperture radar with a low-incidence conical-scanning beam for directional wave spectra and wind, and a Chinese wind scatterometer with a rotating fan-beam antenna. The EUMETSAT satellite METOP-C will carry on ASCAT-C scatterometer as a part of payload including Advanced Microwave Sounding Unit - A (AMSU-A), Advanced Very High Resolution Radiometer / 3 (AVHRR-3), Global Ozone Monitoring Experiment – 2 (GOME-2), and infrared Atmospheric Sounding Interferometer (IASI), and Microwave Humidity Sounding (MHS). The third program is OceanSat-3 satellite operated by the Indian Space Research Organisation (ISRO). OceanSat-3 payload includes ku-band pencil beam scatterometer, 13-band Ocean Colour Monitor (OCM), and 2-band Long Wave InfraRed (LWIR).

Several satellite projects aiming at the observation of surface wind speed and direction over the global oceans are planned. The Post EUMETSAT Polar System (Pot-EPS named) with second generation scatterometer (SCA) is expected for 2022. The China National Space Administration (CNSA) will operate the program HY-3C expected for 2020. The Russian research organisation Research Center for Earth Operative Monitoring will be in charge of operating METEOR-M N3 satellite, expected for 2020. The Japan Aerospace Exploration Agency's (JAXA's) will maintain the satellite series contributing to climate change research and monitoring through the Global Change Observation Mission (GCOM) satellites. GCOM-W2 and GCOM-3 are planned for 2019 and 2022, respectively.

1.4   Climate

1.4.1   Increasing uncertainty and risk due to climate change.

Several studies on the environmental global climate have emerged recently, with a great concern about future climate changes, risks and impacts. The problems regarding the climate changes are much more associated with local impacts of extreme events than the global average, which tends to be smoothed out. Changes in extreme weather and climate events have been observed since 1950. Some of these changes have been linked to human influences, including a decrease in cold temperature extremes, an increase in warm temperature extremes, an increase in extreme high sea levels and an increase in the number of heavy precipitation events in a number of regions. IPCC-AR5(2014) describe that continued emission of greenhouse gases will cause further warming and long-lasting changes in all components of the climate system, increasing the likelihood of severe, pervasive and irreversible impacts for people and ecosystems. The observed changes in the climate were found to be very heterogeneous; therefore, risks are unevenly distributed and are generally greater for disadvantaged people and communities in countries at all levels of development (IPCC-AR5, 2014).

Bitner-Gregersen (2017) corroborates the local dependences of wind and wave climates, affected by local properties of ocean environment, which impact ship design and marine operations, and they challenge ability of ships to maintain manoeuvrability in sea states. Bitner-Gregersen (2017) present differences between open sea and coastal water wind and wave climate using hindcast data. The study discussed the challenges in providing metocean description for assessment of ship manoeuvrability and uncertainties related to it. The risk of climate-related impacts results from the interaction of climate-related hazards with the vulnerability and exposure of human and natural systems, including their ability to adapt (IPCC-AR5, 2014). Rising rates and magnitudes of warming and other changes in the climate system, accompanied by ocean acidification, increase the risk of severe, pervasive and in some cases irreversible detrimental impacts.

1.4.2   Sea Level Rise

Coastal communities throughout the world are exposed to numerous and increasing threats, such as coastal flooding and erosion, saltwater intrusion and wetland degradation (Rueda et al., 2017). Flooding is one of the most dangerous consequences related to climate changes. Rueda et al. (2017) present the first global-scale analysis of the main drivers of coastal flooding due to large-scale oceanographic factors, which is a multidimensional problem (e.g. spatiotemporal variability in flood magnitude and the relative influence of waves, tides and surge levels). Rueda et al. (2017) show that 75% of coastal regions around the globe have the potential for very large flooding events with low probabilities, 82% are tide-dominated, and almost 49% are highly susceptible to increases in flooding frequency due to sea-level rise. Over the period 1901–2010, global mean sea level rose by 0.19 [0.17 to 0.21] m and the rate of sea level rise since the mid-19th century has been larger than the mean rate during the previous two millennia, according to IPCC-AR5 (2014). This report, based on tide gauge and satellite altimeter, shows that is very likely that the mean rate of global averaged sea level rise was 3.2 [2.8 to 3.6] mm/yr between 1993 and 2010. Under all Representative Concentration Pathways

(RCP) scenarios from IPCC-AR5 (2014), the rate of sea level rise will very likely exceed the observed rate of 2.0 [1.7–2.3] mm/yr during 1971–2010, with the rate of rise for RCP8.5 during 2081–2100 of 8 to 16 mm/yr.

2.   LONG TERM STATISTICS AND EXTREME VALUE ANALYSIS

Long-term distributions and Extreme Value Analysis play an important role on marine projects, metocean design criteria and coastal management. The process of estimating extreme quantiles associated with return periods of interest involves large uncertainties and long processes vulnerable to error propagation; as for example from input data with intrinsic biases, storm selection, idealized requirements of distribution functions and extrapolation. Widely-used methods, as Peaks Over Thresholds (POT), assume that events are identically distributed, the process is stationary and events are independent – which is nearly impossible to find in environmental time-series as winds, waves and currents. Thus, several studies have emerged investigating the possible trends in the frequency of events, duration of the storms, statistical models to better extrapolate the quantile functions and spatial techniques.

Godoi et al. (2017) studied extreme events of waves in New Zealand using 44 years of hindcast data. They found the interannual variability is largest along the north coast of the country and on the east coast of the South Island, suggesting relationships with La Niña-like effects and the Southern Annular Mode. They argue the known trend for a more positive Southern Annular Mode may explain the increasing number of extreme events shown in their study. Sartini et al. (2015), at the Italian coast, calculated return levels by the Goda method, the Generalized Extreme Value (GEV) and the Generalized Pareto Distribution–Poisson point process models and the Equivalent Triangular Storm (ETS) algorithm. All models follow the Peak-Over-Threshold (POT) approach which require an optimal threshold implementation, save for the GEV analysis, which is applied to model significant wave height maxima pertaining to time-blocks. Sartini et al. (2015) argues in favor of the versatility of the GPD–Poisson model, while the GEV and ETS models exhibit limitations in assessment of a variety of wave fields, greatly diversified in semi-closed basins. Sulis et al. (2017) compared the results of the most commonly used extreme wave analysis methods applied to a 20 year wave hindcast in the Gulf of Cagliari (South Sardinia, Italy). While conventional distributions recommended by Goda (e.g. the Gumbel and Weibull distribution) represent the most common methods in engineering applications, accurate results in the paper indicate that the community should consider the Generalized Pareto Distribution (GPD) as one of the most performing credible candidates. Sulis et al. (2017) corroborates with several previous studies, including Campos et al. (2016) who achieved the best results using Pareto, Pearson Type-3 and Weibull distributions.

Laface et al. (2016) propose a new solution, in the context of equivalent storm models, for long-term statistics of ocean storms. The paper has proposed a new model for an improvement of the class of equivalent storm models that are widely used in maritime engineering for investigating the long term statistics, coastal processes as well as for the evaluation of progressive damage of coastal structures. Laface et al. (2016) explain that the main concept consists of replacing the actual storm with an equivalent one, from a specific perspective, depending on the scope of the analysis to perform. Finally, in comparison with previous methods, their solution provides a better representation of actual storm duration.

In the structures design, short and long term statistical distributions of wave height, crest height and wave periods, as well as joint distributions, are important for structural integrity assessment. Hagen et al. (2017) combined the short-term statistics with the long-term scatter diagram for an offshore location at the Norwegian and long term scatter diagrams generated. Based on these scatter diagrams, extreme value estimates are calculated for wave height and crest height, and corresponding wave periods determined. They found that wave periods generated are somewhat shorter than prescribed in design recipes. Authors also investigated the

statistical uncertainty of extreme value estimates as function of number of simulations. Mura-leedharan et al. (2015) deeply studied the distribution of significant wave height and associated peak periods using 21 years of wave hindcast in the North Atlantic. The joint distribution of wave heights and periods are extremely important for offshore structures and ship motions. Moving to a multivariate study, Zhou et al. (2017) investigated the extreme water level, current velocity and wave height in Laizhou Bay, China using simulation results from MIKE21 and Gumbel distribution.

Considering that wave spectra often exhibit multiple peaks due to the coexistence of wind waves and swells, Laface et al. (2017) described the waves by partitioned sea states that can be interpreted physically as representing independent wave systems. The sensitivity of return values of significant wave height to swell contribution was investigated via an application of the Equivalent Triangular Storm Model (ETS). The results of Laface et al. (2017) show that the contribution of swell is more significant for storms of small and medium intensity and decreases for increasing storm intensities. Further return values variability neglecting swell is less than 7% at any point for return periods up to 100 years.

As an alternative to extreme value analyses based on hindcast data, Wimmer et al. (2016) estimated return values of significant wave height directly from measurements by satellite altimeters over the North Atlantic. Return values were calculated by fitting a Generalized Pareto Distribution to all values above a threshold, which was allowed to vary spatially. The novel method of Wimmer et al. (2016) gave return values that were up to 37% smaller than those estimated by fitting a Fisher-Tippet distribution to all the data.

The spatial and regional distributions of extreme quantiles have been further explored during the last few years. Sartini et al. (2017) studied the spatial and temporal modelling of extreme wave heights in the Mediterranean Sea based on a 37-year wind and wave hindcast database at 10-km resolution. A point-wise Generalized Extreme Values model was employed to generate the assessments results. Overall, the spatial model proved capable of providing an accurate description of extreme return levels of significant wave heights and their spatial variability, especially on a basin-wide scale and with greatest precision on the mesoscale. However, Sartini et al. (2017) argues that return level estimates are found less reliable in certain coastal areas because the traditional point-wise approach is not refined enough to address the entire wave spectrum of an area as complex as the Mediterranean Sea. Sartini et al. (2017) incorporated the Mean Sea Level Pressure fields as covariates to improve localized assessment. These covariates represent meteorological forcing and allow analysis of the role of different cyclonic regimes in defining wave features and their spatial variability.

A number of studies recently applied the method developed by Hosking and Wallis (1997): Regional Frequency Analysis (RFA) based on L-moments. Although it was initially developed for flood events, it was adapted to extreme winds and waves. The RFA consists of using data from different sites with related statistics to better estimate the quantile function, which can be used for regional or site-specific analyses. The concept comes from the fact that if event frequencies are similar for different observed quantities, more robust conclusions can be reached by analyzing all of the data samples together than by using only a single sample. As most extreme analyses are based on hindcast data with regular grid resolutions, RFA suggests that the inclusion of neighboring grid-points improves the estimate of the quantile functions (Campos and Guedes Soares, 2016). Additionally, RFA is especially suitable for long return values extrapolations and short time-series lengths; because it trades space for time, reducing the confidence interval amplitude even in very long return periods. Campos and Guedes Soares (2016) applied the RFA based on L-moments to calculate spatial extreme return values of significant wave height in the South Atlantic Ocean. They obtained reliable extreme return values at each grid point with very low variance of the distribution parameters estimators and narrow confidence intervals. Considering the return period of 100 years, the significant wave heights vary from 5.5 to 11.2 meters within the considered domain in southern and southeast-

ern Brazil. In the North Atlantic Ocean, Lucas et al. (2017) applied the RFA for several locations at the coast of Portugal using data from HIPOCAS (Hindcast of Dynamic Processes of the Ocean and Coastal Areas of Europe).

The regionalization and exclusion of sites with discordant statistics are essential steps of the RFA, as well as the goodness-of-fit tests applied to the regional quantile functions. Hosking and Wallis (1997) defined a heterogeneity test for selected regions and a goodness-of-fit test based on the kurtosis of the empirical and modeled distributions. Vanem (2017) applied RFA on extreme significant wave heights in the North Atlantic Ocean for historical and projected ocean wave climates. A set of homogeneous regions were identified as ocean regions with similar characteristics, and the effect of climate change on the ocean wave climate could be studied, both with regards to changes in extreme quantiles at certain location and to overall spatial changes. Results from Vanem (2017) confirm that RFA can be useful in the analysis of extreme ocean waves. In particular, regional frequency analysis yields narrower uncertainty bounds and hence more robust estimation of extreme quantiles, corresponding to long return periods.

2.1   Long Term Measurements and Data

Long and reliable environment data is the first step for any climate characterization, extreme value analysis, ship design and coastal management. As it is the primary information in projects at sea, the reliability and accuracy of such data is crucial. Buoy and satellite measurements are preferred sources of data when compared to hindcasts but it must be properly quality controlled, organized and sufficiently long. The Centre ERS d'Archivage et de Traitement (CERSAT) of the French Research Institute for Exploitation of the Sea (IFREMER) is a center that continuously organizes, evaluates, quality controls and calibrates all the altimeter data public available, providing reliable netcdf output files easy to handle, which facilitates the use. They provided a public database with easy access at:

ftp://ftp.ifremer.fr/ifremer/cersat/products/swath/altimeters/waves/data

Queffeulou and Croizé-Fillon (2017) describe in detail the data and the methodology applied in the CERSAT/IFREMER satellite wave data processing and quality control. Regarding heave-pitch-roll buoys, CERSAT/IFREMER has also systematically organized and quality controlled the data joining a vast amount of buoys, which can be downloaded at:

ftp://eftp.ifremer.fr/globwave/insitu_final_format/oceansites/wave_sensor/

ftp://eftp.ifremer.fr/globwave/insitu_final_format/coriolis/wave_sensor/

The National Data Buoy Center has also provided quality controlled buoy data, public available and organized at the following site:

http://www.ndbc.noaa.gov/historical_data.shtml

The crossing information of in-situ buoy data with satellite tracks allows the cross-validation and calibration of datasets. Joining many sources of measurements, Young et al. (2017) performed a calibration and cross validation of global wind and wave database of altimeter, radiometer, and scatterometer measurements. A combined satellite dataset consisting of nine altimeter, 12 radiometer, and two scatterometer missions of wind speed and wave height is calibrated in a consistent manner against NDBC data and independently validated against a separate buoy dataset. Young et al. (2017) investigated the performance of each of the instruments at extreme values using quantile–quantile comparisons with buoy data. The various instruments were cross validated at matchup locations where satellite ground tracks cross. The resulting calibrated and cross-validated dataset from Young et al. (2017) is believed to represent the largest global oceanographic dataset of its type, which includes multiple instrument types calibrated in a similar fashion.

When measurements are not found or insufficiently long, the use of numerical modeling simulated for preterit conditions become important. Numerical hindcasting from surface winds provides essential space-time information to complement buoy and satellite observations for studies of the marine environment. Several reanalyses have been developed and evaluated, becoming nowadays a reasonably trustful source of information, especially in deep waters and open areas. The European Centre for Medium-Range Weather Forecasts (ECMWF) and the National Centers for Environmental Prediction (NCEP) are the main centers continuously generating reanalysis data. In terms of recent developments, ERA-20C is ECMWF's first atmospheric reanalysis of the 20th century, from 1900-2010. It assimilates observations of surface pressure and surface marine winds only, being an outcome of the ERA-CLIM project. Different from the previous reanalysis, ERA-20C is an extremely long source of data which allows deeper investigations on climate changes, projections of long-term events and site characterizations. Poli et al. (2016) describe the reanalysis which can be found at:

https://www.ecmwf.int/en/research/climate-reanalysis/era-20c

The main limitations of the reanalysis products are the simulations under extreme conditions and coastal areas, due to the resolution of the grids. Perez et al. (2017) recently developed a global wave hindcast for coastal applications, GOW2. This information is extremely useful for coastal studies and can be used both directly or as boundary conditions for regional and local downscalings. For developing the GOW2 hindcast, WAVEWATCH III wave model is used in a multigrid two-way nesting configuration from 1979 onwards. The multigrid includes a global grid of half degree spatial resolution, specific grids configured for the Arctic and the Antarctic polar areas, and a grid of higher resolution (about 25 km) for all the coastal locations at a depth shallower than 200 m. Available outputs include hourly sea state parameters (e.g. significant wave height, peak period, mean wave direction) and series of 3-h spectra at more than 40000 locations in coastal areas. Comparisons with instrumental data from Perez et al. (2017) show a clear improvement with respect to existing global hindcasts, especially in semi-enclosed basins and areas with a complex bathymetry. The effect of tropical cyclones is also well-captured thanks to the high resolution of the forcings and the wave model setup. Li et al. (2016) used WAVEWATCH III and SWAN models in a nested grid system to model basin-wide processes as well as high-resolution wave conditions around the Hawaiian Islands from 1979 to 2013. The wind forcing included the Climate Forecast System Reanalysis (CFSR) for the globe and down-scaled regional winds from the Weather Research and Forecasting (WRF) model. The hindcast of Li et al. (2016) captures heightened seas in interisland channels and around prominent headlands, but tends to overestimate the heights of approaching northwest swells and give lower estimates in sheltered areas. With the rapid increase of computational power, the reanalysis and hindcasts in the future tend to have higher resolution, more robust data assimilation, and better physics, which significantly improve the quality of data at coastal regions and under extreme conditions.

Using the wave model WAVEWATCH III, Beya et al. (2017) developed a calibrated hindcast for the coast of Chile. A correction method was applied to the statistical parameters in order to reduce systematic errors of the model. Beya et al. (2017) constructed an Atlas that showed better performance when compared to existing databases under normal wave conditions. They reported deficiencies in estimating of extreme values, which has important consequences in the design of coastal structures.

As an alternative to the use of traditional hindcasts based on numerical models, Jane et al. (2016) investigated the spatial dependence of the wave height at nearby locations applying a new copula-based approach for predicting the wave height at a given location. By working directly with wave heights, it provides an alternative method to hindcasting from observed or predicted wind fields when limited information on the wave climate at a particular location is

available. It is shown to provide predictions of a comparable accuracy to those given by existing numerical models.

Finally, the local knowledge at the coast can be additional important information to evaluate the sea level and wave climate, as discussed by Reineman et al. (2017). By examining the local knowledge of more than one thousand California surfers collected through an online survey, Reineman et al. (2017) extrapolates their evaluations to estimate the susceptibility of California surf-spots to sea level rise based on the principle of tidal extrapolation. Vulnerability classifications are derived from the relationship between wave quality, tide effects, and sea floor conditions.

2.2   Wave Climatology

A number of studies over the last decade have shown that over the last 30 years the ocean surface wind and wave climate has changed on global and regional scales. Although these reports are based on a number of different observational techniques, including ship observations and satellite data, all show a consistent positive trend over the last decades, with extreme values growing faster than the mean. Magnitude of the reported trends can be different, depending on the instrumentation used for observations (for example, global wind trends based on SSM/I radiometers are only half of those reported by altimeter measurements (Young et al., 2011a, b)).

Model hindcasts (reanalyses) did not show such consistency. There are two main third-generation wave models used for global applications, WAVEWATCH-III (American) and WAM (European). Long-term forecasts are available for both of them. Here, we will refer to Durant et al. (2014), which is a 30-year hindcast with WW3 (1979-2009), and Aarnes et al. (2015) reanalysis of the ERA-Interim hindcast with WAM for the period of 1979-2012. The latter was done for two stand-alone ECMWF (European Centre for Medium-range Weather Forecast) operational wave model (EC-WAM) runs with and without wave altimeter assimilation.

Durant et al. (2014) focusses on the Central and South Pacific, which is the main area of controversy with respect to the model hindcasts. Here, it can be noted that trends in the Southern Ocean throughout the full period are not reliable and, contrary to the observations, can be even negative. These are due to discontinuities in the CFSR wind data set used to force the wave model. The discontinuity is apparent around 1993/1994.

Trends in the ERA-Interim wind and wave data were investigated by Aarnes et al (2015). They found that in general the trends in this data set are affected by the introduction of assimilation of the altimeter wave height data in 1991. The authors note that the 48 hour forecast values (t=48), rather than the current analysis at t=0, may be more suitable for calculating the trends. This is because while the data assimilation generally has a large effect at t=0, this effect is somewhat reduced after a few days of model integration. The authors also note that their calculated wind and wave trends are somewhat different to those of Young et al (2011); in general they are smaller and do not show significant positive trends at high latitudes.

Thus, regardless of many details not mentioned here, we can point out two major problems with using the model reanalysis data for investigating weak long-term metocean trends. First, since the wave models are forced by outputs of the wind models, change of practice or tuning the winds may affect the predicted wave trends significantly or even adversely. Second, the introduction of assimilation of in situ and, particularly, satellite remote sensing data makes the model performance inconsistent throughout, particularly as the influence of data assimilation on the model outputs is ever-growing.

Therefore, the satellite observations, which are available for almost the same period as the longest modelling hindcasts, and provide global coverage (although not with the same spatial and temporal resolution), exceedingly become the main benchmark for metocean climate and

its trends. Young et al. (2017) proposed an extended work on the earlier altimeter analysis of wind-wave trends, by combining data of other satellite metocean platforms and by trying to reconcile the earlier discrepancies with radiometers.

The combined satellite dataset consists of nine altimeter, 12 radiometer, and two scatterometer missions of wind speed and wave height and is calibrated in a consistent manner against NDBC data and independently validated against a separate (ECMWF) buoy dataset. The various instruments are cross validated at matchup locations where satellite ground tracks cross. The resulting calibrated and cross-validated dataset is believed to represent the largest global oceanographic dataset of its type, which includes multiple instrument types calibrated in a similar fashion. This work provides satellite calibrations against buoys for all the missions mentioned. Careful analysis of the methods for recovering the wind speed allowed bringing altimeter and radiometer/scatterometer wind trends much closer to each other. It worth noticing here that both systems have a fair weather bias at wind speeds exceeding 20 m/s and hence the extreme wind speeds may be underestimated.

In 2011, Chinese altimeter mission Hai-Yung-2 was launched. Liu et al. (2016) found wave-height trends similar to the other altimeter missions, but wind-speed measurements are not calibrated at this stage.

2.3   *Climate Trends and Uncertainty*

Ocean waves and surface winds significantly affect coastal structures and offshore activities and impact many vulnerable populations of low-lying islands. Therefore, better understanding of their variability plays an important role in potentially reducing risk in such regions. With the increase of in-situ and remotely-sensed data, as well as reanalysis products, the study of climate trends and intrinsic uncertainties has improved in the recent years. Ulbrich et al. (2009) performed a fundamental study on extra-tropical cyclones in the present and future climate. Based on the availability of hemispheric gridded data sets from observations, analysis and global climate models, objective cyclone identification methods were developed and applied. Thus, Ulbrich et al. (2009) give a comprehensive review of the actual knowledge on climatologies of mid-latitude cyclones for the Northern and Southern Hemisphere for the present climate and for its possible changes under anthropogenic climate conditions. In the Northern Hemisphere, Ulbrich et al. (2009) describe that under anthropogenic climate change (ACC) conditions, the number of all cyclones will be reduced in winter, but in specific regions (over the Northeast Atlantic and British Isles, and in the North Pacific) the number of intense cyclones increases in most models. For the average over the hemisphere, an increase in the number of extreme cyclones is found only when "extreme" is defined in terms of core pressure, while there is a decrease in several models when defining "extreme" from the Laplacian of surface pressure or vorticity around the core. In the Southern Hemisphere, Ulbrich et al. (2009) describe that under ACC conditions a southward shift of this band is identified, more or less meridional equally distributed. This will lead to less cyclonic activity around 50°S and increased activity around 60°S. Results of Ulbrich et al. (2009) are in agreement with IPCC AR4 report stating that "*the most consistent results from the majority of the current generation of models show, for a future warmer climate, a poleward shift of storm tracks in both hemispheres that is particularly evident in the SH, with greater storm activity at higher latitudes.*"

Kumar et al. (2016) investigated the influence of climate variability on extreme ocean surface wave heights using ECMWF reanalysis. In this study, global impacts of natural climate variability such as El Niño–Southern Oscillation (ENSO), North Atlantic Oscillation (NAO), and Pacific decadal oscillation (PDO) on extreme significant wave height (SWH) were analyzed using ERA-Interim (1980–2014) and ECMWF twentieth-century reanalysis (ERA-20C; 1952–2010) datasets. The major ENSO influence on Hmax is found over the northeastern North Pacific (NP), with increases during El Niño and decreases during La Niña, and its coun-

ter responses are observed in coastal regions of the western NP. Composite analysis of different ENSO and PDO phase combinations reveals stronger (weaker) influences when both variability modes are of the same (opposite) phase. Overall, Kumar et al. (2016) found that the response of extreme significant wave heights to natural climate variability modes is consistent with seasonal mean responses.

Focused on coastal areas, Barnard et al. (2015) synthesized multi-decadal, co-located data assimilated between 1979 and 2012 that describe wave climate, local water levels and coastal change for 48 beaches throughout the Pacific Ocean basin. They found that observed coastal erosion across the Pacific varies most closely with El Niño/Southern Oscillation, with a smaller influence from the Southern Annular Mode and the Pacific North American pattern. Barnard et al. (2015) concluded that, if projections for an increasing frequency of extreme El Niño and La Niña events over the twenty-first century are confirmed, then populated regions on opposite sides of the Pacific Ocean basin could be alternately exposed to extreme coastal erosion and flooding, independent of sea-level rise.

Important studies were published concerning the prediction of possible climate trends. Martínez-Asensio et al. (2016) studied the ability of statistical wind-wave models to capture the variability and long-term trends of the North Atlantic winter wave climate. Stefanakos and Vanem (2017) obtained very good results of climatic forecasting of wind and waves using fuzzy inference systems. Stefanakos and Vanem (2017) models are coupled with a nonstationary time series modelling, which decomposes the initial time series into a seasonal mean value and a residual part multiplied by a seasonal standard deviation. Two long-term datasets for an area in the North Atlantic Ocean were used, namely NORA10 (57 years) and ExWaCli (30 years in the present and 30 years in the future). Muraleedharan et al. (2016) investigated regression quantile models for estimating trends in extreme significant wave heights in two Portuguese locations, using 44 years hindcast produced in the HIPOCAS project. The regression quantile models of Muraleedharan et al. (2016) showed the ability to model the historical trends that may subsist in long term data sets, a feature that the traditional fitting of extreme distributions does not account for. Hithin et al. (2015) studied trends of wave height and period in the Central Arabian Sea using satellite altimeter data from 1996 to 2012. Hithin et al. (2015) showed a positive trend of 0.63 cm/yr in the annual mean significant wave height. In contrast, a negative trend of 2.66 cm/yr is found for the annual maximum significant wave height due to the decreasing trend of extreme tropical cyclone events. The annual mean and maximum wave period show a decrease of 0.005 s/yr and 0.011 s/yr, respectively.

2.4   More measurement in extreme conditions

Extreme meteorological and oceanographic (metocean) conditions are essentially air-wave-sea interaction phenomena. To describe, simulate and predict the extreme storms, both tropical and extra-tropical, often extrapolations from moderate conditions are used, but physics of air-sea interactions, wave dynamics, atmospheric boundary layer (BL), upper ocean currents and mixing, are very different in extreme weather conditions (see e.g. Babanin (2011) for a review).

In the atmosphere, the effect of sea-drag saturation was confirmed in field and laboratory observations where the critical wind speed at 10 m reference height U10 was found as

$$U_{10} = 32\text{-}33 \text{ ms}^{-1} \tag{1}$$

Physics of the drag saturation, i.e. of change of the dynamic regime of the atmospheric boundary layer, is complex and at this stage not clear. The ocean surface at hurricane winds, even visually, enters a different dynamic regime, with sporadic whitecaps replaced by surface where the foam extends from crest to crest and interface becomes hazy. Wave asymmetry saturates at wind speeds of

$$U_{10} \approx 34 \text{ ms}^{-1} \tag{2}$$

which signifies change of the mechanism for wave breaking: from the breaking being driven by nonlinear evolution of steep water waves to the breaking being caused by the direct wind action. Subtle by comparison are changes of the dynamic regime in the upper ocean at extreme conditions and of the air-sea gas exchanges, but they do occur and occur at approximately the same threshold wind speeds: the fluxes still grow rapidly, but in relative terms at a much lower rate by comparison with the moderately strong winds. Furthermore, bubble injection becomes the dominant mode of gas transfer. Change of regime of the air-sea gas transfer is observed at

$$U_{10} > 35 \text{ ms}^{-1} \tag{3}$$

Thus, the general consensus in the community is that wind speeds in the range of 30-40 ms^{-1} signify a regime change. This means that extrapolations of measurements, dependences and mechanisms obtained in benign and moderately strong conditions should be re-validated and used with extreme caution when applied to tropical cyclones and perhaps extreme extratropical storms too. It is likely that these mechanisms, and therefore the respective dependences, are different, and are yet to be explicitly obtained, described and parameterized.

Progress of in situ observations is vital for extreme-weather science, because of uncertainty of some estimates, for example, source functions for spray production, can be many orders of magnitude. On the atmospheric side, structure and composition of the boundary layer close to the surface needs to be understood. This requires measurements of wind profiles in the constant-flux layer (up to 100-200 m above the surface) and preferably within the wave boundary layer (10-20 m), which is the sublayer with its specific dynamics due to spray and wave-coherent pressure/velocity oscillations (Babanin and McConochie, 2013).

Most of the fluxes are created, moderated or facilitated by the waves on the ocean interface. Therefore, accurate measurements of waves, including their full frequency-wavenumber directional spectra are necessary. Among the wave measurements, significance of wave breaking in formation of the fluxes is hard to overstate. Near-surface turbulence, both on the oceanic and atmospheric sides, radiation stresses, injections of air bubbles into the water, which facilitate gas exchanges, and emission of spray into the air, which accelerates evaporation, disruption of the skin layer and hence intensification of the heat transport - these and other dynamic and thermodynamic features and small-scale processes between the atmosphere and the ocean owe their rates and very existence to the wave breaking. Stereo-imaging, particularly high-speed and high-resolution video recording can provide detailed information of the three-dimensional surface behaviors of this kind (Fedele et al., 2013).

Measurements below the ocean surface may hold the key to the coupled physics of tropical cyclones. Traditionally hurricanes are treated as a meteorological phenomenon, and because of formidable logistical difficulties, ocean response to the hurricane forcing is very rarely measured. To stress that these are not ordinary oceanographic deployments, it has to be understood that significant wave heights in the hurricanes can be in excess of 10 m, and hence, such measurements have to be effectively done within the wave crests, by devices which either tolerate or avoid crossing the air-sea interface. Use of surface following platforms, such as wave gliders, shows a promise in this regard, even in tropical-cyclone conditions (Lenain and Melville, 2014).

3. WAVES & SWELL

3.1 Measurements / Data

3.1.1 Deterministic wave generation in the laboratory

There has been a considerable interest in the precise generation of waves in the laboratory. This concerned mainly very large steep waves that have been used for extreme load cases. Rather than generating very long wave trains and considering the extremes for analysis, a special short wave train with one or a small number of interesting extreme waves is generated on a specified position in the basin. There are several types of these so-called deterministic waves:

- Focusing waves and single wave events: A focusing wave is defined as a superposition of two-dimensional waves consisting of subsequent wave frequencies with increasing propagation speeds, in such a way that all components meet in time and space at the "focusing point".
- Deterministic wave sequences in a sea state: For a given design spectrum of a unidirectional wave train, the phase spectrum contributes to all local characteristics. The most unfavourable event under storm conditions is the in-phase superposition of component waves in the seaway. Randomly, the time series may contain a dangerous wave sequence, a coincidence which would require a much extended test duration. Applying the transient wave technique, a single wave event can be integrated in a random sea deterministically.
- Wave tank realization of observed wave records: Some interesting wave events are reported and registered from field measurements. Depending on water depth and ability of the wave maker, it is possible to generate them in a model basin.

The state of the art methods to generate and calibrate deterministic wave sequences has been described by Schmittner et al. (2014). The most used way to generate an extreme wave is by superposing different frequency components at a specified focal location as introduced by Rapp and Melville, (1990); Clauss, (2002) and Ma et al., (2010). The motions of the wave maker are determined by transforming the desired wave from the focal point backwards to the position of the wave maker. In most cases linear theory is used which often leads to a non-focused wave mainly due to nonlinear effects (Liu et al., 2016). The phase of each wave component should be corrected depending on its steepness (Fernández et al., 2014). Alternatively, non-linear wave models can be used (Duz et al., 2016), but this usually calls for an iterative solution since calculations backwards in time are normally impossible.

A special type of "rogue" or "freak" wave is the so-called breather-solution of the non-linear Schrödinger equations. This wave evolves from a modulation instability known as Benjamin-Freir or Bespalov-Talanov instability. Although it initially appeared to be just a theoretical possibility, these types of freak wave are successfully generated in the wave basin (Chabchoub et al., 2011, 2013, 2016). In the experiment, the localization of the wave energy in both space and time was confirmed. The measured surface elevation agreed quite well with the theoretical solution, the maximum amplification of the carrier wave was close to 3, which is the theoretical value predicted by the NLS equation . This type of wave has recently attracted much attention (Osborne and Ponce de León, 2017); it has been proposed as a prototype of ocean rogue waves due to its intense localization and because it seems to appear from nowhere and disappear without a trace. This latter characteristic has been reported for many known rogue wave events. Shemer and Alperovich (2013) also conducted an experiment to investigate the evolution of the Peregrine breather. The experimental results were compared to the numerical simulations based on the NLS and the Dysthe equations. The comparison indicated that the Dysthe equation can predict the evolution of the Peregrine breather better than

NLS. It was found that, with identical initial conditions, the Dysthe equation yields a lower increase rate of the envelope than predicted by NLS, resulting in a maximum amplification is lower than 3 and a location of the extreme wave crest far away from the one predicted by the NLS equation.

Onorato et al. (2013) conducted experiments to study the interaction between extreme waves, which were generated by a Peregrine breather solution. The devastating effect of such an extreme wave on a model of a 90 m chemical tanker was discussed. Unlike previous experiments conducted in deep water, these extreme waves were generated in a finite water depth to reproduce extreme conditions in the North Sea, such as the Draupner wave.

Deng et al. (2015) conducted an experiment on the evolution of the Peregrine breather in a wave flume with water depth kh = 5.65. They produced a maximum wave crest 2.86 times the initial wave height at a distance of 7 wave lengths from the wave generator. The surface elevation of the extreme did not exactly follow the theoretical shape; this was attributed to imperfections of the wave generation by a flap. The extreme wave was used to study the force on a vertical circular cylinder; the measured force appeared to correlate to the numerical predictions.

The important role played by rogue waves on structural loading of ships and offshore structures is discussed in the DNV-GL position paper (Bitner-Gregersen and Gramstad, 2015). This document reviews several research activities of DNV-GL and discusses generation mechanisms of rogue waves, their probability of occurrence, warning criteria and possible consequences.

Ken Takagi et al. (2017) derived a formulation for wave prediction using multipoint measured data for short crested waves. The formulation can be applied for both stationary process and non-stationary process. Based on this formulation, a convolution integral formula which represents the relation of free surface elevation between multipoint measurement and target point prediction is obtained. Through validation, the method is applicable to the wave warning system in short crested waves.

P.R. Shanas et al. (2017) measured waves in the Red Sea from a buoy located in the central Red Sea in order to show the presence of multi-directional waves. Superimposition occurs that leads to an increase in significant wave height and decrease in mean wave period on a diurnal cycle. Monthly features of superimposed waves have been analysed based on a correlation analysis. The analysis has been further extended to the entire Red Sea by implementing a third generation spectral wave model, WAVEWATCH III. Monthly and spatial variability of the superimposed and non-superimposed have been discussed. The waves at 58% area of the Red Sea are dominated by unidirectional waves, while the 28% area is dominated by superimposed waves and 14% area has nearly the same contribution of two wave systems.

Nagi Abdussamie et al. (2017) conducted model tests to investigate the global responses of a conventional tension leg platform (TLP) due to wave-in-deck loads associated with extreme wave events in irregular long-crested waves of a cyclonic sea state. The obtained results demonstrated the variability of all the measurements and provided insights into the effect of wave-in-deck loads on the platform behavior, tendon tensions and slamming pressures and showed qualitative correlations between these parameters.

Victor A. Godoi et al. (2017) presented a detailed climatology of extreme wave events for New Zealand waters, in addition to estimates of significant wave height (Hs) for up to a 100-year-return period. Extreme events were explored using 44 years (1958-2001) of wave hindcast data. Results indicate some similarities to patterns previously shown in the mean wave climate, with the largest waves found in southern New Zealand, and the smallest ones observed in areas sheltered from southwesterly swells.

Michael Banks et al. (2017) report this paper on results of an experimental investigation into the interaction between unidirectional waves and a horizontally moored semisubmersible model. The magnitudes of heave and pitch motions of the model were found to increase as the wave steepness increased.

3.1.2   Measurement and analysis

Stansberg et al. (2009), give an overview of different methods to measure waves in the laboratory. Different systems for point measurements were compared in a side-by-side experiment in a wave basin; the systems consisted of intrusive (the capacitive and resistive wave probes) and non-intrusive (the servo and acoustic wave probes) sensors. The results indicate the following uncertainties (u95) for the different sensors:

- Capacitive probes: 1.8 mm
- Resistive probes: 1.5 mm
- Servo probe: 2.0 mm
- Acoustic probes: 1.0 mm

Stansberg et al. recognize that the challenge is in spatial/temporal measurements. It is practically impossible to put many sensors in a small area; apart from physical aspects there is also the danger of electronic interference. An array of separate sensors at a distance of typically half the wave length of interest is being used to measure 3D wave spectra. Naaijen et al., (2009) used an array of 10*10 sensors; Hennig et al., (2015) used a relatively small device having 6 sensors arranged on a circle and a 7th sensor in the center for short-crested waves.

Stansberg et al. (2009) also describe optical systems using stereo cameras above the wave surface. These systems have been successfully used in outdoor conditions, but suffer from reflection and lighting problems in laboratory conditions. Another option is to generate a laser sheet that illuminates a line on the water surface over a distance of 2 – 2.5 m. This line is then recorded by a single camera.

Stansberg et al. present an update of their 2009 investigation in 2011 (Stansberg et al. 2011). The focus is on the measurement of a 3D wave surface. Essentially the same sensors and the analysis of the signals are being reviewed. All sensors are in use in at least one of the major European towing tanks, but it is apparent that there is not a clear optimum solution for a given problem. Much depends on local conditions like water depth and lighting, if stationary measurements or measurements at speed are required and if long-crested waves from one direction are to be measured or short-crested waves from a range of directions.

Richon et al. (2009) presented the development of system using a laser pointing vertically downwards to the water surface and a camera to record the intersection point. The accuracy of this system was claimed to be better than ± 1 mm. Day et al. (2011) used a similar system, but used low cost components. He published results of wave measurements using a traditional wave probe, an acoustical probe and the laser system. The first two appeared to give very similar readings while the laser system showed mainly higher wave crests and deeper wave troughs to a lesser extent, Figure 1
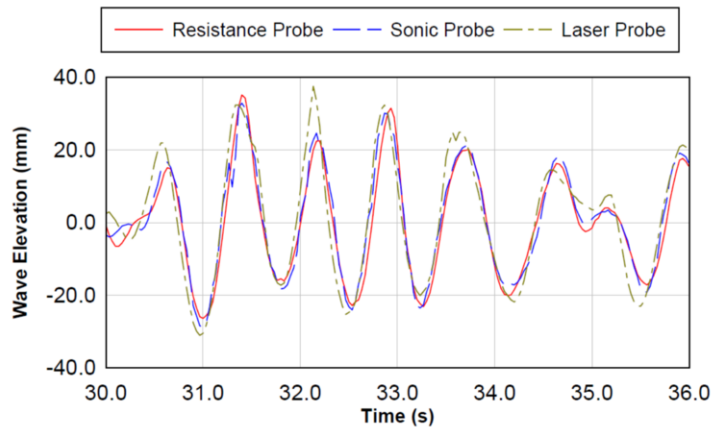
Figure 1: Wave measurement by 3 different sensors: classical resistance probe, acoustical (sonic) probe and a laser point measurement (from Day et al. 2011).

Gomit et al., (2013) describe two systems, the first consisting of stereo cameras measuring the free surface and the second of a combined laser system and one camera below and two other cameras above the wave surface. The first system uses floating particles on the free surface to correlate the images from the two cameras. Since the particles are moved sideways by the passing model, it is not useful to measure the wave pattern in the wake of the model. The second system uses particles floating in the fluid. These particles are illuminated by a laser sheet parallel to the free surface. The position of the particles is then recorded by one camera on the bottom of the basin and two cameras above the water surface. The wave elevation is determined by comparing the undistorted image from below to the distorted (due to refraction) image from above. Since this measurement is done on a fixed position in the basin, it can only be used to measure a stationary wave field.

When a model of a ship at speed is tested in waves, it is of interest to measure the wave just in front of the model. The classical wave probe has some problems due to run-up at the front and ventilation at the back of the wires. Although the errors are not very large, there is a drive to use non-intrusive sensors. An acoustical sensor is one option; the development of a practical system is published by Bouvy et al. (2009). For the problem of a measurement at speed a system above water is required; this system suffers from spikes and/or gaps in the signal when the reflected pulse is not received by the sensor. This problem is solved by reconstructing the signal in the sensor so that a smooth output is achieved. Alternative methods are being discussed by Perelman et al. (2011). They compare results from a single ultrasonic probe to results from the measurement of a line on the wave surface illuminated by a laser sheet from the bottom of the basin and results from a stereo imaging technique. In general, the two measurements agree very well, see Figure 2. For some conditions there is a problem with the signal from because the signal of the ultra-sonic probe is quite noisy, while there is a drop-out in the measurement of the deepest wave trough. The laser sheet measurement suffers from reflection problems although the measurement for the most important area is fine. There is some difference in the measurement of the wave crests in that the wave crest can be quite undefined when it is just overturning and when there are air inclusions. The laser sheet gives a very bright reflection from an air inclusion, so in this case it tends to measure the lower side of the air inclusion while the ultra-sonic probe, measuring from above, tends to measure the upper surface.
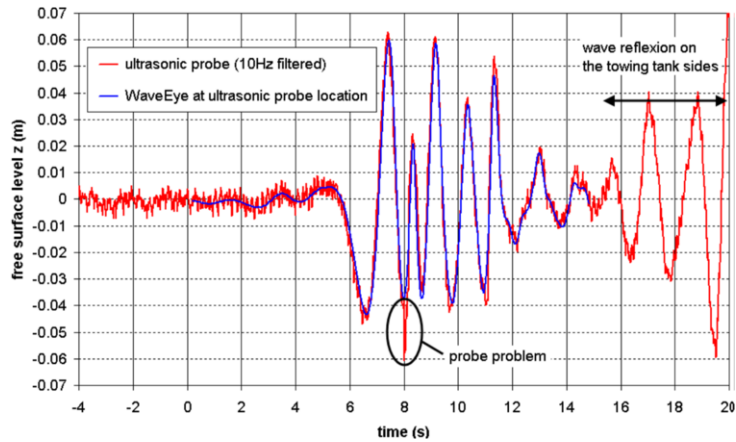
Figure 2: Measurement of a stationary wave field by a single ultra-sonic probe and by a system of 5 video cameras measuring a line on the surface that is illuminated by a laser sheet generated on the bottom of the basin (from Perelman et al. 2011).

3.1.3   Particle Image Velocimetry

Minnick et al. (2010) carried out the experiment employed Particle Image Velocimetry (PIV) techniques to obtain a data set of the vector field below the free surface for regular waves of varying steepness and realizations of irregular seaways both with and without embedded wave groups of large amplitude. In addition to the crest elevation the associated water particle velocities determine the magnitude of the impact load to a large extent. Especially in breaking waves the horizontal particle velocities can become extremely high and difficult to predict by commonly used methods for estimating wave kinematics. Lindeboom and Scharnke (2016) present Particle Image Velocimetry (PIV) measurements to capture the kinematics of different types of near breaking and breaking waves. A difficult problem appeared to be to have sufficient particles in the crest of the wave. A point of consideration is that many repeat tests and repeat measurements are necessary for a reliable (low uncertainty) measurement. Lindeboom and Scharnke used 20 repeat tests, but they concluded that this was insufficient. Nevertheless, their results correlate very well to results from CFD calculations as shown by Duz et al. (2016), Figure 3.
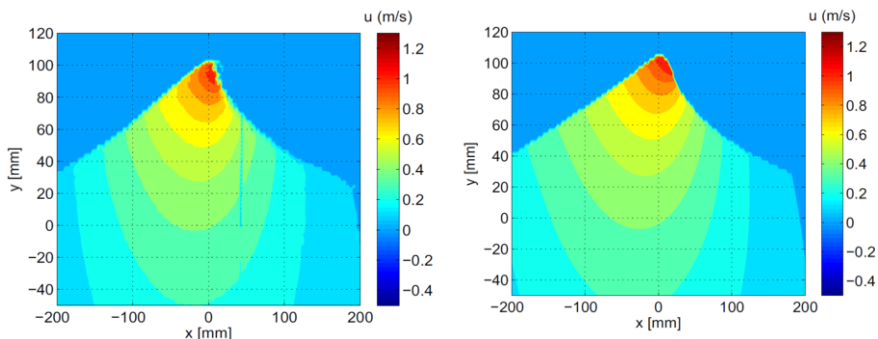
Figure 3: Horizontal velocity in a wave crest. Left: measured velocity using PIV techniques; Right: Velocity as calculated by CFD.(from Duz et al. 2016).

3.2   *Rogue Waves*

Rogue waves, commonly also referred to as freak waves, are waves that are much larger than what is expected for a given sea state, based on averaged properties of this sea state - typically the significant wave height Hs. A recent review on rogue waves and different mechanisms that are suspected to generate such waves can be found in Adcock and Taylor (2014). Another recent review with focus on rogue waves and their impact on ships and offshore structures is given in Bitner-Gregersen and Gramstad (2015).

There is still no consensus on a single unique definition of a rogue wave, but the most common approach is to define a rogue wave as a wave whose wave height or crest height exceeds some thresholds related to Hs. Various criteria exist, but a common definition is

$$\frac{H}{H_s} < 2 \text{ and/or } \frac{C}{H_s} < 1.25,$$

where H and C are the (zero-crossing) wave height and crest height of an individual wave, as illustrated in Figure 4. The significant wave height Hs is typically measured from a 20-minute time series in which the wave was recorded.
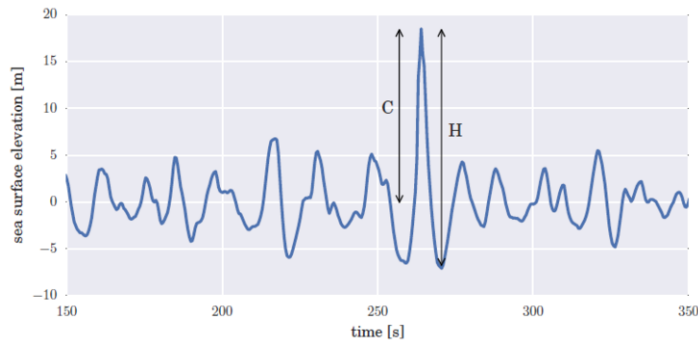
Figure 4: Illustration of wave height and crest height as used in the common definition of a freak wave. From Bitner-Gregersen and Gramstad (2015).

Given such a definition one can quite easily estimate the probability of such waves occurring, for example according to linear or second-order theory, see e.g. Bitner-Gregersen and Gramstad (2015).

Of course, also other properties of large waves may be of interest, for example the typical shape of a rogue wave or the characteristics of the wave group in which a rogue wave is observed. Gemmrich and Thomson (2017) studied surface elevation records from two locations in the northeast Pacific and investigated the properties of the recorded rogue-waves with respect to the characteristics of the wave groups. They also looked at the unexpectedness of the waves defining a rogue and unexpected wave as a wave that in addition to satisfying the criteria above, also is much larger (e.g. more than two times larger) than a given number of surrounding waves, and therefore in a sense is unexpected for a casual observer. This criterion was also studied theoretically by Fedele (2016), deriving some expressions for the probability of occurrence of unexpected waves. Naturally, waves that are both rogue and unexpected have a lower occurrence frequency than just being rogue.

Traditionally, a topic that has received much focus in the context of rogue waves is the effect of modulational instability. Modulational instability is a well-known nonlinear process that is present in water waves, as well as in other many other systems of nonlinear and dispersive waves. Modulational instability has the effect that different wave components in a spectrum can exchange energy through so-called nonlinear near-resonant four-wave interactions. Naturally, this effect is not described by the standard linear or second-order wave models, and there has therefore been some focus on nonlinear wave models in this respect, see also Section 3.3.2, and Onorato and Suret (2016) for a recent review. Typically, the modulational instability is studied through the framework of the Nonlinear Schrödinger (NLS) equation. An approach based on the NLS framework is the so-called nonlinear Fourier-transform (Osborne, 2010) that gives some insight into to effect of modulational instability. It has been suggested that this methodology can be applied to ocean engineering applications (Jeans et al., 2017, Osborne and Leon, 2017, Yim et al., 2017). Using a phase averaged framework - the Alber equation - the modulational instability in real ocean conditions was studied by Gramstad (2017), who showed that the spectral width at the base of the spectrum is more relevant than the width of the peak when it comes to predicting the importance of modulational instability in a sea state. It should also be mentioned that there has been a lot of interest lately on the presence of rogue waves also in other fields of physics, and on the fact that that this phenomenon is really multidisciplinary (Residori et al., 2017).

As discussed in Section 3.3.2, the effect of modulational instability is described by the Nonlinear Schrödinger-type equations for water waves, in terms of its so-called breather solutions. In recent years, there has been an increasing interest in these analytical solutions both from a theoretical point of view and from a more practical point of view as a prototype for oceanic rogue waves and with ocean engineering applications in mind (Onorato et al., 2013). It has been shown in several experimental studies that these solutions can quite well be reproduced in experimental wave-tank facilities by carefully controlling the condition at the wave-maker (e.g. Chabchoub et al., 2011). Also various properties of these solutions in experimental conditions have been investigated. Peric et al. (2014) studied the breaking dynamics of a breather-type rogue wave experimentally and numerically. Chabchoub (2016) showed that the evolution of a Peregrine breather survived and could be tracked also when superposed on top of a random JONSWAP background spectrum. It has been suggested that such breather solutions (e.g. the Peregrine breather) could be used as a "design wave" for studying the effect of large waves on ships and other marine structures, e.g. in sea-keeping tests (Onorato et al., 2013, Klein et al., 2016). This approach of using the breather solutions to study wave-structure interactions was for example recently used to study slamming for a chemical tanker advancing in extreme waves (Wang et al., 2016) and the structural response of deck structures from events caused by rogue waves (Qin et al., 2017a, Qin et al., 2017b).

Although there during the last two decades has been much focus on the effects related to modulational instability in the context of rogue waves, there has also been an increasing concern whether such dynamics are relevant for realistic ocean conditions. It is very well documented that modulational instability effects are relevant also for irregular random waves if the sea state is sufficiently narrow banded and sufficiently long-crested (e.g. Gramstad and Trulsen, 2007, Onorato et al., 2009). However, one may argue that very few realistic ocean spectra are sufficiently narrow and unidirectional for modulational instability to be an important effect. Based on this some authors have the view that the most important generation mechanism for the generation of oceanic rogue waves is simply spatio-temporal focusing due to the dispersive nature of water waves, enhanced by second-order non-resonant nonlinearities - also referred to as constructive interference or linear focusing (e.g. Fedele, 2015, Fedele et al., 2016). This view is also supported by some recent studies (Christou and Ewans, 2014, Fedele et al., 2016, Benetazzo et al., 2017) that through analysis of field data show that the occurrence of rogue waves in their data does not exceed linear wave theory enhanced with second-order nonlinear corrections - i.e. second-order wave theory. On the other hand, other

studies have shown that enhanced rogue wave occurrence in the ocean is observed more often in sea states with narrow directional wave spectra (Waseda et al., 2011), consistent with the physical mechanism of modulational instability.

In another recent paper, Donelan and Magnusson (2017) carried out directional analyses on the well-known rogue wave Andrea, recorded at the Ekofisk platform in the North-Sea. They argued that the generation of this wave could be explained simply by constructive interference. Based on their analysis Donelan and Magnusson (2017) also suggested that the breaking-limited maximum crest height of a rogue waves is C/Hs=1.7, where C denote the crest height.

Another recent focus in the research on rogue waves is the importance of considering rogue waves as space-time maxima of the sea-surface. Naturally, most recordings of the sea surface, for example from wave buoys, wave probes, etc. measure the surface in a single point. However, such measurements may greatly underestimate (especially in short-crested seas) the actual maximum wave displacements that can occur on sea surface areas even smaller than the wave characteristics dimensions, namely, the wavelength and the crest length (Benetazzo et al., 2015). Hence, the probability that a marine structure (which always has a footprint larger than zero) encountering a rogue wave is significantly larger than the probability of observing a rogue wave in a time series recorded in a single point. This is illustrated in Figure 5 which shows the theoretical probability density function of spatial-temporal (ST) extreme second-order nonlinear crest heights in five different ST regions considered by Benetazzo et al. (2017) using stereo wave imaging systems that measure the sea surface over a large spatial region.
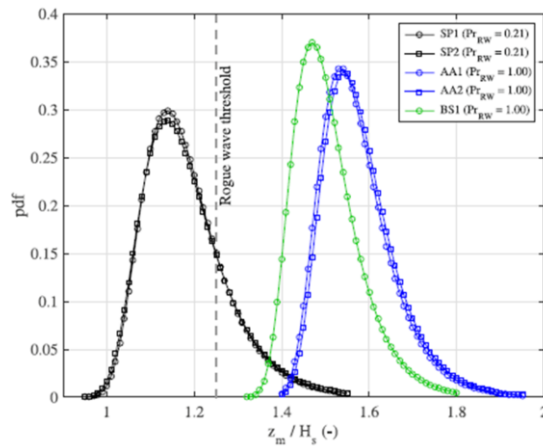
Figure 5: Theoretical probability density function (pdf) of spatial-temporal (ST) extreme second-order nonlinear crest heights in five different ST regions. In the legend, PrRW = Pr(max[z(x, y, t)] > 1.25Hs | (x, y) ∈ Ω, t ∈ D) is the probability that the maxim

Another situation that has been suggested to be associated with higher occurrence probability of rogue waves is crossing sea states. Theoretically, this is based on properties of the coupled Nonlinear Schrödinger equations that predict some amplification of the modulational instability for two Stokes waves propagating with an oblique angle of about 50 degrees (Onorato et al., 2006). An increase in occurrence probability of rogue waves in crossing sea states has also been shown in numerical simulations using HOSM (Toffoli et al., 2011), although for quite special type of crossing seas, namely two directionally narrow identical wave spectra with the same energy and same peak frequency. Trulsen et al. (2015) investigated the crossing sea

state associated with the sinking of the oil-tanker Prestige in 2002, and found no evidence for increased occurrence of rogue waves. In this case, however, the two wave systems had a crossing angle of about 90 degrees, a situation where the NLS theory does not predict any enhancement of the modulational instability. Fedele et al. (2016) also discussed the possible effect of crossing sea in the case of the Draupner wave and carried out HOSM simulations for different crossing angles, concluding that in any case the second-order effects were dominant and third-order contributions on skewness and kurtosis were negligible.

Based on some recent results it has also been suggested that rogue waves may occur as a result of a wave field being brought out of equilibrium, for example by changing bottom bathymetry or currents (Onorato and Suret, 2016, Trulsen, 2017). Thus, this is suggested to be an effect of nonlinear dynamics, but not directly attributed to the effect of modulational instability. Such effects was recently studied numerically by Ducrozet and Gouin (2017), who studied waves propagating over variable bathymetry. Consistent with previous numerical and experimental results they found increased occurrence of rogue waves on the shallower side of a slope when the waves were propagating from deeper to shallower depths. They found, however, that this effect was weakened when considering directionally spread wave fields.

Murray Rudman et al. (2016) applied Smoothed Particle Hydrodynamics to model rogue wave impact on a semi-submersible platform with a focus on the effect that different mooring systems have on platform motion and mooring tension. The results show that a hybrid of the Tension Leg Platform and Taut Spread Mooring systems could have advantages over non-hybrid systems.

Zhe Hu et al. (2015) proposed a combined wave-dam-breaking (CWDB) model in this paper. This model is deduced from the Ritter's solution, by including the influence of the rogue wave propagation as well as the delayed effect of the dam-breaking problem. The CWDB model is validated by making comparisons with both numerical results and existing experimental measurements.

Zhe Hu et al. (2017) simulated the nonlinear rogue-wave overtopping phenomenon in a numerical wave tank in this paper. The simulation results are compared against the theoretical solution predicted by the dam-breaking model. Hydroelastic effects are considered by applying a fully-coupled fluid-structure interaction model.

3.3   Analytical & Numerical Models

Struthi et al. (2017) used an improvised methodology to estimate impact forces on a jacket structure and proposed a slamming coefficient for the structure. The slamming coefficient estimated in this study was in agreement with the theoretical formulas and existing literature. The result shows that the slamming coefficient should be found exclusively for structure configurations rather than using slamming coefficient used for a single cylinder.

Hao Qin et al. (2017) used a 2-D numerical wave flume to generate freak wave. A simplified method is proposed to approximate the deck-house wall as an Euler beam with intermediate elastic bearings. The fluid-structure interaction is considered by applying an implicit iterative algorithm. By comparing the crest shapes and the impact forces of the nonlinear freak wave and a regular wave with the same wave length and height, it is seen that the impact caused by the nonlinear freak wave is more severe.

Chengdi Wang et al. (2017) develop a new significant wave height (Hs) and dominant wave period (Tp) scheme (termed as WHP) for open oceans, using 15 years of hourly observational wind-wave data from eight buoys off the northwest coast of the United States (US). Comparison results show that the WHP scheme gives an almost best performance in predicting Hs and Tp for the open oceans across different regions.

'Jorge Perez et al. (2017) presented the GOW2 database, along-term wave hindcast covering the world coastline with improved resolution in coastal areas and along ocean islands. For developing the GOW2 hindcast, WAVEWATCH III wave model is used in a multigrid two-way nesting configuration from 1979 onwards. Comparisons with instrumental data show an improvement with respect to existing global hindcasts, especially in semi-enclosed basins and areas with a complex bathymetry.

3.3.1   Spectral

Wave modelling efforts and applications can be broadly classified into two large groups: phase resolving (or direct) models (see Section below) and phase average (usually spectral) models – subject of this Section. Direct models can explicitly simulate basic equations of fluid mechanics, but at oceanic scales such models are not practical or even feasible, and therefore spectral models are employed for wind-wave forecast. These are based on parametric, often speculative approaches, but their physics has been advancing lately (see e.g. Rogers et al., 2012, Zieger et al., 2015, Stopa et al., 2016, Babanin et al., 2017).

Evolution of wind-generated waves can be described by the wave action $N=F/\omega$ balance equation

$$\frac{\partial N}{\partial t} + \nabla \cdot [(\mathbf{c}_g + \mathbf{U})N] + \nabla_\mathbf{k} \cdot [\mathbf{c_k}N] = \frac{I + L + D + B}{\omega} \tag{4}$$

where $F(\omega,\mathbf{k})$ is wave energy density spectrum, ω is intrinsic (from the frame of reference relative to any local current) radian frequency, $\mathbf{k}$ is wavenumber (bold symbols signify vector properties). In linear case, temporal and spatial scales of the waves are linked through the dispersion relationship

$$\omega^2 = gk \cdot \tanh(kd) \tag{5}$$

where g is the gravitational constant, d is water depth. The left-hand side of (4) represents time/space evolution of the wave action density as a result of the energy source terms on the right. Here, $\mathbf{c}_g$ is group velocity, $\mathbf{c_k}$ means the spectral advection velocity, $\mathbf{U}$ is the current speed. ∇ here is the horizontal divergence operator, and $\nabla_\mathbf{k}$ is such operator in spectral space.

On the right, source terms are phenomenologically represented by atmospheric energy input from the wind, I; nonlinear interactions of various orders within the wave spectrum, L, whose role is to redistribute the energy within the spectrum; dissipation energy sinks, D; wave-bottom interaction processes, B; and more sources are possible in specific circumstances. Note that all the source terms, as well as the group and advection velocities and the advection current are spectra themselves. L is a conservative term, i.e. its integral is zero, but the other integrals define energy fluxes in and out the wave system (see Babanin et al. (2017) for more details).

Ideas of predicting the wave spectrum can be traced back to the 50s, and but only since the 90s the technical developments of computing facilities made the modern third-generation models practical in the context of the global wave forecast and hindcast. Global applications, however, come at a cost, and not only computational. In finite-depth and shallow environments, waves essentially become a different physical object. Dispersion is reduced or even ceases, nonlinearity grows, but active nonlinear mechanisms change, balance between energy input and dissipation is no longer maintained, and a variety of new physical processes come into existence because of various wave-bottom interactions and sediment response. Respective wave models are notable for a lesser degree of physics and larger degree of parametric and ad hoc tuning.

In this regard, resent NOPP effort (Tolman et al., 2013) produced a most essential update of the deep-water physics of spectral models since inception of the third-generation models. It resulted in new packages of such physics, ST4 and ST6, developed, tested and implemented in WAVEWATCH-III – the American national global wave-forecast model (WAVEWATCH III Development Group, 2016).

ST6 (Rogers et al., 2012, Zieger et al., 2015, Aijaz et al., 2016) signify the observation–based physics. New wind-input and and a number of dissipation functions for the phase-average spectral models were introduced. The input, whitecapping (breaking) dissipation and negative input (wave attenuation due to adverse winds) were obtained in field in situ observations in Lake George (Australia), at moderate-to-strong wind-wave conditions. The respective parameterisations are built on quantitative measurements and incorporate new observed physical features, which until very recently were not known and hence missing. Two novel features of the wind-input source function are those that account for the effects of full airflow separation (and therefore relative reduction of the input at strong wind forcing) and for nonlinear behavior of this term. The breaking term also incorporates two new features evident from observational studies. First, the dissipation consists of two parts—a strictly local (in wavenumber space) dissipation term and a cumulative term which includes integral of the spectrum. Second, there is a threshold for wave breaking, below which no breaking occurs. Such threshold means zero whitecapping dissipation, and therefore, for wave spectra below the threshold (full development, decaying seas, swell) a new dissipation function due to wave/water-turbulence interactions was developed and implemented. It was proposed theoretically (Babanin, 2012, 2017) and is consistent with the observed decay rate of ocean swell (Young et al., 2013). Further development of ST6 saw a new nonlinear interaction term, which accommodates both resonant and quasi-resonant interactions (Gramstad and Babanin, 2016). ST6 version of SWAN (the coastal engineering spectral wave model), in addition to the above, also accommodates observation-based terms for coupled for wave-bottom interactions including ripple formation/dissolution (Smith et al., 2011), for infragravity waves (Nose et al., 2016), for nonlinear wave-current interactions (Rapizo et al., 2017).

ST4 is a physics package with new dissipation functions (WAVEWATCH III Development Group, 2016). Like in the Lake George physics, whitecapping dissipation has a threshold and cumulative term, and because of the breaking threshold the swell dissipation is described by a separate term whose formulation appeals to the swell/air-turbulence interactions, but functionally is similar to ST6. Stopa et al. (2016) conducted a detailed comparison of performance of ST4 and ST6, which highlighted a need for spectral metrics in addition to the traditional integral properties (wave height, mean wave period, direction).

While parameterizations of whitecapping dissipation and wind input, and therefore spectral wave modelling in typical storms have progressed essentially over the last years, large uncertainties remain in the prediction of swell, extreme metocean circumstances, wave-current and wave-ice interactions. Most of these conditions are rare, but have high impact.

Swell, however, is not rare and is present in more than 80% of ocean spectra. It is not extreme, but provides significant adverse impacts on maritime operations such as shipping, loading, dredging. Yet, its prediction by wave-forecast models is poor, both in terms of wave amplitude and, particularly, arrival time. The very definition of ocean swell is ambiguous: while it is usually perceived as former wind-generated waves, in fact it may reconnect with the local wind through nonlinear interactions. Jiang et al. (2016) developed a method for identifying swell events and verifying swell arrival time in the models by means of buoy data. The results indicated that the model (WAVEWATCH-III) usually predicts an early arrival of swell, about 4 h on average. Furthermore, histogram of the arrival time shows that swells can be as early as 20 hours and as late as 20 hours. Since the model/observation error is not consistent even in its sign, it cannot be tune-fixed, and understanding the physics of swell propagation is necessary. As discussed in the paper, many mechanisms can contribute both to acceleration and

deceleration of swell on its way across the oceans. Those need to be separated, understood, parameterized and then reunited in the models, in order to improve the forecast. Observations and experiments of such mechanisms are extremely difficult. Changes to the swell forced by these processes are slow, respective time and length scales are of the order of thousands of wave periods and lengths. Wave flumes are not large enough for simulating these phenomena, and observation of the propagating and dispersing swell packages over global oceans is only possible with satellites, whose capability in this regard still appears marginal.

At the other extreme of metocean conditions, Liu et al. (2017) evaluated the current state of wave modelling in tropical cyclones, and the potential for improvements. Using the well-observed hurricane case of Ivan (2004) as an example, they investigated and inter-compared the performance of two wave models under hurricane conditions: WAVEWATCH-III and the University of Miami Wave Model (UMWM). Within WW3, all the four different source term packages (ST2/3/4/6), old and new, were employed for comparison purposes. Based on the comparisons between model results and measurements from various platforms, it was concluded that UMWM shows less accuracy than WW3 in integral wave parameters. Among the four WW3 source term packages, the older parameterization ST2 systematically underestimates high waves. The remaining three packages (ST3/4/6) perform reasonably well, but tend to overestimate energy of waves traveling in oblique and opposing winds which is typical occurrence in the hurricanes. It was shown that enhancing the strength of negative wind input can somewhat improve model skills in such situations, but uncertainty of the DIA parameterization of the nonlinear interactions remains the dominant source of errors, not possible to fix at this stage as the computational cost prevents the use of exact nonlinear integral.

As far as ocean currents are concerned, these are common conditions both in the open ocean and coastal areas. Major currents such as Gulfstream, Kuroshio or Agulhas are well known for harsh seas and high likelihood of abnormal (rogue) waves. Tidal inlets with waves on strong and variable currents are a typical feature of shipping routes in coastal areas. While linear effects of currents on waves, such as refraction, Doppler shift or relative speed with respect to the wind are assumed to be implicitly or explicitly included in wave-forecast models (often unverified and not validated), nonlinear effects are usually left out or even unknown. These include changes to nonlinear interactions in presence of currents with horizontal or vertical velocity gradients, wave/current energy and momentum exchanges, nonlinear modifications of the wave spectrum. Babanin et al. (2017) review the state of the art of this problem. Linear and nonlinear dynamics of waves on currents are discussed, depth-integrated and depth-varying approaches are described and examples of numerical model performance for waves on currents in realistic oceanic scenarios are presented.

Wave-ice interactions have been an exotic field of research for a long time, but with the Arctic opening from ice in summer months, the wave-ice modelling acquires important practical meaning. Among various theories for the wave-ice interactions some are different qualitatively, i.e. wave scattering (without dissipation) and dissipation (with or without scattering), others differ quantitatively, to the extent that some theories predict wavelength to increase in presence of ice, whereas others to decrease. In the field, all the mechanisms are acting together, depending on their relative magnitude, and practical guidance of the existing theoretical knowledge in forecasting waves in marginal ice zones is limited. Additional complications in this regards are due to necessity of also knowing initial conditions for the ice coverage and properties, and to be able to predict effects of waves on ice – this makes wave-ice interaction an essentially coupled problem. Developments of this aspect of wave modelling are very rapid: from no wave-ice modules some five years ago, to 5 new modules in WAVEWATCH-III alone presently. We refer the reader to Rogers et al. (2016) for the most recent update.

3.3.2   Phase Resolved

Spectral (phase averaged) models, as described in section 3.3.1, provide sea state description in terms of the wave spectrum and parameters that can be derived from the wave spectrum, such as the significant wave height, period, wave direction, and so on. Naturally, phase-averaged models do not provide any information about the instantaneous sea surface and e.g. associated water particle kinematics. To obtain such information wave models that also describe the wave phases, so-called phase-resolving models, are needed. Essentially, such models are based on the basic hydrodynamic equations (Navier-Stokes equation or Euler equations for potential flow), but numerous models exist that provide simplifications and special cases under various conditions and assumptions.

Most such simplified models assume that waves are weakly nonlinear. This is an assumption that usually can be justified for the evolution of realistic ocean waves. Of course, some processes, for example the breaking and overturning of waves or waves hitting a structure, are generally strongly nonlinear in their local dynamics. However, the general dynamics of propagating sea waves is generally weakly nonlinear. Based on this, one may distinguish between three classes of wave models: (i) linear wave model, (iii) second-order wave model, and (iii) higher order (nonlinear) wave models.

The linear wave model provides the linear approximation to the basic equations for waves, and for a given wave spectrum it assumes that the sea surface is a superposition of independent wave components. That is, the wave phases are assumed independent. This assumption provides a particularly simple description that is both efficient to simulate numerically, easy to analyze analytically and can be used to derive various properties such as statistical distributions (e.g. Gaussian distributed sea surface and Rayleigh distributed wave crests and wave height) or information about water particle kinematics, for example. For waves on deep or intermediate constant water depth, the natural extension of the linear wave model is the second-order wave model, in which the second order bound waves components are also taken in to account. Hence, the second-order wave model can in a sense be viewed as a generalization of the Second-order Stokes wave for random waves. Yet, the second-order model still assumes that the wave field consists of independent free wave components and consequently ignore more complicated nonlinear effects such as energy exchange between wave components. Second-order remains an important tool in many engineering applications and is currently the main model used to provide short-time wave information in the offshore industry. For example, many of the widely used statistical distributions for wave-heights and crest-heights are based on second-order theory.

For more accurate phase-resolving description of ocean waves higher-order models must be applied. Different from the linear and second-order theory, typically there are no analytical solutions in higher-order models, and applications of higher-order models normally involve numerical simulations of partial differential equations describing the evolution of the waves. Although there is a rapid increase in the use of Computational Fluid Dynamics (CFD) tools that simulate the full Navier-Stokes equation, also in applications to water waves and wave-structure interaction, such tools are generally still too computationally demanding to be used for large-scale problems that require wave information over a large spatial area over a long period. This is particularly the case for full 3D modelling of short-crested waves. Nevertheless, in the future CFD is expected to become an increasingly important tool also for wave simulations, and several commercial and open-source CFD simulations tools have modules for simulations of waves.

Simplified models based on potential flow theory combined with additional simplifications of the full equations remain very important for the modelling of waves in engineering applications. Typically, approximate/simplified models rely on some simplifications based on assumptions for which some parameters are assumed small. As already described, weak nonlin-

earity is one such assumption where the wave amplitude is assumed small compared to the wave length and/or water depth. Others common simplifications rely on small wave-length compared to water depth (deep water), small depth compared to wave-length (shallow water), or weakly varying depth or wave modulations (e.g. narrow-band assumption or assumption of weakly varying bathymetry).

Models that assume shallow water include models such as the Korteweg-de Vries (KdV) equation, the Kadomtsev-Petviashvili (KP) equation and Boussinesq-type equations. In their classical forms these models assumes shallow water depth and weak nonlinearity. During the last decades, there has been a development of improved Boussinesq-type models that are valid also for quite deep water conditions (improved dispersion properties) including also highly and fully nonlinear formulations (e.g. Memos et al., 2016); see also Kirby (2016) for a recent review. There are also continuous efforts to include other physical effects into such models (Kirby, 2016) such as wave breaking (e.g. Kim et al., 2017) and wind growth (e.g. Liu et al., 2016).

Another important class of simplified nonlinear models is those that in addition to weak non-linearity also assume that the wave-field is represented by a narrow wave spectrum so that modulations of the wave field takes place on longer temporal and spatial scales than the dominant wave period and wavelength of the wave train. The most basic of these models is the so-called cubic Nonlinear Schrödinger equation (NLS) for water waves (Zakharov, 1968). Numerous extension and modifications of the basic cubic NLS equation have been presented, including NLS-type equations valid to higher order of nonlinearity and/or bandwidth, for finite and variable water depth, for interaction with currents, for two crossing wave systems, to mention some.

Traditionally, due to their relative simplicity, and most importantly, the existence of exact analytical solutions, NLS-type equation has played an important role in the understanding of the nonlinear dynamics of water waves. The so-called breather solutions of NLS-type equations represents the effect of modulational instability and are often linked to the generation of rogue waves in the ocean, see more detailed discussion in section 3.3. In recent years, there has been an increasing interest in these analytical solutions in the context of rogue waves. However, most of the work on this topic is quite theoretical and the direct relevance for real-world engineering applications is sometimes difficult to see. The strict mathematical validity of the NLS equation was recently studied by Düll et al. (2016). Another recent focus within the topic of NLS equations has been the analogy to other fields of physics where nonlinear dispersive waves are present and where NLS-like equations also can be applied and where rogue wave solutions are observed (Chabchoub et al., 2015, Residori et al., 2017).

An important strength of the NLS-type equations is that they are very efficient to simulate numerically. Traditionally they have therefore been applied in many studies where large scale numerical wave simulations are desired, such as investigation of statistical properties of waves. In more recent years, with the increase in available computational power, there has been a shift towards more accurate and more computationally demanding models such as other models discussed in this section, such as HOSM, Boussinesq-models or even CFD and fully nonlinear potential flow codes. It should be mentioned that one advantage of NLS-type equations compared to many other models is that they can be formulated as space-evolution equations as well as time-evolution equations. The space-evolution form is particularly suitable for direct comparison with wave-tank experiments (i.e. waves propagating in space from a wave-paddle). The relation between the temporal and spatial forms of the NLS equation is recently discussed in Chabchoub and Grimshaw (2016).

An illustration of the applicability of various phase-resolving models, including the cubic NLS equation and the higher order NLS equation (Dysthe), for deep and intermediate water-depth with respect to nonlinearity and spectral bandwidth is shown in Figure 6.
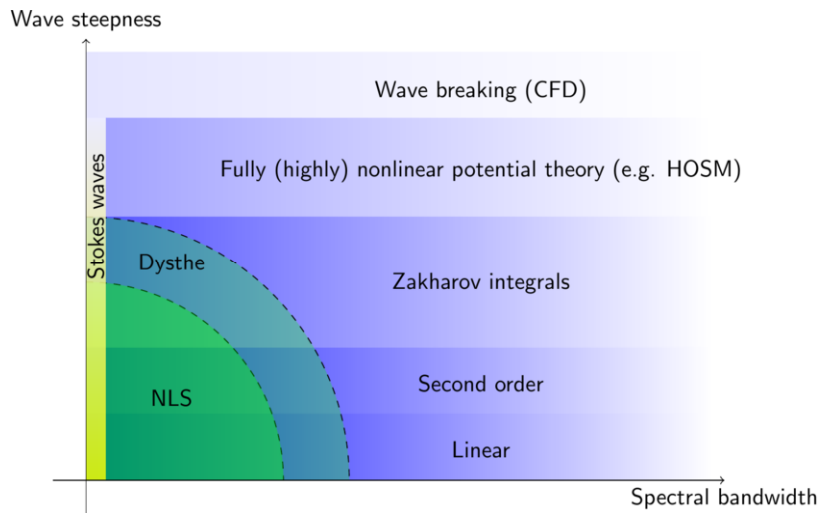
Wave steepness

Figure 6: Illustration of the range of validity for various wave descriptions for deep and intermediate depth water waves. From Bitner-Gregersen and Gramstad (2015).

Because of the continuous increase available computational power there has been an increase in applications of more accurate models based on the fully nonlinear potential flow equations. Some overview of this topic can be found in the recent book Chalikov (2016). Common approaches for such models include Boundary Element Methods (BEM) for which the equations are solved via Greens functions and integral equations at the boundaries, and volume methods for which the solution is found numerically by discretizing the fluid domain and solving the equations by finite difference of finite element methods. In general, both such models may be quite flexible in the sense that they can handle complex computational domains or wave-structure interactions. On the other hand, such models are typically quite computationally heavy.

Another model that has seen many applications to phase-resolved modelling of waves is the so-called Higher Order Spectral Model, often abbreviated HOS or HOSM. The original HOSM formulation is due to Dommermuth and Yue (1987) and West et al. (1987), and it has later been shown that other models derived independently using other approaches (e.g. Craig and Sulem, 1993) are numerically equivalent to the original HOSM formulation. Currently, there is an available open-source HOSM code named HOS-ocean (Ducrozet et al., 2016). The same group has also released a HOSM code (HOS-NWT) that can be used as a numerical wave tank, including features of an ocean wave basin: directional wavemaker, reflective walls and absorbing beach (Ducrozet et al., 2012).

HOSM is based on an expansion of the fully nonlinear free surface boundary conditions under the assumption that the wave steepness (ratio of amplitude to wave-length) is relatively small. Since this expansion in principle can be taken to very high order by adjusting the nonlinear order (often denoted M) in the code, HOSM is sometimes referred to as a fully-nonlinear model. However, in practice HOSM is normally used with some relatively low order truncation of nonlinearity (M=3 or 5 for example), although higher order may be applied, so "highly-nonlinear" is probably a more appropriate term. HOSM has the advantage that it discretizes the horizontal plane only and applies a pseudo-spectral approach where highly efficient FFT routines are used. This makes HOSM very numerically efficient, and it is a particularly useful tool for large-scale problems for which more advanced methods are too computationally demanding. HOSM can also quite efficiently provide the water particle kinematics in the fluid

domain (Bateman et al., 2003). On the other hand, HOSM is less flexible with respect to its computational domain, where it is typically restricted to a periodic square domain over a flat bottom. There are however modifications to the HOSM formulation that allow variable bathymetry (Gouin et al., 2016, 2017).

HOSM also has the limitation that the expansions do not converge if waves become very steep and close to the breaking limit, and naturally it cannot describe breaking waves without further modifications. Traditionally, dissipation due to breaking have been modelled in HOSM in a very simple manner based on smoothing (Fourier-filtering) of the solution (see e.g. Xiao et al., 2013). Recently, there has been some effort to introduce more realistic breaking models into HOSM, as well as into other nonlinear wave models. Seiffert and Ducrozet (2016) implemented a criterion for the onset of breaking into HOSM based on the works of Barthelemy et al. (2015) and Saket et al. (2016). In the work of Seiffert and Ducrozet (2017) two different breaking models were added to a HOSM model and validated against wave tank experiments.

3.3.3 *Short Term Stochastic / Probabilistic / Machine Learning*

The short-term wave characteristics are required for design and operation of offshore structures and industrial facilities within the coastal areas. These extreme single waves, for example, cause the highest loads and wave overtopping volumes on structures and thereby represent the design conditions important to be accurately defined. Under-prediction of the design maximum wave height causes unsafe designs, while over-prediction causes too conservative and thus expensive designs. Nayak and Panchang (2015) analyzed short-term wave height distributions in intermediate water depths using spectral wave data from two gauges and NDBC buoy 42035 during Hurricane Ike. They compared frequently used distributions such as the Rayleigh, the scaled Rayleigh and the 2-parameter Weibull distributions. Their analysis of wave heights suggests a good fit to the scaled Rayleigh distribution, which over-predicts by 1% to 9% for the data examined, and the average of the highest ten percent the waves, H1/10 was also over-predicted by similar magnitude (< 10%). However, Nayak and Panchang (2015) found that the over-prediction was more pronounced for the maximum wave height by as much as 40% in some cases. The two-parameter Weibull distribution was observed to provide a good fit, but the parameters of the distribution were not consistent with those developed by Forristal. Nayak and Panchang (2015) which concluded that the analysis using the scaled Rayleigh distribution (which utilizes the spectral width) showed a better prediction than the original Rayleigh distribution, but with a high variability.

Amrutha and Kumar (2015) analyzed the water surface displacement measured using waverider buoy moored at 13 m water depth in the west coast of India to study the short-term statistics of waves covering full one year period. The study indicates that the values of the observed maximum wave height as a function of duration are not consistent with the theoretical expected value, with a significant variation (1.29–2.19) in the ratio between highest 1% wave and significant wave height compared to the theoretical value of 1.67. Unlike Nayak and Panchang (2015), Amrutha and Kumar (2015) found the significant wave height ~8% lower than that predicted by the conventional Rayleigh distribution periods for the study area. Nørgaard and Andersen (2016) examined if Rayleigh distribution can be used to determine extreme wave heights in non-breaking swell conditions in deep waters. Nørgaard and Andersen (2016) concluded that the Rayleigh-distribution is under-predicting the low-exceedance wave heights in irregular swell waves. This is expected to be caused by wave non-linearity and thus a new modified wave height distribution is suggested, where the shape parameter in the distribution is dependent on the wave non-linearity, represented by the Ursell-number. The new proposed wave height distribution for non-linear and non-breaking waves is highly applicable for practical engineering design of both near-shore and offshore structures under influence of swell-waves.

In terms of predictions of individual waves especially important for warning systems, Zhu et al. (2016) proposed a novel feature extraction approach for identifying ocean wave characteristics in real time. The algorithm was developed through the integration of the fuzzy C-means clustering algorithm, statistics formulation, short-time Fourier transforms, high frequency radar data processing and window function analysis. In order to demonstrate the proposed algorithm developed by Zhu et al. (2016), two Wellen radar systems were installed in South Korea. The testing results demonstrated that the proposed algorithm is effective in extracting characteristic features from a variety of ocean waves. It is expected that system will accurately predict natural hazards and provide adequate warning time for people to evacuate from threatened coastal areas. Takagi et al. (2017) derived a formulation for the prediction of individual wave using multi-point measurements, which can be applied not only for the stationary process but also the non-stationary process. Examples based on numerical experiments of long crested waves show that prediction error is small when the prediction time is short and the measurement point is sufficiently far from target. Takagi et al. (2017) concluded that the method is applicable to the wave warning system in short crested waves.

Moving to the frequency domain, Giske et al. (2017) presented a new method for efficient calculation of auto- and cross-spectral densities in the stochastic modelling of ocean waves and wave loads, which may contribute to more efficient long-term response prediction. The cross-spectral densities of the first order wave excitation forces are considered, but the method is straightforwardly generalized to other cross-spectral densities, e.g. for wave elevation, wave kinematics or second order loads.

New researches on spatial-temporal characteristics of ocean waves have been produced recently. Alvise et al. (2017) presented the analysis of the temporal profile and height of space-time (ST) extreme wind waves to verify, to what extent, one can estimate the shape and the crest-to-trough height of near-focusing large 3D wave groups. Wave data were gathered from an observational ST sample of sea surface and they were examined to detect the highest waves (exceeding the rogue wave threshold) of specific 3D wave groups close to the apex of their development. First Alvise et al. (2017) examined the local maximum elevations of the groups within the framework of statistical models for ST extreme waves, and compared with observations and predictions of maxima derived by one-point time series of sea surface elevations. Then they analyzed the temporal profile near the maximum wave crests and compared with the expectations of the linear and second-order nonlinear extension of the Quasi-Determinism (QD) theory. Alvise et al. (2017) showed that the elevations close to the crest apex are narrowly distributed around a mean profile, whilst a larger dispersion is observed away from the maximum elevation. The developments Alvise et al. (2017) are currently in process of being implemented in a numerical spectral model for wave extreme prediction. Podgorski and Rychlik (2016) proposed measures of three-dimensional spatial wave size, expressed in terms of properly defined characteristics: the crest-height, the length, and the wave front location. Their statistical distributions are presented in explicit integral forms for the deep water seas modeled as Gaussian fields. The approach of Podgorski and Rychlik (2016) allows for investigation of the effect that shape and directionality of the sea spectrum have on the joint distributions of the size characteristics.

In terms of new developments on probabilistic distributions, Antão and Guedes Soares (2016) studied a bivariate gamma distribution fitted to an empirical joint probability density of wave steepness and height for deep water waves. A transformation of this distribution was also fitted to waves from a wave tank experiment in order to observe how the skewness of the bivariate gamma distribution changes. Antão and Guedes Soares (2016) concluded that the quality of the obtained fits compared with fits of a Gumbel copula for the same data. Seyffert et al. (2016) contributed to the theoretical basis for the occurrence of rare wave groups. The theory is compared with numerical Monte Carlo simulations in addition to physical oceanographic data. Seyffert et al. (2016) argued that the wave groups, in run length, shape, and amplitude,

are shown to be dependent on the wave spectrum and its spectral moments, a prescribed exposure time, and a pre-selected mean wavegroup period.

<u>Error/Bias correction applied to numerical models</u>

Wind and wave forecasting represent a useful tool for safety assessment of maritime works and activities. Metocean forecasting uncertainty is usually corrected by using either the mean calibration factor or the time series method, and has been widely used. However, within the frame of maritime work management it is necessary to forecast, with an acceptable probability of error, whether or not the wind speed and wave height at a given location will exceed prefixed thresholds within a specified temporal window. Models that seek to predict environmental variables invariably demonstrate bias when compared to observations. Although the numerical models have shown a significant improvement over the last decades, bias correction (BC) algorithms are still necessary and important, both for forecast and hindcast simulations. Wang et al. (2017) constructed a new non-parametric correction model to improve wave model accuracy through modifying a previous approach. The new correction model introduces a kernel algorithm to learn error information from both value magnitude and series trend through training datasets, and utilizes the information to correct potential errors in hindcast outputs. Wang et al. (2017) argued that the two-dimensional learning method is more effective than the previous one-dimensional which only learns error information from the value magnitude.

Parker and Hill (2017) introduced and compared a subset of BC methods with the goal of clarifying a "best practice" methodology for application of BC in studies of wave-related processes. Specific focus was paid to comparing parametric vs. empirical methods as well as univariate vs. bivariate methods. The techniques were tested on global WAVEWATCH III datasets compared to buoy observations at multiple locations, for both wave heights and periods. Results from Parker and Hill (2017) showed that all methods performed uniformly in terms of correcting statistical moments for individual variables with the exception of a copula based method underperforming for wave period. When comparing parametric and empirical methods, no difference was found. Between bivariate and univariate methods, Parker and Hill (2017) showed that bivariate methods greatly improve inter-variable correlations, emphasizing that is essential to employ methods that consider dependence between variables. Girolamo et al. (2017) illustrated a general criterion useful to correct wave forecast, providing an engineering tool able to assess the safety of the temporal window needed to complete a specified maritime work. The paper provided a detailed description of the method, together with the application to a real case.

<u>Ensembles and Probabilistic Forecasts</u>

Although the atmospheric ensemble forecasting is utilized since the 90s, the wave ensemble forecasts have become more popular during the last few years. The use of probabilistic forecasts based on ensembles has the benefit of calculating the uncertainties associated with the numerical prediction as well as improving the skill of the model especially after the fifth day of forecast. It is known that accurate wave forecasts during typhoon events are extremely important in aiding the mitigation and minimization of their potential damage to the coastal infrastructure, and the protection of coastal communities. Therefore, it is expected the development and use of wave forecasts will increase significantly in the next years. Pan et al. (2016) presented a practical approach to optimizing model-ensemble wave heights in an attempt to improve the accuracy of real-time typhoon wave forecasting. A locally weighted learning algorithm was used to obtain the weights for the wave heights computed by the WAVEWATCH III wave model driven by winds from four different weather models (model-ensembles). The optimized weights are subsequently used to calculate the resulting wave heights from the model-ensembles. Results of Pan et al. (2016) showed that the optimization is capable of capturing the different behavioral effects of the different weather models on

wave generation. Comparison with the measurements at the selected wave buoy locations shows that the optimized weights, obtained through a training process, can significantly improve the accuracy of the forecasted wave heights over the standard mean values, particularly for typhoon-induced peak waves. Pan et al. (2016) indicated that the algorithm is easy to implement and practical for real-time wave forecasting. Pezzutto et al. (2016) compared the performance of two wind and wave short range ensemble forecast systems for the Mediterranean Sea, based on the respective systems: the Met Office Global-Regional Ensemble Prediction System and the Nettuno Ensemble Prediction System. Attention is focused on the differences between the two implementations (e.g. grid resolution and initial ensemble members sampling) and their effects on the prediction skill. Pezzutto et al. (2016) state that assessment of the added value of the ensemble techniques at short range in comparison with the deterministic forecast from Nettuno reveals that adopting the ensemble approach has small, but substantive, advantages.

The statistical characteristic of ocean wave could consist of two parts that are used for long-term prediction and short-term prediction. In general, the different method/approximations are used for both of long-term and short-term prediction.

Duan et al (2016) proposed a hybrid EMD-SVR model in order to predict the short term of significant wave height. With this method, the limitation from conventional statistical model in the forecasting of nonlinear and non-stationary waves could be improved. The validation of the method is compared with that of AR, EMD-AR, SVR and EMD-SVR models by using the same data from NDBC buoys.

Minoura, M (2016) also proposed stochastic sea state models by employing Fourier series expansions. All components of sea state, significant wave height, mean wave period, wave direction, mean wind speed, and wind direction are found in good correlation with that of the hindcasting seastate data. Several aspects are used in order to clarify the accuracy of the proposed model. These are probability density function, mean value, variance value, cross relation function and persistence duration of sea-state.

3.4   *Tropical & Extratropical Cyclones*

Tropical cyclones can develop a heavy force circular wind that is characterized from a low pressure in the center and a closed low-level atmosphere circulation. Since a heavy wind force is developed, the extreme wave or freak wave might be generated simultaneously. It is commonly known that the direction of circulation depends on the location, counterclockwise wind blowing in the northern hemisphere and clockwise blowing in the southern hemisphere. The different names for a tropical cyclone are typhoon, hurricane, tropical storm, etc.

The tropical cyclone, i.e. hurricane wave, might become a catastrophic disaster that causes heavy damage on the land or infrastructure on the coast or port, i.e. coastal bridge (Guo, et all (2015). The failure of the coastal bridge could impact the transportation and cause economic losses. In order to predict sufficient clearance on the coastal bridge from hurricane wave force, Gao develop an analytical solution by using Eigen function matching method so that the boundary value problem of the submerged coastal bridge deck is derived.

Since a tropical cyclone can also generate an extreme wave or freak wave, it is very important to know the characteristics of the newly generated wave swell source. Sandhya et al (2016) conducted study of the Indian coast in order to describe the in situ field data during extreme cyclone conditions. Then, he investigated the all components of wave energy spectra by using linear wave theory (ridge analysis).

The freak wave or rogue wave is the other extreme wave condition, with very steep, and a much larger wave. The condition of very steep, much larger than the common sea state is a given that the maritime community to handle and work with these conditions (Bitner-Gregersen E, 2017).

The freak wave could categorized based on nonlinearity and irregularity of nearshore waves, such as power spectral, occurrence frequency of freak waves, skewness kurtosis, wave grouping and its distribution (Zhuo, Z and Sato S). It is concluded that the occurrence of freak waves is dependent on the kurtosis and the groupiness factor based on the two typhoon observation on the Suruga coast Shizoka Prefecture of Japan in 2013.

Deng et al (2016) conducted an experimental investigation on deterministic freak waves. The experimental condition is setup so that four freak waves were generated with different steepness values. A phase amplitude iteration scheme was applied in order to optimize the deterministic wave sequences by taking into account the different wave steepness values. The third order stokes wave theory was used to predict wave speed by adopting local trough to trough periods and freak wave height.

Kai Yin et al. (2017) used the coupled ADCIRC+SWAN models to investigate the effects of potential sea level rise (SLR) and typhoon intensification (TI) on storm surges and waves in Pearl River Estuary, China. The results demonstrated that TI has a greater impact on storm surge, whereas SLR has a greater impact on wave heights in the estuary.

Zhilin Sun et al. (2015) carried out a numerical study based on the ECOMSED model to investigate the storm surge induced by super typhoon 5612 (WANDA) along Zhengjiang coast, China. The results presented good agreement with the observed data. Overtopping probabilities of seawalls corresponding to each track designed based on WANDA were achieved.

P.L.N. Murty et al. (2014) implemented a coupled wave + surge hydrodynamic modeling system (ADCIRC+SWAN) to simulate storm surge, still water level landfall in the Odisha State, east coast of India, during October, 2013. This coupled model provides a realistic description on the dynamic interaction of tides, wind, waves and currents.

Zhantao Zhuo and Shiji Sato (2015) investigated typhoon wave characteristics with an objective to extract essential wave parameters influential to stability of coastal structures. The relationships among various parameters were examined regarding the nonlinearity and the irregularity of nearshore waves, such as power spectrum, occurrence of freak waves, skewness and kurtosis, wave grouping and distribution of wave height.

H.Q. Zhang and B.C. Nie (2016) analysed typical wave parameters caused by typhoon near Donghai Bridge, a demonstration area of offshore wind farm. Anisotropic energy dissipation in the wave propagation direction is considered and further applied in this model. This new model is used to simulate and forecast wave evolution caused by Chan-Hom (201509).

Jin-hai Zheng et al. (2017) investigated the central pressure and the maximum wind speed of three categories, which are typhoons making straight landfall, typhoons active in offshore areas and typhoons moving northward after landfall, on basis of a 65-year dataset (1949-2013). Statistical analysis suggested that the minimum central pressure increased northward and shoreward gradually. The relationship between the maximum wind speed and the minimum central pressure was established through second-order polynomial fitting.

Shun-qi Pan et al. (2016) presented a practical approach to optimizing model-ensemble wave height in an attempt to improve the accuracy of real-time typhoon wave forecasting. A locally weighted learning algorithm is used to obtain the weights for the wave heights computed by the WAVEWATCH III wave model driven by winds from four different weather models (model-ensembles). The optimized weights are subsequently used to calculate the resulting wave heights from the model-ensembles.

4.   CURRENTS

Fossen and Lekkas (2017) presented a globally κ-exponentially stable adaptive disturbance observer intended for an indirect adaptive control approach and a globally convergent direct adaptive control law for estimation and compensation of ocean currents, which could be ap-

plied to the horizontal-plane motion of surface vessels and autonomous underwater vehicles. These two nonlinear adaptive path-following algorithms were based on a classical LOS guidance principle for marine craft, and integral action is obtained by parameter adaptation.

Hu et al. (2016) designed a three-dimensional current sensor which could measure the horizontal velocity and small upwelling. The horizontal flow velocity was measured by the ball and the vertical flow velocity was measured by the thin disc through the results of horizontal flow velocity measurement. The device could be used to measure the velocity in the range of 0mm/s~400mm/s and the minimum flow velocity which could be accurately measured is about 8 mm/s.

Mayerle et al. (2015) constructed a three-dimensional process-based model for sediment transport coupled with wave-current models based on the Delft3D modelling system in conjunction with the field measurements for the sediment motion and presented transport of a mixture of cohesive sediments and sands in the Paranagua Estuarine Complex in the south of Brazil.

Zhang et al. (2017) established a set of three-dimensional numerical models to investigate the mechanisms of local scour around three adjacent piles with different arrangements under steady currents. The results revealed that the dimensionless pile spacing had a significant effect on the flow field and local scour around the three adjacent piles.

Almar et al. (2016) presented a method based on the application of the Radon transform on longshore spatio-temporal images and the results showed an overall good agreement with the synthetic field in-situ currents. This remote sensing method allowed a long term monitoring of the longshore current and its cross-shore structure.

Xu and Lin (2017) proposed a new two-step projection method in connection with an ISPH model that used both current time step and future time step, which achieved much better energy conservation than the traditional ISPH model, even with the use of a much larger time step.

Scott et al. (2016) demonstrated that strong boundary-controlled rip flows existed in association with groynes, and that the development of these currents in a fetch-limited environment is principally related to the deflection of the alongshore current by the coastal structure through field measurements from Boscombe beach. A calibrated and validated numerical model (XBeach) was used to explore the key environmental controls on rip behaviour across a range of groyne configurations and wave conditions not observed in the field.

Choi et al. (2015) used the Boussinesq model FUNWAVE to perform a numerical simulation of the SandyDuck field experiment for 2 October 1997 in order to investigate surf zone hydrodynamics in a directional random wave environment with the observed directional offshore spectrum and field topography, including the scoured depression below the FRF pier structure. The simulation results agreed well with the experimental data to reveal a wave height distribution of the random waves as well as the well-developed longshore current and its energetic fluctuation.

Yang et al. (2015) carried out a numerical model investigation with COULWAVE to study the wave-induced flow in wetland mound–channel systems at different water levels, vegetated conditions, and mound configurations. Numerical results showed that rip current strength and primary circulation size depend on mound spacing, water depth, wave height, and vegetation cover.

Chen and Christensen (2017) developed a numerical model for fluid-structure interaction analysis of flow through and around an aquaculture net cage, which was based on the coupling between the porous media model and the lumped mass structural model. Since the interaction effects between the net cage and the flow were considered and the time stepping procedure was introduced, the solver could be applied in both steady and unsteady conditions.

Liu et al. (2017) established the ocean-current-induced electric field model for current movement and obtained the measurement principle of an expendable current profiler (XCP) through model analysis. Based on this analysis, a method was proposed for the measurement of the nanovolt-scale ocean-current-induced electric field.

Xiao et al. (2017) described a novel non-intrusive reduction model which was based on the Smolyak sparse grid method and implemented under the framework of advanced 3D unstructured mesh finite element ocean model (Fluidity) for three-dimensional (3D) free surface flows. It was shown that the accuracy of solutions from free surface flow NIROM, which showed a good agreement with the high fidelity full ocean model, was maintained while the CPU cost was reduced by several orders of magnitude.

Yang et al. (2016) investigated the two-dimensional flow over two inclined flat plates with the same length and thickness in a staggered arrangement at low Reynolds numbers by numerical simulation and recommend the IBM method to handle the location and boundary condition for the plates.

Chen et al. (2015) conducted several groups of numerical simulations of ship navigation based on the Princeton Ocean Model (POM) in the North Pacific Ocean and focuses on the ocean surface current in the East China Sea (ECS) to investigate the effect of the Kuroshio Current on ship navigation quantitatively as well as the next step of making a weather routing system and found that the POM model could generate a high-quality Kuroshio Current distribution that could be applied to conduct numerical simulations of ship navigation.

Wang and Zou (2015) established a comprehensive set of data, consisting of current velocity measurements on barred beaches with slopes of 1:100 and 1:40, as well as wave transformation and setup data in order to examine the bimodal longshore current velocity profile for purely wave-driven currents, with emphasis on the second peak and ratio of two peaks. The 2-D model based on vertically integrated equations (external mode) of Nearshore POM was performed to compute the measured velocity profile.

Klebert et al. (2015) presented the full-scale measurements of the deformation and current reduction of a large-scale fish sea cage submitted to high currents and applied a simulation model based on super-elements describing the cage shape whose results showed good agreement with the cage deformations.

4.1 Measurements / Data

Ocean currents have received tremendous attention for decades on the basis of its important role in marine engineering. The parameters of velocity and direction are the main concerns of measurement of ocean currents in the field of ocean engineering.

4.1.1 In-situ current measurements

Field measurement is extremely essential for researchers to study the ocean currents. Scott et al. (2016) used fixed instruments and GPS-drifters to conduct a 10-day field experiment at Boscombe and found that there was a close correspondence between the existence of strong boundary-controlled rip flows and groynes.

There are a variety of flow velocity measuring instruments and the Acoustic Doppler Current Profiler is the most widely used equipment in the modern testing field. In order to study the interaction between the sea cage and the bathymetry chart, Klebert et al. (2015) conducted a field experiment to measure the deformation and current reduction using an Acoustic Doppler Current Profiler and Acoustic Doppler Velocimeter. However, the Acoustic Doppler Current Profiler can hardly be used to measure the vertical velocity owing to its lower accuracy. To compensate for this shortcoming, Hu et al. (2016) designed a three-dimensional current sensor which could measure the horizontal velocity and small upwelling. Because of the powerful

facility to measure the horizontal and vertical flow velocity separately, the device can fit the needs of small, three-dimensional, transient and deep sea.

Some new detection methods are proposed recent years. Fossen and Lekkas (2017) presented two nonlinear adaptive path-following algorithms which can be used for estimation and compensation of ocean currents. Liu et al. (2017) established the ocean-current-induced electric field model for current movement and obtained the measurement principle of an expendable current profiler by model analysis. On this basis, they gave a new way of measurement of the nanovolt-scale ocean-current-induced electric field.

Ocean current observations can be found at a number of web-sites. NOAA's National Oceanographic Data Center (NODC), http://www.nodc.noaa.gov/, provides current data from a number of sources as does the Bundesamt für Seeschifffahrt und Hydrographie (Federal Maritime and Hydrographic Agency), http://www.bsh.de/en/index.jsp, of the German Federal Ministry of Transport, Building and Urban Development. The Southern Oscillation Index/El Nino web site, http://www.pmel.noaa.gov/tao/elnino/nino-home.html provides access to a number of links to a number of data products including surface currents.

4.1.2   Remotely sensed current measurements

Due to the advantages of low cost and intuitive use, video remote sensing has become more and more common as an efficient tool to monitor the offshore environment. Uiboupin and Laanemets (2015) used the bias-corrected SST imagery to estimate the mean upwelling characterics in the Gulf of Finland (Baltic Sea). In this method, the information of the upwelling is extracted from sea surface temperature obtained from satellite remote sensing technology. Almar et al. (2016) presented a method to estimate the longshore current from video based on the Radon transform and the results showed an overall good agreement with the synthetic fields and in-situ currents. Wijaya (2017) proposed an alternative method to determine the surface current from radar images based on Dynamic Averaging and Evolution Scenario method.

Near-realtime global ocean surface currents derived from satellite altimeter and scatterometer data can be found at NOAA's Ocean Surface Current Analyses – Real Time (OSCAR) web site (http://www.oscar.noaa.gov/index.html). The data is validated against moored and floating buoy data, and the method to derive surface currents with satellite altimeter and scatterometer data is the outcome of several years NASA sponsored research.

4.2   Analytical & Numerical Models

Some ocean current models are applied to solve the practical engineering problems and promote further development. Sediment transport, which proves to be closely related to harbors and navigation channels, has received much attention in recent years. Mayerle et al. (2015) constructed a three-dimensional process-based model coupled with wave-current models to investigate the sediment transport in the Paranagua Estuary Complex in Brazil. The ocean model clearly illustrates the sediment transport and morphological changes in estuaries. Wang et al. (2016) applied the Aqua-FE^{TM} model to simulate the effects of wave and current on gravity cage with two different meshes. Lamas et al. (2017) analyzed the response on yaw motions of a Tension Leg Wellhead Platform on flow-induced motions with CFD dynamic analysis. Zhang et al. (2017) conducted a systematic analysis on the mechanisms of local scour around three adjacent piles by establishing a set of numerical models, which successfully described the impact of the pile spacing on the flow field, bed elevation contours and scour depth.

Ocean model outputs have been employed to describe the interaction of currents and structure, which has been becoming the focus of research and the hotspot. Chen et al. (2015) used the POM ocean model to study the impact of the Kuroshio Current on ship navigation. It is found that the POM model performs well in generating a high-quality Kuroshio Current dis-

tribution. Pan et al. (2016) applied WADAM, MULDIF and WASIM to investigate the impact of a current on the relative motions and wave drift forces for two offshore floaters and gave the comparison analyses on these three models. Chen and Christensen (2017) developed a numerical model based on the coupling between the porous media model and the lumped mass structural model to analyze the interaction of flow and an aquaculture net cage.

Some new algorithms and new numerical models have been put forward in recent years. Xu and Lin (2017) proposed a new two-step projection method in connection with an ISPH model that used both current time step pressure and future time step pressure, which was able to get better energy conservation than the traditional ISPH model, even if a much larger time step was used. Xiao et al. (2017) described a novel non-intrusive reduction model which was based on the Smolyak sparse grid method and implemented under the framework of advanced 3D unstructured mesh finite element ocean model for three-dimensional free surface flows. It was shown that the accuracy of solutions from free surface flow NIROM, which was well fitted with the high fidelity full ocean model, was maintained while the CPU cost was much lower.

5.   WIND

Umesh et al. (2017) summarized the results of validation performed with wave spectra using SWAN model off coastal Puducherry, located in the east coast of India and studied the impact of wind forcing from ECMWF ERA Interim winds and QuikSCAT-NCEP blended winds on resultant wave spectra. They found that wave model output was critically sensitive to the choice of the wind field product and blended winds generated more realistic wave fields in coastal location and could reproduce the growth and decay of waves in the real-time based on model simulations.

Chen et al. (2017) numerically investigated the energy harvesting performance of a fully-activated flapping foil under wind gust conditions and the effects of the gust frequency, the oscillation amplitude of gust, and the phase difference between the gust and the pitch were systematically examined. By comparing with the results from the uniform flow, they found that the energy harvesting efficiency under wind gust conditions can be changed greatly.

Campos and Soares (2016) performed two pairs of comparisons between HIPOCAS and ERA reanalysis by considering the wind speed and significant wave height and found that ERA-Interim presented the best results against measurements but suggests some underestimation under extreme events at mid-high latitudes, while HIPOCAS tended to overestimate the measurements and over-predict both ERA reanalyses in the range of extreme values.

Cambazoglu et al. (2016) evaluated the impact of resolution on wind predictions within regions of Turkish Straits System and Chesapeake Bay using a quadruple nest of CO-AMPS® (27 km to 1 km) to find an optimal configuration of spatial and temporal resolution and suggested the use of hourly atmospheric products at 3-km resolution for oceanic forcing purposes.

Stefanakos (2016) obtained the wind and wave parameters by coupling the well-known Fuzzy Inference Systems (FIS) in combination with Adaptive Network-based Fuzzy Inference Systems (ANFIS) with a nonstationary time series and found that the forecasts based on the proposed methodology outperform the ones using only FIS/ANFIS models through the comparison of the error measures from the two approaches.

Tagliaferri et al. (2015) proposed two methods for short term forecasting of wind direction with the aim to provide input for tactic decisions during yacht races based on artificial neural networks (ANN) and support vector machines (SVM), respectively. They found that although the ANN forecast based on the ensemble average of ten networks showed a larger mean absolute error and a similar mean effectiveness index than the SVM forecast, its accuracy increased significantly with the size of the ensemble.

Chen et al. (2015) proposed a new algorithm to retrieve wind speed and wind direction from marine X-band radar image sequence, which related wind vector not only to the gray level intensities of radar images, but also to the sea states explicitly. The method of preprocessing radar image was proved to be effective implemented and was suitable for identifying barriers from the sea clutter.

Bennett and Mulligan (2017) investigated three different spatially-varying surface wind which included two 2D parametric wind models and a 3D atmospheric model with data assimilation, and atmospheric pressure fields used for forecasting or hindcasting hurricane waves on the continental shelf. They suggested that the results of this study were relevant for other tropical cyclones that undergo extratropical transition or were influenced by other atmospheric disturbances at mid-latitudes, resulting in storms with large spatial size and high asymmetry.

Caires et al. (2016) proposed a semi-parametric method based on the theory of max-stable processes that could be used to determine the time- and space-evolving wind fields associated with a given return value of wind speed at a specified reference location. The main recommendation of this study is that the proposed method be considered further for the determination of temporally and spatially evolving hydraulic conditions.

Pillai et al. (2017) explored the application of a wind farm layout evaluation function and layout optimization framework to Middelgrunden wind farm in Denmark, which has been built considering the interests of wind farm developers in order to aid in the planning of future offshore wind farms using the UK Round 3 wind farms as a point of reference to calibrate the model. The results showed that both optimization algorithms were capable of identifying layouts with reduced levelized cost of energy compared to the existing layout while still considering the specific conditions and constraints at this site and those typical of future projects.

Castro-Santos and Diaz-Casas (2015) determined the influence that location had in the life-cycle of a floating offshore wind farm and applied the methodology to a floating offshore wind farm with semisubmersible platforms and located in the Galicia area (North-West of Spain), which could clarify the importance of the economic and strategic location settings when a floating offshore wind farm was constructed in any region.

Lakshmi et al. (2017) performed a comprehensive analysis on storm surge computation utilizing WRF-ARW winds run with three different grid resolutions for the recent very severe cyclonic storms Phailin and Hudhud that had landfall along the east coast of India by considering two different sets of WRF-ARW winds constructed using GFS and FNL initial conditions under three varied horizontal grid resolutions.

Emanuel (2017) presented a fast, physically motivated intensity algorithm consisting of two coupled ordinary differential equations predicting the evolution of a wind speed and an inner core moisture variable, which included the effects of ocean coupling and environmental wind shear but does not explicitly simulate spatial structure and produced a smaller increase in global tropical cyclone frequency in response to global warming, but a comparable increase in power dissipation compared to the existing method.

Wang et al. (2017) proposed a new gradient wind field model for translating TCs, based on the vector summation of the rotational wind speed and the translation speed, which could better describe the realistic wind field than the existing Georgiou's model incorporating Blaton's adjusted curvature.

5.1   *Current State of the Art*

The assessment of the environment impact over global ocean as well as over regional basins requires the knowledge of high accurate wind speed and direction with high space and time resolutions. The wind variables would be derived from the operational numerical weather prediction models (NWP) such as European Center for Medium Weather Forecasts (ECMWF)

analyses and from ECMWF re-analyses ERA Interim. Indeed NWP provide estimates of winds and of additional parameters such as sea state, air temperature and humidity, sea surface temperature (SST) on a regular grid with a high temporal resolution generally between 3:00 and 6:00. However, their spatial resolution is relatively low, especially for the needs of local and coastal environmental studies. For example, in these areas the coastal topography has a significant impact on the spatio-temporal changes of marine meteorology which in turn produce fine scale variability of surface parameters. A feature of the coastal dynamics atmospheric production of expansion vessels supercritical downstream structures marked mountain. This acceleration of the winds causes significant spatial variations of surface wind not included in the analyses and the impact weather and ocean level is poorly determined. Another feature of the coastal winds is the sea breeze. It is produced by strong contrasts of temperature and can reach 10 m/s and assign a coastal strip of tens of kilometers. Accurate prediction of sea breeze is necessary for operational wind farms to assess energy intake to the power grid.

For further improvement of the surface wind space and time characteristics relied on the main weather conditions occurring over global and/or regional oceanic scales. The scientific community makes use of remotely sensed data and of the associated surface wind analyses. Radars and radiometers onboard polar satellites provide valuable information on surface winds, with high spatial resolution, and global coverage. Satellite observations allow access to synoptic and global estimates of geophysical parameters with high spatial resolution ranging between 1km and 50km with an accuracy equivalent to that estimated from the buoy measurements. The characteristics of the satellite surface wind speeds and directions useful for environmental impact achievements are summarized in Table 1. It provides satellite mission, onboard instrument of interest for surface wind observation, period of data availability, repeat orbit (i.e. requiring time between two successive observations at same location) for polar sun-synchronous satellites, space grid resolution (i.e. also called Wind Vector Cell (WVC)), and the centers producing and distributing data. Most of these data are also archived by IFREMER for scientific use. Table 1: Characteristics of sources providing satellite surface winds required for environmental impact shows about 30 independent wind sources, including 12 scatterometers, 2 SAR, 10 radiometers, and 8 altimeters. For instance, the European Space Agency (ESA) operated two scatterometers onboard the European Remote Sensing Satellites ERS-1 (1991 – 1996) and ERS-2 (1995 – 2011). Three scatterometers have been operated by the National Aeronautic Space Administration (NASA): NASA scatterometer (NSCAT) (1996 – 1997) onboard the Japanese Advanced Earth Observing Satellite (ADEOS-1), Sea-Winds onboard QuikSCAT satellite (1999 - 2009), and SeaWinds onboard (ADEOS-2/Midori) (2002 – 2003). The latest European scatterometers are the Advanced SCATterometer ASCAT-A (2006 – present) and ASCAT-B (2013 – present) onboard METOP-A and –B satellites, Ocean SCATterometer (OSCAT) onboard OCEANSAT2 satellite (2009 – present), and HY-2A scatterometer (2011 – present). ASCAT-A/B, OSCAT, and HY-2A are operated by European Meteorological Satellite organization (EUMETSAT), and the Indian Space Research Organization (ISRO), respectively.

Higher wind speed and direction retrievals will be derived from two SAR onboard ENVISAT and SENTINEL 1A ESA satellites, respectively.

To enhance surface wind sampling in space and time over oceanic areas, winds from radiometers such as the Special Sensor Microwave Imager (SSM/I) on board Defense Meteorological Satellite Program (DMSP) F10, F11, F13, F14, and F15, F16, F17, and F18 satellites, the polarimetric radiometer WindSat onboard CORIOLIS satellite, and the altimeters onboard ERS-1, ERS-2, Topex/Poseidon, ENVISAT, JASON1, and JASON2 satellites.

All wind speeds and directions available for the project are related to level 2 product (data over instrument swath or along tracks) associated with each satellite mission and provided by the producer agencies (CNES, ESA, EUMETSAT OSI SAF, IFREMER, ISRO, KNMI, NASA, RSS)

Scatterometers, SAR, and WindSat provide valuable information on both wind speed and direction, whereas passive microwave imagers (e.g. SSM/I) and altimeters provide information on wind speed (only). Radars and radiometers provide accurate retrievals in almost all atmospheric and oceanic conditions. In general, they are available with a spatial resolution lower than 1km for SAR, 7km along altimeter tracks, and varying between 25 and 12.5 km² for scatterometers and radiometers. Figure 7 shows examples of sampling length distributions of remotely sensed wind derived from ASCAT-A/B and SSM/I-F16/F17 over the European of interest, available for one day (**left panel**) and one month (right panel). Areas located 12km to 25km off coasts exhibit significant sampling that would meet the requirements dealing with the potential assessment of wind renewable marine energy. To overcome near coast winds not available from scatterometers and radiometers, the project will use SAR data. Figure 8 shows an example of sampling length of SENTINEL 1A SAR observations occurring during the period January – April 2016.
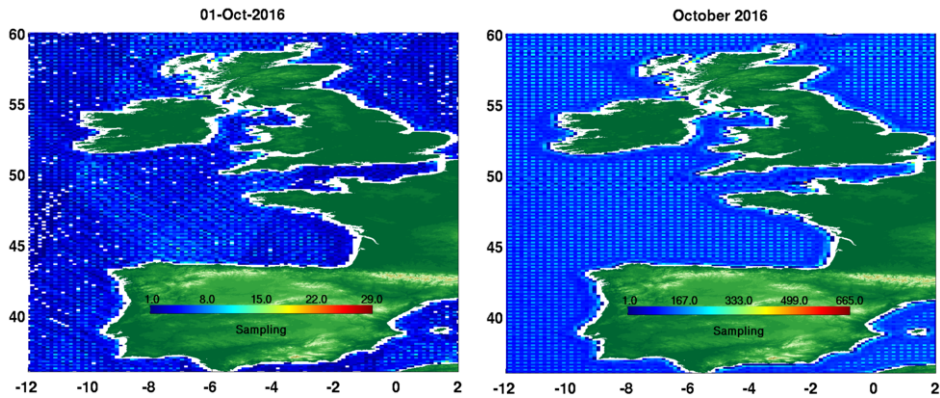

Figure 7: Spatial distributions of remotely sensed winds derived from ASCAT-A/B and SSM/I-F16/F17 over ARCWIND oceanic zone calculated for October, 1st 2016 (left panel) and for full October 2016 (right).
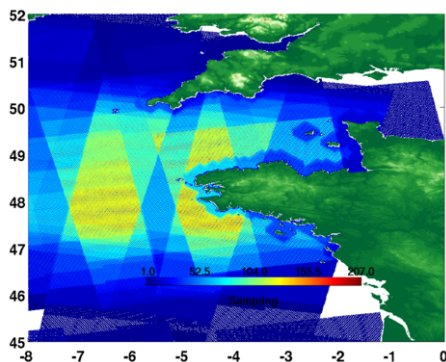

Figure 8: Spatial distributions of remotely sensed winds over a North West Atlantic oceanic area calculated from SENTINEL 1A SAR data occurring during the period Jan. – April 2016

Table 1: Characteristics of sources providing satellite surface winds required for environmental impact

Satellite	Instruments	Period	Orbit (days)	Spatial grid	Sources
ERS-1	Scatterometer altimeter	1992 - 1996	3	50/25km² 7km	ESA/IFREMER
ERS-2	Scatterometer altimeter	1996 - 2011	35	50/25km² 7km	ESA/IFREMER
ADEOS-1	Scatterometer (NSCAT)	1996 - 1997	4	25km²	NASA/JPL
QuikSCAT	Scatterometer (SeaWinds)	1999 - 2009	4	12.5km²	NASA/JPL
ADEOS-2	Scatterometer (SeaWinds)	2002 - 2003	4	25km²	NASA/JPL
OceanSat2	Scatterometer (OSCAT2)	2009 - 2013	2	25km²	ISRO/KNMI
Metop-A	Scatterometer (ASCAT-A)	2007 - Present	29	25/12.5km²	OSI SAF
Metop-B	Scatterometer (ASCAT-B)	2012 - Present	29	12.5km²	OSI SAF
HY-2A	Scatterometer	2012 - Present	14	25km²	NSOAS/KNMI
ISS	Scatterometer (RapidScat)	2014 - Present		12.5km²	NASA/JPL
ENVISAT	SAR altimeter	2002 - 2011	35	1km²	ESA
SENTINEL 1A	SAR	2015 - Present		1km²	ESA
SENTINEL 3	Altimeter	2015 - Present	27	300m	ESA
Topex/ Poseidon	altimeter	1992 - 2005	10	7km	CNES
Jason1	altimeter	2001 - 2013	10	7km	CNES/NASA
Jason2	altimeter	2008 - Present	10	7km	CNES/NASA
Jason3	altimeter	2006 - Present	10	7km	CNES/NASA
DMSP F10-F18	Radiometers(SSM/I)	1992 - Present		25km²	RSS
CORIOLIS	Radiometer(WindSat)	2003 - Present	8	25km²	RSS
SMAP	Radiometer	2015 – Present	8	25km²	NASA/JPL
SCATSAT-1	Scatterometer	2016- Present	2	25km²	ISRO
CFOSAT	Scatterometer	2018 -	13	50km² / 25km²	CNSA/CNES

5.2   *Accuracy Issues*

The remotely sensed wind accuracy is mainly determined through comprehensive comparisons with mooring wind data. The comparison issues require proper spatial and temporal procedures aiming at generating satellite and in-situ collocated data (matchup data). The agreement between the two sources is good. The root mean square difference is about 1.10m/s and 18°, for wind speed and direction, respectively. To assess the consistency between retrievals from various satellite instruments, inter-comparisons are performed between space and time collocated data derived from two satellite sensors. For instance, Figure 9 shows an example of comparisons between wind speed (left panel) and direction (right panel) matchups from ASCAT and Sentinel 1A SAR.
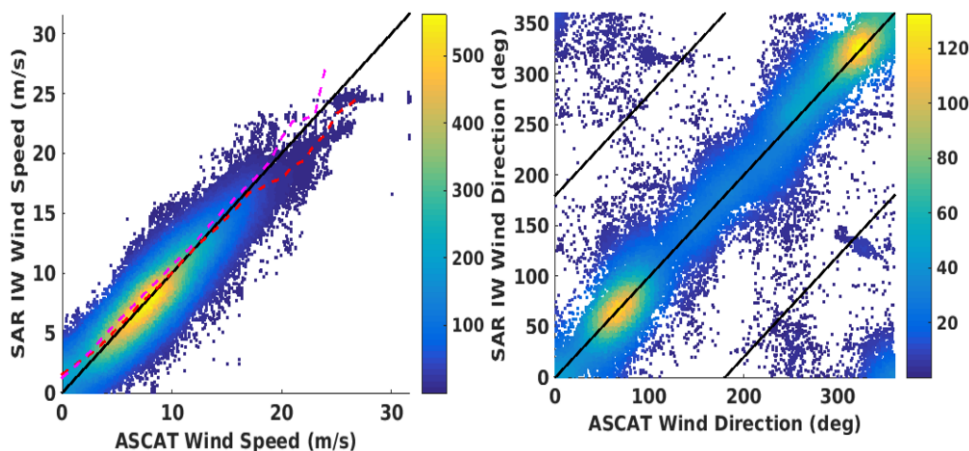
Figure 9: Sentinel SAR IW wind speed (left panel) and direction (right panel) versus ASCAT retrievals. Results are shown for all scatterometer and SAR matchups occurring over the North West Atlantic oceanic area.

5.3   *Measurements / Data*

Wind measurements are perhaps one of the most ambiguous metocean properties. The standard wind speed at 10 m height is almost never measured directly. Even if an anemometer mast has a sensor at 10 m above the mean water surface, it is always located in finite depth where the level of this surface varies in response to tides, seiches and other forcings. Measurements at deep-water offshore rigs are placed at elevations much higher than 10 m, and measurements from offshore discus buoys are typically below 10 m height and are also subject to buoys' heave and tilt. Therefore, any of the in situ measurements require interpolation to the standard 10 m level before being used.

Such extrapolations are not unambiguous. They usually invoke the assumption of the wall boundary layer and logarithmic profile associated with it. Both are problematic if applied in a broad range conditions. For light winds (less than 5 m/s), the 10 m height can be outside the constant-flux layer , and for extreme conditions wave crests can be higher than 10 m, and certainly the buoy masts will be below crests over a wave period.

Babanin and McConochie (2013) conducted comparisons of mean wind speeds and wind-momentum fluxes, based on measurements throughout the wave boundary layer, including wave-follower measurements very near the surface. Significant deviations from the constant-

flux expectations are found, even if corrected for the Monin-Obukhov stratification effects. The turbulent stress towards the surface is reduced dramatically, some 7 times in their measurements, whereas the mean wind speed is increased by some 5% compared to predictions based on the logarithmic profile. Practical significance of such observations is large, for example, for measurements conducted within the Wave Boundary Layer by buoys. If such buoy wind speeds extrapolated away from the surface by means of logarithmic profiles, to the 10 m standard height or above, the actual values of wind speeds may be overestimated. If the buoys are used to directly measure turbulent stresses, then, depending on the height of the anemometer mast on the buoy, such stresses can be very essentially underestimated. In the meteorological context, implications of these results are not very clear. On one hand, the concept of the constant flux layer needs serious modifications. On the other hand, the observed reduction of the turbulent stresses can be expected, since near the wavy surface part of the momentum flux is supported by wave-induced pressure/velocity fluctuations (e.g. Hara and Sullivan, 2015). Relative change of the total vertical flux of horizontal momentum, if any, needs to be determined by means of detailed modelling of the boundary layer with account on wave-induced effects.

Measurements of winds in extreme tropical cyclones have been, and remain subject to controversy for the last decade due to a number of dynamics and thermodynamics involved due to presence of spray in the air, extended whitecapping on the surface, changes to the surface roughness and aerodynamics at extreme winds – all of which influence the wind profile in the boundary layer. Smith and Montgomery (2014) provide theoretical reasoning supported by observational evidence as to why significant departures from the normally assumed logarithmic layer might be expected, questioning its use in the inference of the drag coefficient at high wind speeds. They also draw attention to a study examining a range of boundary-layer schemes demonstrating that a recently articulated boundary-layer spin-up mechanism transcends the presence of a log layer.

Apart from in situ measurements, satellite remote sensing has become a broadly employed technology for metocean observations including estimates of the winds. Young et al. (2017) evaluated the performance of the satellite systems across the full magnitude of the measured values of U10. Their analysis shows that across the range 0–15 m/s, altimeter, radiometer, and scatterometer instruments provide values of U10 that are consistent with buoy data and between the various instrument systems. For wind speeds above 15m/s, the altimeter appears to underestimate U10, whereas the radiometer/scatterometer data appear in reasonable agreement with the limited fixed-platform anemometer data. The radiometer and scatterometer cannot accurately measure wind speed in heavy rain. The exclusion of these cases, which often are associated with high winds, produces a fair weather bias. The distance between altimeter tracks is often many hundreds of kilometers and the repeat time for a given track up to 10 days. This relatively course spatial coverage means that the altimeter potentially under-sampled storm events and may miss wind speed extremes. Cross validation between the instruments confirms that the altimeter underestimates extreme wind speeds. As reliable ground truth calibration data at high wind speeds are very limited, all systems (altimeter, radiometer, scatterometer) should be used with caution for wind speeds greater than 20m/s.

The final calibrated combined satellite database provides a valuable resource for the study of a wide range of metocean properties including the wind speeds. The datasets are available in the public domain (altimeter—Globwave, http://globwave.ifremer.fr/; radiometer/scatterometer—Remote Sensing Systems (REMSS), http://www.remss.com/).

5.4   *Analytical & Numerical Methods*

In Mao and Rychlik (2016), and Rychlik (2015), the spatio-temporal random model for variability of mean wind speed in Northern Atlantic was proposed. The model can be used to derive long-term wind speed distributions at fixed location and encountered by a vessel. Means

to evaluate parameters of the Weibull distribution for encountered wind speeds are given. The model can also be used to find the distribution of yearly maximums at fixed location and maximum wind speed along a rout. The model can also be used to simulate time series of mean wind speeds.

6.   ICE /ICEBERGS

6.1   Measurements / Data

With the Arctic Ocean becoming open of ice in summer, shipping and offshore industry are advancing into Arctic and other freezing seas. Moreover, because of the summer melt, multi-year ice is being replaced by the first-year ice in the Arctic which makes navigation potentially possible round the year. As a result, there is a surge of efforts on modelling the waves in ice in order to enable metocean forecast for the Arctic. Such forecast requires knowledge of the ice cover, its thickness and other properties such as floe size distribution in the Marginal Ice Zones (MIZ) in real time. Therefore, Arctic expeditions which include ice measurements are on the rise. In 2012-2017, U.S. Office of Naval Research funded two five-year campaigns through the MIZ and Sea State Departmental Research Initiatives (DRI) broadly dedicated to different aspects of wave-ice interactions, with significant ice component in both of them. The latter DRI focused on Arctic conditions during the late summer and early autumn, especially the freeze-up of the Beaufort and Chukchi seas, to capture the strongest storms and maximum open water. This focus complemented the MIZ DRI that was studying the summer breakup and ice retreat. In situ observations were collected primarily during respective two cruises in spring and autumn of 2015, supplemented by long-term moorings, autonomous platforms and satellite remote sensing (Thomson et al., 2013). A special issue of the Journal of Geophysical Research, dedicated to these filed campaigns, is in progress at the time of writing, where state-of-the-art methods of in situ ice measurements, as well as outcomes of the field campaigns will be described in detail.

Satellite measurements of ice, both in the Arctic and Antarctica, are largely limited to the percentage of water surface covered by ice (ice cover). Radiometers conduct and provide the ice cover routinely, but do not measure waves, and hence there was a need to distinguish water surface from icescape (i.e. to measure ice cover) by altimeters which also take direct measurements of wave height and estimate the surface winds over the open water as described above. Such method was developed in Liu et al. (2016). Because of the heterogeneous nature of sea ice (e.g. leads, cracks, and ripples), individual altimeter waveforms exhibit a greater variability than those from the open water. A threshold value for the standard deviation of Ku-band backscatter was used to detect waveforms over sea ice, with 0.2 dB being found to provide optimal results in comparison to the three-parameter classifier proposed earlier for the microwave radiometer. Thus, the one-parameter classifier was obtained and tested and the 0.2 dB threshold can be applied to all altimeter missions to measure ice cover.

New satellite technologies are able, in addition to the ice cover, to measure ice thickness and ice-floe distribution necessary for the operational wave forecast, are rapidly emerging. NASA's Ice, Cloud, and land Elevation Satellite (ICESat) ran a series of campaigns over Antarctica from 2003 to 2008 that were used by Kurtz and Markus (2012) to calculate ice thickness. The ICESat data produced ice thickness averages at a 25 km resolution with an uncertainty of 23 cm. High-resolution ice-floe imaging of MIZ is possible by means of TerraSAR-X or in optical diapason, but such data are not routinely acquired and computer requirements for storage and processing of such images in large quantities are still prohibitive.

6.1.1   Space-borne Measurements

According to Cooley et al. (2016), remote sensing techniques must have the appropriate balance of spatial and temporal resolution to effectively examine river break up processes. In their study, they apply an automated ice detection algorithm using MODerate-Resolution Im-

aging Spectroradiometer (MODIS) satellite imagery data to identify ice breakup patterns. MODIS reflectance is used to classify each pixel of an area as snow/ice, mixed ice/water or open water. The algorithm is used to examine the Mackenzie, Lena, Ob' and Yenisey rivers from 2000–2014. Results from the analysis identify many possible drivers for the breakup progression however they are dependent on the river system.

The Cloud-Aerosol Lidar with Orthogonal Polarization (CALIOP) is a satellite that has been making continuous global snow and ice measurements since 2006. The polar-orbiting CALIOP obtains data between 82°S to 82°N which provides insight into the Arctic ice cover. CALIOP has an advantage over the MODerate-Resolution Imaging Spectroradiometer (MODIS) passive remote sensor because it can make reliable measurements during both the daytime and night-time seasons. Lu et al. (2017) have developed a new retrieval method for surface type identification which they apply to the past 10 years of available data. Their results are validated against data taken from the MODIS/Aqua, NASA team and AMSR-E which indicate good agreement. Overall, CALIOP provides the ability to study ice cover year-round at higher temporal and spatial resolution compared to previous passive sensors.

The Finnish Meteorological Institute (FMI) has developed a new approach for generating real-time automated ice thickness charts. Karvonen et al. (2016) present the methodology and compare their results against reference data sets from the Russian Caspian ice charts provided by the Scientific Research Center Planeta. The ice thickness is estimated by combining a thermodynamic snow/ice model with Synthetic Aperture Radar (SAR) data that has been segmented using a series of algorithms. Karvonen et al. (2016) conclude that this method can estimate ice thickness with a relative error less than 30%.

A regional coupled model system, HAMMER, was developed as part of the IRO-2 project to provide sea ice forecasting. In March 2014, Dobrynin et al. (2015) completed a field campaign in the Barents Sea to test the HAMMER system. HAMMER is made up of an atmospheric model, a sea ice model, and an ocean circulation model. The ice concentration and ice thickness are initialized using remote sensing data. The system incorporates global weather and ice forecasting data from the European Centre for Medium Range Weather Forecasts (ECMWF) and the Arctic wide ice-ocean forecast (ICEDAS). The system updates the model initialization parameters daily based on new forecast and measurement data. Furthermore, this system has the capability to feed forecast data directly into a route optimization system. Overall, the researchers found that the HAMMER results were within reasonable agreement with the ship-borne observations.

6.1.2   Airborne Measurements

Airborne Electromagnetic (AEM) induction is a method of measuring sea ice thickness via an electromagnetic (EM) induction device suspended from helicopter or plane. With an EM induction device, it is possible to identify the water-ice interface from their contrasting electrical conductivity. With the addition of a laser altimeter, which ranges the air-ice interface, the thickness of the ice can be found. Hendricks et al. (2014) employed this measurement technique near Barrow, Alaska on their field campaign in April 2013 as a proof-of-concept. They found that one of the most significant advantages of this technique is that it can be used for surveys of shallow regions with grounded sea ice that would otherwise be inaccessible by boat. Further validation work including systematic surveys paired with satellite data will be needed to refine this technique.

6.1.3   Ice Management Trials

On the Offshore Newfoundland Research Expedition in April 2015, Neville et al. (2016) participated in a series of ice management trials near the south-east coast of Labrador. These trials were completed to gather data to support numerical models used to simulate ice management operations. Collected data was used to quantify the rate of ice management in terms of

the incoming and outgoing ice conditions. Methods used to collect field data involved aerial footage taken from a helicopter, ice drift beacons, and footage taken from the ship.

Oden Arctic Technology Research Cruise 2015 (OATRC 2015)

In autumn 2015, the Norwegian University of Science and Technology and the Swedish Polar Research Secretariat (SPRS) conducted a research cruise named the "Oden Arctic Technology Research Cruise 2015" (OATRC 2015) which was supported by the ExxonMobil Upstream Research Company. The research cruise involved two icebreakers, Oden and Frej, who sailed north of Svalbard to conduct full scale trials of new technologies relating to ice management (Lubbad et al. (2016)).

One of the technologies tested on OATRC 2015 was a shipborne sea ice thickness and concentration measurement system. Lu et al. (2016) installed a series of shipboard Ice Concentration and Ice Thickness Cameras which worked with their corresponding image detection algorithms to provide a real-time quantification of the surrounding ice. The Ice Concentration Cameras were set up on the bridge facing obliquely towards the transiting direction. This provided a 180° view of the ice conditions towards the horizon. The Ice Thickness Camera was installed off the port side of the bridge looking vertically downward. This was done in order to obtain images of ice tilted up which exposed their thickness. The results of their trials indicated good agreement between the measured concentration and the ice observer's documentation. Measurements from the Ice Thickness Camera were compared against the measurements of an Electromagnetic (EM) inductive device which was mounted on the bow of the ship. The Ice Thickness Camera illustrated good agreement with the EM inductive device measurements.

Using the data collected from OATRC 2015, Holub et al. (2017) describe a system which can provide real-time ice drift measurements by applying photogrammetric feature detection and matching algorithms to marine radar or synthetic aperture radar (SAR) satellite data. The ship's radar data is evaluated and compared against GPS drift beacons deployed during the research cruise. The initial results showed that radar and SAR can successfully be used to measure ice drift.

6.1.4   Subsea Measurements

Upward Looking Sonar (ULS) instruments can be used to examine the underwater profile of ice with a temporal resolution of about 1 second, and horizontal and vertical spatial resolutions of about 1 m and 0.05m respectively. Fissel et al. (2015) applied methods of geometrical characterization to seven-years of ULS data to identify large ice keels, hummocky ice features, and massive ice features. Continuous year-long ULS data was obtained from the Chukchi Sea, Beaufort Sea and off the coast of North East Greenland. The results of the analysis allowed the researchers to identify geographical variability of massive ice features (MIF) between NE Greenland and the Canadian Beaufort Sea. The number of MIF detected in NE Greenland was found to be 5.5 times greater than the number of MIF in the Beaufort Sea location.

6.1.5   Icebergs

Detection

Iceberg detection is most commonly performed by visual inspection, sometimes with the aid of satellite imagery or marine radar. However, these methods tend to lose their effectiveness in low visibility, poor weather conditions and high sea states. Abdel-Moati et al. (2017) propose the application of infrared based optical imaging technology in automated iceberg detection. The primary advantages of infrared sensors are their higher immunity to fog and ability to work in the dark. Abdel-Moati et al. completed a series of laboratory experiments investi-

gating three infrared regions while varying the polarization. They found that none of the combinations of imagers and polarization filters worked in all scenarios and instead suggested that a multi-spectral camera could be used instead.

Drift Forecasting

An operational iceberg drift forecast model was developed by Turnbull et al. (2015) in support of a scientific coring campaign off Northwest Greenland. The coring operations took place from August-October 2012 in Melville Bay where there was a high concentration of icebergs. The model was designed to incorporate near real-time input including, in-situ metocean parameters, observed iceberg drift and size, tidal currents, and weather forecasts. Hindcast simulations were used, applying observed iceberg trajectories to tune the air and water drag coefficients of a given iceberg. During the campaign, researchers found that the model performed well in locations with strong and persistent non-tidal currents. The model did not perform as well in locations where ocean currents were dominated by tidal and inertial forcings.

Profiling

Due to the considerable threat of icebergs to offshore facilities and operations, iceberg modelling has been an important area of research for the design of offshore structures, drift forecasting and iceberg management systems. In recent years, photogrammetric methods have been used to obtain accurate 3D profiles of numerous icebergs.

In the summer of 2014, a group from Memorial University of Newfoundland completed a series of autonomous iceberg mapping missions by using an Autonomous Surface Craft (ASC) (Wang et al. (2015)) and a Slocum underwater glider (Zhou et al. (2014)). For the above-water surveys, the ASC collected iceberg images, GPS positions, laser range information and vehicle orientation information. Wang et al. (2015) applied methods of volume intersection and occluding contour finding to generate 3D models of the icebergs. Underwater mapping of an iceberg was performed by Zhou et al. (2014) using a mechanical scanning sonar. Insufficient data was collected to form a closed surface; however these trials confirmed the potential of this system.

In June of 2012, Younan et al. (2016) conducted a field program offshore Newfoundland and Labrador collecting 3D profiles of grounded and floating icebergs. The above-water profile of the iceberg was obtained by circumnavigating an iceberg while collecting: photographs from 3 ship-mounted cameras, position and heading data, and laser range data. Photogrammetric methods were then used to generate a 3D model. The underwater iceberg mapping was completed using a remotely operated vehicle (ROV) outfitted with a multibeam sonar. During this program 35 high definition iceberg models were successfully logged and generated.

6.1.6   Thermodynamics

According to Turnbull et al. (2016), thermodynamic models of sea ice can be used in predicting seasonal patterns in ice concentration, thickness, and flexural strength. In February 2016, Turnbull et al. deployed six Temperature Acquisition Cables (TACs), along with two anemometers on snow-free, land-fast sea ice in Pistolet Bay, Newfoundland. Combining these measurements with the available meteorological data, an alternative method for solving the sea ice surface temperature was developed. This method consists of a linear function which depends on the surface meteorological parameters. With further development of this model, Turnbull et al. suggests that it could be used for remote estimation of ice compressive and flexural strength.

6.2   ICE-STRUCTURE INTERACTION

6.2.1   Sea Ice

When a ship is transiting in sea ice, its hull is subjected to a variety of ice impact pressures. Since the 1980's, computerized measurement techniques have been used to collect time-series impact loads on various vessels. This has allowed for the development of structural design criteria based on the pressure versus contact area relationship obtained from full scale data. Most recently, a large shuttle tanker, the M/T Timofey Guzhenko was outfitted with state-of-the-art sensors capable recording continuous long-term ice pressures and structural responses. Between 2009 and 2013, the system recorded close to 30,000 bow impact events. From this dataset, Kim et al. (2016) investigate three impact events representing peak force and peak local pressure events. Using finite element (FE) analysis, the measured ice pressure data was applied to an FE model of the ship's grillage. The results of this analysis were used as a verification check for the ice load monitoring system which confirmed the structure did not experience yielding.

Development of a numerical ice simulator was undertaken as part of DYPIC (Dynamic Positioning in ICE), an international research project focused on developing Dynamic Positioning technology in ice (Kerkeni et al, 2014). The Norwegian University of Science and Technology started developing the model in 2010 using a physics engine to model rigid body motions and evaluate contact forces of a DP vessel operating in floe ice. Some of the latest model developments are presented in Scibilia et al. (2014) with the incorporation of an ice splitting model along with an ice fracture solver which simulates local ice compaction around an icebreaker. Scibilia et al. use data obtained on the OATRC 2012/2013 trials to make qualitative comparisons of observed physical processes with the results of the numerical model. Based on their simulations, they found that the results exhibited the same visual behaviour as observed in the field.

The GEM simulation tool (Daley et al. (2014)) was initially developed as part of the STePS2 project at Memorial University of Newfoundland as a tool used to estimate local ice loads on a vessel operating in pack ice. In this simulation, every ship-ice and ice-ice collision is modelled. One of the key features of GEM is that simulations can be run much faster than real-time. This is partly attributed to underlying assumptions of the collision model which reduces 2D collisions into equivalent 1D collisions. In Daley et al. (2014) a sample simulation is provided along with the resulting impact load statistics. These results are then compared against the available data concerning ice impact loads in sea ice.

Through incorporating a 2D discrete element method, Zhou and Peng (2014) propose a numerical method for simulating the performance of a dynamically controlled vessel in level ice. The waterline of the hull and ice edge are modelled using a series of nodes. In the case of the hull waterline, a closed polygon is formed; whereas the nodes of the ice edge will form a broken line. Ship-ice interaction is detected using a polygon-based detection technique. Three separate contact scenarios are used in solving for the ice induced forces. The results of the model were validated against sea trials of a full-scale R-class icebreaker. A dynamic positioning model was implemented using a line of sight guidance scheme and a PID algorithm.

A similar 2D discrete element method is used by Dai (2016), however instead of modelling level ice, pack ice was modelled using circular floes. In addition to ship-ice collisions, ice-ice collisions were also considered.

Hisette et al. (2017) created a simulation using the discrete element method to model a ship breaking through an ice ridge. Artificial ice ridges are generated in the simulation using buoyancy, where a series of submerged ice blocks are released below the surface and float up to form an ice ridge. The simulation results are compared against model tests which include a

qualitative comparison of underwater videos of the ridge and a quantitative comparison of time-series data.

6.2.2   Laboratory Testing

A series of dynamic positioning (DP) model scale tests were complete by Wang et al. (2016) in the ice tank facility at OCRE-NRC in 2015. The trials consisted of 372 runs using 17 different ice sheets. The test variables included floe size, floe thickness, concentration, inclusion of brash ice, ice drift speed, and heading direction. The ice loads were not directly measured during the tests, but instead estimated from the thruster response. An NRC developed DP algorithm was used in the model and provided satisfactory behavior in most cases. Manual control of the model was required during some of the more severe ice conditions tested.

Bergsma et al. (2014) examine the use of artificial ice as an alternative to refrigerated ice for testing the ice submersion resistance of a ship at model scale. A series of towing tank tests were completed at the Maritime Research Institute Netherlands (MARIN) using pre-sawn polypropylene for artificial ice. The results of the tests with artificial ice were validated against the Lindqvist formula. It was found that the submersion resistance of the artificial ice was higher than the Lindqvist prediction at low ship speeds. Bergsma et al. assume that this is due to the friction of the material at low velocities. Good agreement with the Lindqvist prediction was achieved at higher ship velocities.

6.2.3   Iceberg Loading

In cases where icebergs pose a risk to offshore gravity based structures (GBS), special consideration must be given to ensure that the risk of a topsides impact is reduced to an acceptable level Stuckey et al. (2016). This is typically done by altering the geometry of the structure, either by elevating the topsides, or enlarging the footprint. To optimize the geometry of a GBS, Stuckey et al. (2016) developed a numerical model to estimate the frequency of icebergs that impact the topsides using 3D models of a given platform and iceberg models of various shapes and sizes. Iceberg models were generated from a database of iceberg profile measurements and set adrift next to the platform. The simulation was completed multiple times to gain a statistical understanding of the initial point of contact and crushing behaviour of the various iceberg shapes that might be encountered.

6.2.4   Ice Hydrodynamics

A review of the hydrodynamics of icebergs was undertaken in Sayeed et al. (2017). This review examines the current literature on iceberg and bergy bit motion during interaction and impact with an offshore structure. This topic is broken down into four main parts: the far field wave induced motions; the near field interaction effects; collision modeling; and a summary of past full-scale trials. It is brought to light that with the current state of research is lacking in many aspects of understanding the near field hydrodynamic effects of icebergs. It is argued that the inability to properly model these effects often lead to overestimations in impact velocity and therefore impact energy. Better understanding of hydrodynamic interaction could lead to improved load predictions allowing for more efficient design of offshore structures.

Sayeed et al. (2015) conducted model tests investigating the hydrodynamic interaction between ice masses and offshore structures. The variables tested included the size and shape of the ice masses as well as the wave particulars. Three spheres of different diameter along with an irregular shaped ice block were used as model icebergs. Their work showed that hydrodynamic proximity and wave reflection had a considerable effect on small ice masses near larger structures. A reduction in impact velocity is observed which indicates that the hydrodynamic effects cause a reduction in the impact load.

Experiments were performed by Chander et al. (2015) to investigate the forces involved in submerged ice collisions. This was done in Memorial University's Fluids lab using a high-speed camera to film the trajectory and impact of a spherical ice model (10cm polypropylene) with a model ship hull. A waterproof load cell was used to record the impact forces. Added mass was calculated using the velocity and acceleration data obtained from image analysis performed using MatLab. In their experiments, the added mass coefficients were found to be close to 0.5 for lower values of Reynolds number but increased suddenly as the ice model approached the plate. For all tests, the added mass coefficient was at a maximum at the point of impact.

6.2.5   Ice Accretion

Ice accretion can pose a significant hazard to vessels and offshore structures in cold regions. Not only does ice accretion lead to unsafe working conditions for crew on deck, but can also threaten the stability of the vessel which may cause the vessel to capsize. Mintu et al. (2016) provide a review of existing literature related to ice accretion covering: field measurements, experimental studies and numerical models. A critique of the current international standards is also provided.

In their review, Mintu et al. (2016) emphasize the complexity of ice accretion where the amount of icing will depend on several parameters including the meteorological conditions, the wave heights, vessel speed and direction relative to the waves. Experience also shows that the amount of icing is also dependant on the location of the structure/vessel relative to the location of the spray and waterline.

Examining the state-of-the-art research on ice accretion, Mintu et al. (2016) found that many research approaches tend to focus on just one aspect of ice accretion due to high level of complexity. On the other hand, they have found that classification societies and regulatory authorities have oversimplified the problem, providing generalized equations for determining icing allowances. Furthermore, they have found a lack of consistency between the standards, indicating further research on ice accretion is needed to develop a more consistent design standard.

Through analysis of infrared and visual images, Fazelpour et al. (2016) proposes a method for measuring the ice thickness on a cylindrical component. Laboratory experiments were conducted in a cold room using two cylindrical components: one covered by saline ice, and one covered by fresh ice. The experimental results indicate that the method is reliable in determining the thickness of ice.

6.3   Analytical & Numerical Models

Shu et al. (2015) make an assessment of sea ice simulations in the Coupled Model Inter-comparison Project Phase 5 (CMIP5) during 1979 to 2005. Forty-nine models, almost all of the CMIP5 climate models and earth system models with historical simulation, are used. For the Antarctic, multi-model ensemble mean results can give good climatology of sea ice extent (SIE), but the linear trend is incorrect. For the Arctic, both climatology and linear trend are better reproduced. Sea ice volume is first evaluated but with too small results as a result of sea ice thickness simulated in CMIP5 is too thin.

Croxall et al. (2015) present the new 3.6 version of the Louvain-la-Neuve sea ice model (LIM), which will be used for the next Climate Model Inter-comparison Project (CMIP6). In the new model, the robustness, versatility and sophistication of the code are focused on and improved. The model simulated sea distributions at a global scale with nominal 2-degree resolution and at a regional scale with 2 km resolution around the Svalbard Archipelago. The results are consistent with the observed data.

Rae et al. (2015) adopt the new sea ice configuration GSI6.0 to simulate the sea ice extent, thickness and volume compared with the previous configuration and with observationally-based datasets. In the Arctic, the sea ice is thicker in all seasons than in the previous configuration, and there is now better agreement of the modelled concentration and extent with the HadISST dataset. In the Antarctic, a warm bias in the ocean model has been exacerbated at the higher resolution of GC2.0, leading to a large reduction in ice extent and volume.

Stroeve and Notz (2015) present the insights on past and future sea-ice evolution from combining observations and models. It is concluded that models and observations agree well on the sensitivity of Arctic sea ice to global warming. In contrast, a robust reduction of the uncertainty range of future sea-ice evolution remains difficult, in particular since the observational record is often too short to robustly examine the impact of internal variability on model biases. Process based model evaluation and model evaluation based on seasonal-prediction systems provide promising ways to overcome these limitations.

Interaction of ice and structures

Yu et al. (2015) simulate the wind turbine dynamic response under surface ice loads using FAST. For conditions in which the ice forcing is essentially decoupled from the structural response, ice forces are established from existing models for brittle and ductile ice failure. For conditions in which the ice failure and the structural response are coupled, a rate-dependent ice model is described. Analytical ice mechanics models are presented that incorporate ice floe forcing, deformation, and failure. For lower speeds, forces slowly build until the ice strength is reached and ice fails resulting in a quasi-static condition. For intermediate speeds, the ice failure can be coupled with the structural response and resulting in coinciding periods of the ice failure and the structural response. A third regime occurs at high speeds of encounter in which brittle fracturing of the ice feature occurs in a random pattern, which results in a random vibration excitation of the structure.

Shu et al. (2017) study on small wind turbine icing and its performance. Results show that ice rapidly reduces the rotation speed and load power of the wind turbine. The ice growth rate rises initially and then declines with time. Ice linearly increases from the root to the tip and mainly accumulates at the leading edge. As the rotation speed slows down, the ice-covered area moves to the pressure side. Higher wind velocity and lower temperature lead to more severe ice, but they do not change the ice shape.

Metrikin et al. (2015) investigates dynamic positioning (DP) in level ice conditions using experimental and numerical approaches. A novel numerical model for simulating DP operations in level ice is presented. The fracture of level ice is calculated on-the-fly based on numerical solution of the ice material failure equations, i.e., the breaking patterns of the ice are not pre-calculated. Several ice basin experiments are reproduced in the numerical simulator, and the results of the physical and numerical tests are consistent.

Bae et al. (2016) present the numerical simulation for the collision between side structure and level ice in event of side impact scenario. Different models of indenter were taken into account in order to observe structural responses and influences of external parameters, namely ice topology, while the described location parameters were taken as the ship's internal parameters. Impact force was presented with total energy, as well as the ratio between kinetic and internal energy. The deformation pattern was used as a verification of the collision process and its subsequent results.

Song et al. (2015) present the fluid-structure-interaction analysis of an ice block-structure collision. Numerical simulations of a collision between an ice block and a floating structure have been carried out using the FSI analysis technique of the LS-DYNA code for a more realistic and accurate prediction of the impact loadings. The simulation results were compared with laboratory experiments where a floating structure was impacted with an approximately

one ton ice block at a speed of 2 m/s. The results of the numerical simulations compared favorably with actual experiments using freshwater ice blocks.

Mierke et al. (2015) study the applicability of the Lattice Boltzmann based free surface flow solver elbe to the simulation of complex ship-ice interactions in marine engineering. Basic methodology and initial validation of the fluid-structure coupling of elbe and ODE is presented. As elbe uses graphics processing units (GPUs) to accelerate the numerical calculations, the coupled numerical tool allows for investigations of ship-ice interactions in very competitive computational time and on off-the-shelf desktop hardware.

Hu and Zhou (2015) make an experimental and numerical study on ice resistance for ice-breaking vessels. Different numerical methods are presented to calculate ice resistance, including semi-analytical method and empirical methods. A model test of an icebreaking vessel that was done in an ice basin has been introduced for going straight ahead in level ice at low speed, with a good comparison between model test results and numerical results.

Huisman et al. (2016) present a numerical model to predict the interaction between floating objects and the surrounding level ice, especially breaking of level ice due to bending. This method assumes the formation of circumferential cracks as a result of the bending moment in order to achieve a more realistic breaking pattern. The ice-breaking model is validated for a two-dimensional elastic beam.

7.   COUPLED PHENOMENA

Wave-induced effects in the lower atmosphere and the upper ocean have been a major research topic over the last decade (see e.g. Babanin et al. (2012) for introduction). It is rapidly becoming clear that many large-scale geophysical processes are essentially coupled with the surface waves, and those include weather, tropical cyclones, storm surges, climate and other phenomena in the atmosphere, at air/sea and sea/land interface, and many issues of the upper-ocean mixing and ocean currents below the surface. Besides, the wind-wave climate itself experiences large-scale trends and fluctuations (Young et al., 2011), and is subject to changes in the weather climate.

Before that, coupling of the wave-related air-sea interactions into weather and climate research had not been conducted due to two main reasons. In terms of geophysics, the reason is the traditional perception that processes of such distant scales can be studied and modeled separately, and exchange between the scales can be parameterized as some larger-scale average (mean fluxes of energy and momentum in this case). In technical terms, the computational costs of such coupling have been prohibitive until recently. Things, however, are changing.

7.1   Wave Breaking

Wave breaking, if it did not exist, would have to be invented. Its role in the coupled air-surface-ocean systems is hard to overestimate. On the surface, it limits the wave growth and hence prevents occurrence of very high waves, and serves as a major dissipation mechanism in wave models. Above the surface, it facilitates the fluxes of momentum and energy, heat and moisture. Breaking produces spray and spume, which links waves to the aerosol production and thus all the way to inland corrosion, cloud physics, climate. Below the surface, breaking is a major source of turbulence and the main source of bubbles. The former is relevant for ocean mixing, sediment sediment suspension and transport, the latter to gas exchange, aeration and thus to biology, underwater acoustics. Wave momentum lost due to the breaking goes to surface currents and contributes to scattering of surface debris and pollutants.

Wave breaking is closely related to the problem of rogue waves. Those are waves of maximal possible height, and this height is controlled by the breaking. Babanin and Rogers (2014) argued that the enhancement above the mean wave height can be due to quasi-linear superposition of waves and/or because of nonlinear effects such as instabilities of wave trains. Both

appear to be important and possible. Individual waves can be focused into a superposition due to either dispersive or directional features of wave fields. While probability of the former in oceanic conditions is very low, the directional focusing appears to be rare, but regular events. Nonlinear wave fields should be separated into stable and unstable conditions, with different probability distributions for wave heights/crests and therefore wave breaking. In stable conditions, wave statistics are determined by the quasi-linear focusing, whereas in unstable wave trains high transient wave events can occur. Their maximal height/steepness is determined by combined dynamics of the instability growth and the limiting wave breaking. Research argument about relative importance of linear superposition and nonlinear dynamics, leading to wave breaking, is continuing (e.g. Chalikov and Bulgakov, 2017).

With the growing interest to the wave-coupled phenomena, wave-breaking effects in the coupled systems have been actively studied. Brumer et al. (2017) considered concurrent wave-field and turbulent flux measurements acquired during the Southern Ocean (SO) Gas Exchange (GasEx) and the High Wind Speed Gas Exchange Study (HiWinGS) projects. These permitted evaluation of the dependence of the whitecap coverage on wind speed, wave age, wave steepness, mean square slope, and wind-wave and breaking Reynolds numbers. Xie (2016) considered effects of winds on breaking in surf zone, using a two-phase flow model. Both spilling and plunging breakers over a steep (1:35) sloping beach have been studied under the influence of wind, with a focus during wave breaking. Detailed information of the distribution of wave amplitudes and mean water level, wave-height-to-water-depth ratio, the water surface profiles, velocity, vorticity, and turbulence fields have been presented and discussed. The inclusion of wind alters the air flow structure above water waves, increases the generation of vorticity, and affects the wave shoaling, breaking, overturning, and splash-up processes.

The important role of wave breaking in dissipation and models for wave forecast remain in focus of research. Zieger et al. (2015) discussed a new whitecapping dissipation function in WAVEWATCH-III. The new dissipation term features the inherent breaking term and a cumulative dissipation term, which is due to breaking of short waves caused by longer waves in the spectrum. Salmon et al. (2015) considered scaling of depth-induced breaking in spectral models. A joint scaling dependent on both local bottom slope and normalized wavenumber is presented. In order to account for the inherent differences between uni-directional (1D) and directionally spread (2D) wave conditions, an extension of the wave breaking dissipation models is proposed. By including the effects of wave directionality, rms errors for the significant wave height are reduced for the best performing parameterizations in conditions with strong directional spreading. Linking wave models with the coupling problem, Scanlon et al. (2016) estimated whitecap coverage from such models. High-resolution measurements of actively breaking whitecap fraction and total whitecap fraction from the Knorr11 field experiment in the Atlantic Ocean are compared with estimates of whitecap fraction modeled from the dissipation source term of the ECMWF wave model. The results reveal a strong linear relationship between model results and observed measurements, thus indicating that the wave model dissipation is an accurate estimate of total whitecap fraction.

7.2   *Wave-current interactions*

The surface waves are wind-generated, but the respective fluid motion is mostly part of the water side of interface and is strongly linked to the upper-ocean dynamics including the ocean currents. Wave-current interactions are common conditions both in the open ocean and in coastal areas. Major currents such as the Gulfstream, Kuroshio, or Agulhas are well known for harsh seas and high likelihood of abnormal (rogue) waves. Tidal inlets with waves on strong and variable currents are a typical feature of shipping routes in coastal areas. While linear effects of currents on waves, such as refraction, Doppler shift, or relative speed with respect to the wind are assumed to be implicitly or explicitly included in wave-forecast models (often unverified and not validated), nonlinear effects are usually left out or, at this stage, even unknown. These include changes to nonlinear interactions in the presence of currents

with horizontal or vertical velocity gradients, wave–current energy and momentum exchanges, nonlinear modifications of the wave spectrum.

The review paper by Babanin et al. (2017) outlines principles of phase-resolving and phase-average wave models, with emphasis on the state of the art of wave-current interaction physics. They argue that these interactions are the least well-developed part of such models. Linear and nonlinear dynamics of waves on currents are discussed; depth-integrated and depth-varying approaches are described; examples of numerical model performance for waves on currents in realistic oceanic scenarios are presented.

Waves, in turn, can substantially influence the surface currents through their Stokes drift, and even more so through radiation stress due to the momentum lost in wave breaking (even in deep water). These influences are largely missing in modelling the ocean circulation of open oceans, and they certainly need to be reinstated because of their importance, for example, in search and rescue missions. In principle, this can be done by coupling the wave models with the circulation models, but this should be done with caution. The present-day wave forecast models were not designed to produce correct fluxes for input and dissipation of energy, but rather to provide an approximate balance of those in order to predict the resulting wave growth and wave height reasonably well.

Most essential is the role of waves in influencing and even producing currents in finite depths. Here wave breaking is extensive, and this role is known and well accounted for in coastal circulation and coastal engineering models. Apart from direct wave-current applications, a more complex suit of wave current-turbulence interactions, both on the atmospheric and ocean sides, is gaining attention over the recent years. While energies involved are small in the context of changes to the waves or currents, they may play an additional and missing feedback in the atmospheric boundary layer, where airflow then generates both surface waves and currents, and in the upper ocean mixing.

A number of laboratory and field experiments have been conducted to pin down elements of the missing wave-current physics recently. In laboratory, Rapizo et al. (2016) investigated the effects of a co-flowing current field on the spectral shape of water waves. The results indicate that refraction is the main factor in modulating wave height and overall wave energy. The structure of the current field varies considerably, some current-induced patterns in the wave spectrum were observed. At high frequencies, the energy cascading generated by nonlinear interactions is suppressed, and the development of a spectral tail is disturbed, as a consequence of the detuning of the four-wave resonance conditions. Furthermore, the presence of currents slows the downshifting of the spectral peak. The suppression of the high-frequency energy under the influence of currents is more prominent as the spectral steepness increases. The energy suppression is also more accentuated and long-standing along the fetch when the directional spreading of waves is sufficiently broad. Additionally, the directional analysis shows that the highly variable currents broaden the directional spreading of waves. The broadening is suggested to be related to random refraction and scattering of wave rays. Thus, the variable currents have significant implications both on spectral and phase-revolving (i.e. rogue waves) evolution of wave fields.

Laboratory study by Toffoli et al. (2015) investigated specifically rogue waves in opposing currents. Interaction with an opposing current amplifies wave modulation and accelerates nonlinear wave focusing in regular wavepackets. This results in rogue waves, even if the wave conditions are less prone to extremes. Laboratory experiments in three independent facilities were presented to assess the role of opposing currents in changing the statistical properties of unidirectional and directional mechanically generated random wavefields. The results demonstrate in a consistent and robust manner that opposing currents induce a sharp and rapid transition from weakly to strongly non-Gaussian properties. This is associated with a substantial increase in the probability of occurrence of rogue waves for unidirectional and directional

sea states, for which the occurrence of extreme and rogue waves is normally the least expected.

The stronger nonlinearity in adverse currents signifies higher wave steepness, which must affect the rate of energy dissipation. Rapizo et al. (2017) studied the current-induced dissipation through a data set in the tidal inlet of Port Phillip Heads, Australia. The wave parameters analysed were significantly modulated by the tidal currents. Wave height in conditions of opposing currents (ebb tide) can reach twice the offshore value, whereas during co-flowing currents (flood), it can be reduced to half. The wind-wave model SWAN is able to reproduce the tide-induced modulation of waves and the results show that the variation of currents is the dominant factor in modifying the wave field. In stationary simulations, the model provides an accurate representation of wave height for slack and flood tides. During ebb tides, wave energy is highly overestimated over the opposing current jet. A modification to enhance dissipation as a function of the local currents was proposed. It consists of the addition of a factor that represents current-induced wave steepening and it is scaled by the ratio of spectral energy to the threshold breaking level. The new term asymptotes to the original form (Zieger et al., 2015) as the current in the wave direction tends to zero. The proposed modification considerably improves wave height and mean period in conditions of adverse currents, whereas the good model performance in co-flowing currents is unaltered.

Overall, wave-current interactions are the last loose element of physics of wave forecast models, and, to an extent, of ocean circulation modeling. A rich variety of dynamics are involved, some of which are not well understood, and complicated mathematics to describe such dynamics, make it an exciting research field at the boarder of wave, ocean and meteorological applications.

7.3   *Wave-ice interactions*

Wave-ice interactions have long been an exotic field of research, but with the Arctic opening from ice in summer months, epy wave-ice modeling acquires important practical meaning. Among the various theories to explain wave-ice interactions, some differ qualitatively, i.e. wave scattering (without dissipation) and dissipation (with or without scattering); others differ quantitatively to the extent that some theories predict wavelength to increase in presence of ice, whereas others predict wavelength to decrease. In the field, all the mechanisms are acting together, depending on their relative magnitude, and practical guidance of the existing theoretical knowledge in forecasting waves in marginal ice zones is limited. Additional complications in this regard are due to necessity of also knowing initial conditions for the ice coverage and properties, and to be able to predict effects of waves on ice—this makes wave-ice interaction an essentially coupled problem.

The wave-ice problem can be roughly subdivided into three large groups of interactions. First is the interaction of waves with solid or uniform ice. Note that solid and uniform is not the same. Solid ice can consist, for example, of pancake ice floes frozen together, whose structure is then not uniform. At the other end of extremes, the frazil ice is uniform, but not solid. Visco-elastic properties of ice in such conditions cause dissipation and change of rate of propagation of wave energy. Below the ice, additional turbulent dissipation occurs in the ice-water boundary layer, and scattering of wave energy by ice ridges further contributes to wave-energy attenuation in the main wave propagation direction (without dissipating he energy).

Once the ice is broken, which is the definition of the Marginal Ice Zone (MIZ), the dissipation mechanism is different. It is due to various interactions of ice floes with each other, such as collisions, rafting etc. – all of which take energy from the mean wave motion.

For wave models to be able to predict waves in ice automatically, they should be able to identify the moment of ice breakage by waves. Dimensionless criteria of such breakage in the

broad range of ice conditions remain an open research issue, particularly as the ice conditions are also not usually known in the operational regime.

A few field experiments have demonstrated the fracture and break up of ice pack and therefore the retreat of ice edge induced by strong wave events in both the Arctic and Antarctic MIZs (e.g. Collins et al., 2015, Kohout et al., 2016). A potential and more effective mechanism that accelerates ice retreat may be the positive wave-ice feedback discussed by Thomson and Rogers (2014): due to the fetch effect, the gradual reduction of ice cover provides more opportunities for the emerging of energetic waves, and subsequently such waves can propagate much farther into ice and cause much more ice break-up. The influences of turbulent characteristics of under-ice currents and ice drift on the energy dissipation rates of waves propagating below continuous ice cover were investigated in situ by Marchenko et al. (2016).

Remote sensing methods, like in the other branches of Metocean applications, are increasingly becoming an essential method of field research of wave-ice interactions in their own right. Given the novelty of the problem, some of the emerging methods are highly innovative. Cambell et al. (2014) conducted observation of waves interacting with ice by using stereo imaging. This was applied to three distinct ice types: brash, frazil, and pancake. Ardhuin et al. (2017) offered a new method of measuring waves in ice by using SAR imagery. The iterative nonlinear algorithm estimates phase-resolved deterministic maps of wave-induced orbital velocities, from which elevation spectra can be derived.

Analytical research was the strong part of the wave-ice discipline even before the present boom, and with the new motivation it continued to offer new theories and advances to existing theoretical mechanisms. Mosig et al. (2015) conducted comparison of visco-elastic models for wave attenuation. Montiel et al. (2016) proposed a new method to solve the traditional time-harmonic multiple scattering problem under a multidirectional incident wave forcing with random phases. Zhao and Shen (2016) suggested a continuum approach by means of diffusion approximation to the ocean wave scattering by ice floes. A problem of wave-ice speed, connected with the dissipation and yet separate, was comprehensively addressed by Collins et al. (2016) whose investigation considers theoretical models and empirical studies related to the dispersion of ocean surface gravity waves propagating in ice covered seas.

Field and analytical research is usually underpinned by laboratory experiments which allow us to look in details on physical mechanisms involved. Bennets et al. (2015) offered an experimental model of transmission of ocean waves by an ice floe. Thin plastic plates with different material properties and thicknesses were used to model the floe. Toffoli et al. (2015) used the model to validate in laboratory conditions the canonical, solitary floe version of contemporary theoretical models of wave attenuation. Amplitudes of waves transmitted by the floe were presented as functions of incident wave steepness for different incident wavelengths.

Thus, the rich and complex nature of wave-ice interactions caused a surge of dedicated research in recent years. This combined the relative novelty of the topic with the sudden demand on the practical outcomes for wave forecast in the freezing seas and specifically in MIZ. The research topic however remains fragmented at this stage and is in still need of some common thread to be established.

7.4   *Atmospheric wave boundary layer*

Connection of the surface waves with the wind is most intimate and makes the Wave Boundary Layer different to any other boundary layer in fluid mechanics or geophysics. The wind generates the waves, but the waves then change the very wind which produced them. The waves do not provide a constant roughness because they grow, they move and they break. In the classical wall-layer sense, the waves are not roughness at all, as the roughness scale of the logarithmic profiles in the constant-flux layer is orders of magnitude smaller than the wave height. The logarithmic profile is characteristic of the constant turbulent flux, and in WBL

this is not the case. The total flux in WBL is indeed constant, but apart from the turbulent flux, it is also supported by form drag which goes into wave growth and tangential drag which passes momentum to the surface currents. As a result, the actual turbulent flux in the constant-flux layer is reduced towards the surface and the wind profile in WBL deviates from the logarithmic profile (see Babanin and McConochie, 2013, Hara and Sallivan, 2014). We refer to the new book of Chalikov (2016) which has chapters on wind-wave interactions and Wave Boundary Layer written by one of the leading experts in this field.

Since the concept of constant-flux layer and the role of the surface waves in modifying the balance of turbulent stresses very near the surface have already been discussed in Section 5A, here we will concentrate on the atmospheric wave boundary layer in other less common conditions. There are also specific changes to the atmospheric boundary layer at very light winds and very strong winds. In the latter case, the air is full of water droplets due to continuous wave breaking, and with water being 1000 times heavier than air, the spray can impact on the boundary layer substantially. This topic has been a subject of extensive research over the last decade.

Starting the review from extreme wind conditions, Smith et al. (2014) challenged the very concept of the logarithmic boundary layer in the inner core of the hurricanes. While their argument is meteorological, it refers to near surface peculiarities of the wind stress vector. This stress must be connected with the complex nature of wave spectrum in the hurricanes, i.e. the waves are always at angle to the wind in the tropical cyclones, up to 180 degrees in some quadrants (Liu et al., 2017).

Troitskaya et al. (2016) continued research of the boundary-layer spray in extreme-wind conditions by means of a theoretical model. Air-sea momentum exchange was investigated during the entire life cycle of a droplet, torn off the crest of a steep surface wave, and its fall down to the water, - in the framework of a model covering the following aspects of the phenomenon: (1) motion of a heavy particle in the air flow (equations of motion); (2) structure of the wind field (wind velocity, wave-induced disturbances, turbulent fluctuations); (3) generation of the sea spray; and (4) statistics of droplets (size distribution, wind speed dependence). Contrary to some other models of the sea spray, it is demonstrated that the spray in strong winds leads to an increase in the surface drag up to 40% on the assumption that the velocity profile is neutral.

In precision laboratory tests, Troitskaya et al. (2017) investigated the physical mechanism behind the sea-spray production in hurricanes experimentally. By means of high-speed video, they identified it as the bag-breakup mode of fragmentation of liquid in gaseous flows. This regime is characterized by inflating and consequent bursting of the short-lived objects, 'bags', comprising sail-like water films surrounded by massive liquid rims then fragmented to giant droplets with sizes exceeding 500 micrometers. From first principles of statistical physics, they develop a statistical description of these phenomena and showed that at extreme winds the bag-breakup is the dominant spray-production mechanism.

Cox et al. (2017) revisited another extreme-wind problem, the remarkable 1883 sea rescue where oil was used to reduce large breakers during a storm. Modeling of the oil film's extent and waves under the film suggests that large breakers were suppressed by a reduction of wind energy input. Modification of surface roughness by the film is hypothesized to alter the wind profile above the sea and the energy flow.

Behaviour of the atmospheric boundary layer at the other extreme, light wind, is probably understood even less than the hurricane conditions. In the meantime, it has practical significance in a broad range of applications, for example, water evaporation in ponds. Wen and Mobbs (2014, 2015) simulated laminar air–water flow of a non-linear progressive wave at low to moderate wind speeds. While in the water differences between the solutions of potential and viscous flows are very small, in the air they are substantial (Wen and Mobbs, 2014).

The velocity distribution in the airflow in the wave boundary layer is strongly influenced by the background wind speed and it is found that three wind speeds, U = 0, U = umax (the maximum orbital velocity of a water wave), and U = c (the wave phase speed), are important in distinguishing different features of the flow patterns. In the opposing wind from zero to 1.5 times the wave phase speed, it is revealed that at any speed of the opposing wind there exist two rotating airflows, one anti-clockwise above the wave peak and one clockwise above the wave trough. These rotating airflows form a buffer layer between the main stream of the opposing wind and the wave surface. The thickness of the buffer layer decreases and the strength of rotation increases as the wind speed increases. The profile of the average x-component of velocity reveals that the water wave behaves as a solid surface producing larger wind stress compared to the following-wind case.

Thus, in spite of being one of the oldest topics in the context of wave interactions with marine environments, the atmospheric boundary layer and wave influences there remain the active area of research. New features are being revealed not only at extreme ends of wind-wave interactions, i.e. light winds and hurricane, but also in benign and moderate wind conditions.

7.5   *Wave influences in the upper ocean*

Dynamic wave influences in the upper ocean can be subdivided into two parts: momentum which the waves pass to the surface currents and the energy which is passed to the upper layer of the ocean. The latter, apart from the currents, goes to the turbulence and mixes the ocean. If the mixing is limited to the ocean's mixed layer, then its effect is limited to sediment suspension and transport of other admixtures. If, however, the mixing through the picnocline occurs because it is close enough to the surface (which is usually the case in spring-summer period), then such mixing can affect thermohaline circulation, cool the surface – with important consequences for large-scale processes discussed in Section 7.6 below. Note that we do not include wave breaking influences here, which were the topic of Section 7.1 they are powerful bursts of momentum and energy transfer, but are different: random, sporadic and concentrated very near the surface, at the scale of wave height.

Wave momentum is present in the ocean as Stokes drift and is ultimately passed to the ocean through wave breaking (although some amount of it goes back to the air (Iafrati et al., 2014)). The Stokes drift is easily derived for monochromatic waves, but not so directly for spectral waves which the real ocean seas always are. Breivik et al. (2016) explored a new approximation to the Stokes drift velocity profile based on the exact solution for the Phillips spectrum. The profile is compared with the monochromatic profile and the recently proposed exponential integral profile. ERA-Interim spectra and spectra from a wave buoy in the central North Sea are used to investigate the behavior of the profile. It is found that the new profile has a much stronger gradient near the surface and lower normalised deviation from the profile computed from the spectra. Based on estimates from two open-ocean locations, an average value was estimated for a key parameter of the profile. Given this parameter, the profile can be computed from the same two parameters as the monochromatic profile, namely the transport and the surface Stokes drift velocity.

Another attempt on Stokes forces in phase-average equations was done by Suzuki and Fox-Kemper (2016). This interesting paper describes Craik-Leibovich equations of the dynamics of upper ocean flow interacting with nonbreaking, not steep, surface gravity waves. It formulates the wave effects in these equations in terms of three contributions to momentum: Stokes advection, Stokes Coriolis force, and Stokes shear force. Each contribution scales with a distinctive parameter. Moreover, these contributions affect the turbulence energetics differently from each other such that the classification of instabilities is possible accordingly. Stokes advection transfers energy between turbulence and Eulerian mean-flow kinetic energy, and its form also parallels the advection of tracers such as salinity, buoyancy, and potential vorticity. Stokes shear force transfers energy between turbulence and surface waves. The Stokes Corio-

lis force can also transfer energy between turbulence and waves, but this occurs only if the Stokes drift fluctuates. Furthermore, this formulation elucidates the unique nature of Stokes shear force and also allows direct comparison of Stokes shear force with buoyancy. As a result, the classic Langmuir instabilities of Craik and Leibovich, wave-balanced fronts and filaments, Stokes perturbations of symmetric and geostrophic instabilities, the wavy Ekman layer, and the wavy hydrostatic balance are framed in terms of intuitive physical balances.

In terms of the wave-induced turbulence, unrelated to the breaking, there are three different mechanisms proposed for generation of such turbulence over the years. None of them cancels the other two - all are feasible, so the upper-ocean dynamics is a matter of their relative significance. Historically the first one was due to viscous solutions of wave equations being able to produce vorticity which, stretched by random waves, becomes turbulence. The second mechanism (see Benilov (2012) for a recent update), is turbulence generated by potential (non-viscous) waves, hence the turbulence must be pre-existing, which is always the case in the ocean. The Benilov theory is a linear instability theory of 3D turbulence to 2D wave orbital motion, hence it is a mechanism different to Langmuir turbulence which requires Stokes drift and therefore nonlinear waves, and three-dimensional ocean. Therefore, Langmuir turbulence is a yet different mechanism. This is a phase-average theory where the Stokes drift shear plays a role of mean flow shear.

Over the reported period, all the three mechanisms were further explored by researchers. Filatov et al. (2016) considered nonlinear generation of vorticity by surface waves in water with non-zero viscosity, hence the first mechanism. They demonstrated that waves excited on a fluid surface produce local surface rotation owing to hydrodynamic nonlinearity. The effect was examined theoretically and an explicit formula for the vertical vorticity in terms of the surface elevation was obtained. The theoretical predictions were confirmed by measurements of surface motion in a cell with water where surface waves are excited by vertical and harmonic shaking of the cell. The experimental data are in good agreement with the theoretical predictions.

Tsai et al. (2015) worked with the second mechanism of wave-induced turbulence. Numerical simulation of monochromatic surface waves propagating over a turbulent field was conducted to understand the turbulence production by nonbreaking waves. The numerical model solves the primitive equations subject to the fully nonlinear boundary conditions on the exact water surface. The result predicts growth rates of turbulent kinetic energy consistent with previous measurements and modelling. It also validates the observed horizontal anisotropy of the near-surface turbulence that the spanwise turbulent intensity exceeds the streamwise component. Such a flow structure is found to be attributed to the formation of streamwise vortices near the water surface, which also induces elongated surface streaks. It could be mentioned that such behaviour is consistent with expectations of the Benilov theory, where the 3D vortexes are unstable to the wave orbits in planes perpendicular to the orbits. The averaged spacing between the streaks and the depth of the vortical cells approximates that of Langmuir turbulence. The strength of the vortices arising from the wave–turbulence interaction, however, is one order of magnitude less than that of Langmuir cells, which arises from the interaction between the surface waves and the turbulent shear flow. In contrast to Langmuir turbulence, production from the Stokes shear does not dominate the energetics budget in wave-induced turbulence. The dominant production is the advection of turbulence by the velocity straining of waves.

D'Asaro et al. (2014) works in the more traditional Langmuir-turbulence paradigm. They tested the wave-turbulence assumptions using parallel experiments in a lake with small waves and in the open ocean with much bigger waves. Under the same wind stress and adjusting for buoyancy flux, they find the mixed layer average turbulent vertical kinetic energy in the open ocean typically twice that in the lake. The increase is consistent with models of Langmuir turbulence, in which the wave Stokes drift, and not wave breaking, is the dominant mecha-

nism by which waves energize turbulence in the mixed layer. Applying these same theories globally, they found enhanced mixing and deeper mixed layers resulting from the inclusion of Langmuir turbulence in the boundary layer parameterization, especially in the Southern Ocean. It should be pointed out, however, that the enhancement of turbulence once the wind/waves increase, and this is observed, is not a direct verification of the Langmuir turbulence as all the above mechanisms also predict such enhancement if waves grow.

Therefore, with wave-induced turbulence and mixing being a relatively new topic, research in this field concentrates on clarifying and validating physical concepts responsible for such turbulence. While qualitatively three different mechanisms possible, and all of them appear to be relevant, their quantitative significance is subject to active research.

7.6   *Waves in large-scale air-system – climate*

The wave-coupled effects in large-scale air-sea systems were singled out the previous Section because they bring the wave modelling into uncharted waters of large-scale and long-term simulations of weather, climate and general oceanic circulation. Here, 'large-scale' means large by comparison with the scale of wind-generated waves. Weather and climate are phenomena of very different scales (days and years or even longer in time, hundreds of kilometers and global in space). Both scales, however, are much larger with respect to the scale of ocean surface waves (seconds in time and hundreds of meters in space).

Zambon et al. (2014), Reichl et al. (2016), Yablonsky et al. (2015), Aijaz et al. (2017), Stoney et al. (2017) all investigated impact of wave-induced mixing on Tropical Cyclones (TC). TCs, or hurricanes as they are called in the Americas and typhoons in Asia, feed on the energy of the warm ocean, and therefore the Sea Surface Temperature (SST) feedback can have in impact on their intensity. Prediction of Cyclone intensity has resisted improvements over decades, and waves is one of physical phenomena which is missing in the hurricane models.

Zambon et al. (2014) applied coupled ocean-atmosphere-wave-sediment transport (COAWST) model to Hurricane Ivan and highlighted the significance of the wind-wave-current interactions during tropical cyclones. The wind-generated currents and waves produce a vertical shear leading to turbulence, which then mixes the upper ocean layer by entraining cooler water from the thermocline up into the well-mixed ocean surface (Yablonsky et al., 2015, Reichl et al., 2016)] ultimately cooling the SST. Aijaz et al. (2017) describe an implementation of a new wave model that simulates the turbulence generated by nonbreaking waves in a coupled ocean-wave-hurricane modelling system. The Princeton Ocean Model (POM) with hurricane forcing was coupled with the WAVEWATCH-III surface wave model. The SST response from the modelling experiments indicates that the nonbreaking wave-induced mixing leads to significant cooling of the SST and deepening of the mixed layer. In a similar study, Stoney et al. (2017) implemented a wave-mixing parameterisation as a modification to the k-ε turbulence scheme, used within MOM5 ocean model. The inclusion of surface wave mixing led to surface temperature differences of around 0.6C near the storm track, typically with warm anomalies on the side with the strongest winds and cool anomalies in other regions. This pattern was explained by an initial wave-induced deepening of the mixed layer, which can modify the subsequent shear-induced entrainment and upwelling.

Staneva et al. (2016) investigated the effect of wind waves on water level and currents during two storms in the North Sea by using a high-resolution Nucleus for European Modelling of the Ocean (NEMO) model forced with fluxes and fields from a high-resolution wave model. The additional terms accounting for wave-current interaction in this study were the Stokes-Coriolis force, the sea-state-dependent energy and momentum fluxes. The individual and collective role of these processes was quantified and the results were compared with a control run without wave effects as well as against current and water-level measurements from coastal stations. A better agreement with observations was found when the circulation model is forced by sea-state-dependent fluxes, especially in extreme events. Moreover, the modelled

vertical velocity profile fits the observations very well when the wave forcing is accounted for. The contribution of wave-induced forcing was quantified indicating that this represents an important mechanism for improving water-level and current predictions.

Walsh et al. (2017) tested a new parameterization of mixing processes in the upper ocean in a ¼ degree resolution global ocean-climate model MOM5. The parameterization represents the effect of turbulent mixing by unbroken waves as an additional turbulent shear production term in the k-ε mixing scheme. The results show that the inclusion of this parameterization has a noticeable effect on ocean climate, particularly in regions of high wave activity such as the Southern Ocean. Inclusion of this process also leads to some reduction in the biases of the simulated climate, including mixed layer depth, compared with available observations.

A large review of wave-induced mixing on ocean and climate modelling was offered by Qiao et al. (2016). Heated from above, the oceans are stably stratified. Therefore, the performance of general ocean circulation models and climate studies through coupled atmosphere–ocean models depends critically on vertical mixing of energy and momentum in the water column. Many of the traditional general circulation models are based on total kinetic energy (TKE), in which the roles of waves are averaged out. Although theoretical calculations suggest that waves could greatly enhance coexisting turbulence, no field measurements on turbulence have ever validated this mechanism directly. To address this problem, a specially designed field experiment was conducted. The experimental results indicate that the wave–turbulence interaction-induced enhancement of the background turbulence is indeed the predominant mechanism for turbulence generation and enhancement. Based on this understanding, the authors propose a new parametrization for vertical mixing as an additive part to the traditional TKE approach. This new result reconfirmed the past theoretical model that had been tested and validated in numerical model experiments and field observations. It establishes the critical role of wave–turbulence interaction effects in both general ocean circulation models and atmosphere–ocean coupled models, which could greatly improve the understanding of the sea surface temperature and water column properties distributions, and hence model-based climate forecasting capability.

In Summary, Section 7 outlines multiple effects and feedbacks which surface ocean waves have in the lower atmosphere and upper ocean. These include wave breaking, wave-current and wave-ice interactions, Wave Boundary Layer in the wind flow, wave-induced currents and mixing in the upper ocean. Taken beyond the problem of wave dynamics and wave forecast, these effects can have impact on large-scale processes such as weather, including tropical cyclones, ocean circulation and climate.

8.   UNCERTAINTY

Many parameters cause uncertainties in environmental modeling and measurements. Data analysis also contributes to uncertainties in measurements and numerical predictions, such as the applied mathematical model, filters and choice of data samples. This section summarizes the uncertainties in prediction models, full-scale measurements and model-scale measurements as well as the challenges in quantifying the uncertainties.

8.1   *Uncertainty in prediction models*

In general, uncertainties in prediction models depend on the choice of method, equations to describe the real physics, level of approximation, introduction of empirical parameters, rounding errors, grid generation and understanding of the physical model by practicians.

Wave-forecast models, apart from uncertainties due to limitations of their physics, whose many aspects have been discussed above, critically depend on uncertainties of their forcing fields: winds, currents, ice, and bottom topography. As a rule of thumb, for example, 10% of wind-speed error translates into 20% error in wave height.

Errors in wind speed have many sources, one of the main of which is uncertainties of the physics of meteorological models. This is particularly noticeable for extreme winds, where, for instance, high-resolution hurricane-wind model tuned for one region (e.g. Gulf of Mexico) do not perform well in another region such as South-Eastern Asia (Liu et a., 2017). Assimilation of in situ data has its own problems because of extrapolation of measurements to the standard 10 m height (e.g. Babanin and McConochie, 2013), which is especially difficult for high seas. Satellite wind measurement, assimilated broadly nowadays, differ depending on the platform (i.e. altimeters or radiometers), and again with particular biases towards high end of wind speeds (Young et al., 2017). We refer to Section 5.1 on the wind measurements issues, and here will comment that the common practice to overcome the wind-forcing problem these days, is the use of ensemble of the winds produced by different models, in order to provide a likely wave-forecast outcome.

Surface currents are less common forcing fields for wave forecast, often not even taken into account, but their impact on uncertainties in wave prediction is not limited to local areas of strong currents. Ardhuin et al. (2016) demonstrate that small-scale variability of currents in the open ocean has large impact on wave heights in the North Atlantic. Such impact should be even bigger in the Southern Ocean where strong currents, and their eddies, are common features of oceanographic environment, superposed under powerful storms which radiate swells all over the globe round the year. Improving this uncertainty is feasible as high resolution currents are becoming increasingly available through satellite observations and oceanographic forecast, but this would require dedicated efforts on advancing of the physics of wave models (see Section 7.2).

Uncertainties due to ice-field inputs into wave-forecast models are only essential in certain geographic regions and seasons, but these uncertainties are big. At operational scale, it is only relative percentage of the ice cover with respect to the open water that is usually available, whereas wave-ice interactions critically depend on more detailed knowledge of ice properties (e.g. Rogers et al., 2016). Here, however, even if the full information on ice were available, quality of the physics of wave modelling in Marginal Ice Zone is still marginal.

8.2   *Uncertainty in measurements*

There are many sources of uncertainties in measurements, such as instruments used for full-scale and model-scale measurements, remote sensing technique and associated software, location of measurement and reference point, and calibration of instrument.

Uncertainty in measurements of winds and ice were partially addressed in Section 8.1 above. With respect to the winds, we would also reiterate the discussion of Section 5.1, and in particular the fact that the standard wind input in modelling is the wind speed at 10 m height which is almost never measured directly, but is inferred on the basis of extrapolations which are approximate and do not cover the full range of metocean conditions.

The wave-measurement uncertainties are of different nature. A variety of reliable in situ methods and instrumentations are available these days, and the satellites provide the global coverage. Satellites, however, require in situ calibrations, and there are very few in the Southern Hemisphere. Thus, the remote sensing of waves in the Northern Hemisphere is available and well calibrated, but south of equator they are known for their biases.

In the model-scale tests, parameters, such as physical property of water, initial conditions, wavemaker control, wave reflection from beaches and model, interaction between wind and wave, refraction due to uneven seabed on shallow water, wave-current interaction and test duration, cause uncertainties in measurements. With respect to instrumentation, errors in wave probes, current meters and power supply contribute to the measurement uncertainties. Examples of quantifying the uncertainties in model tests are presented in the work of Qiu et al. (2017) and Kim and Hermansky (2014).

8.3 Challenges in uncertainty quantification

Quantification of uncertainties and associated methodology in the aspects discussed above remain as challenges. It should be pointed out that human factors are an important factor contributing to uncertainties in measurements and predictions. It is a real challenge to quantify the uncertainties caused by human factors.

According to the ISO-GUM methodology (ISO, 2008), uncertainties in measurements are quantified by using Type A and Type B categories. An example of applying this methodology is presented in the work of Qiu et al. (2014). While it has been widely used by the ITTC, its applications by the ISSC community for environmental modeling and measurement are limited. Progress is being made by the joint ITTC-ISSC Committee to identify the gaps in quantifying uncertainties with the objective to develop a unified methodology.

9. SPECIAL TOPICS

9.1 Future Trends

9.1.1 Big Data

Big Data and Machine Learning have rapidly grown over the last years in different areas and applications, including the environmental sciences. Alternative methods using data mining and neural networks, for example, have shown great improvement compared to traditional approaches – suggesting that its applications tend to significantly expand in the next years. As an introductive data mining relevant for future studies, Hashim et al. (2016) focused on finding the sequence of the most influential parameters among the factors that affect the offshore wave height. A dataset comprising of four climatic input parameters: sea surface wind speed, wind direction, air temperature, and sea surface temperature; as well as one output parameter (significant wave height) was generated. As a result, the following sequence of parameters has the most to least influence on the predictions of Hs: wind speed, air temperature, sea surface temperature and wind direction. In addition, Hashim et al. (2016) found that combination of three variables, namely wind speed, air temperature, and wind direction, forms the most influential set of input parameters with RMSEs of 0.82, 0.44 and 0.62, respectively for the predicted Hs. Hashim et al. (2016) suggest that the accuracy of wave height prediction may improve when air temperature and sea surface temperature are included as inputs along with wind speed and direction. Ghorbani et al. (2017) investigated the potential of the Chaos theory integrated with multiple linear regression (Chaos-MLR) in prediction of wave heights and wave periods, collected at four moorings in the coastal environment of Tasmania. The intercomparisons demonstrated that the Chaos-MLR and pure MLR models yield almost the same accuracy in predicting the significant wave heights and the zero-up-crossing wave periods. Whereas, the augmented Chaos-MLR model is performed better results in term of the prediction accuracy compared to previous prediction applications of the same case study.

Statistical models have advantages in short-term wave prediction as complex phenomena are substantially simplified; however, conventional statistical models have limitations in forecasting nonlinear and non-stationary waves. Duan et al. (2016) developed a hybrid empirical model decomposition (EMD) support vector regression (SVR) model designated as EMD-SVR for nonlinear and non-stationary wave prediction. Auto-regressive (AR) model, single SVR model and EMD-AR model were studied to validate the performance of the proposed model. Considerable improvements were found in the comparisons among the EMD-SVR and other models. The coefficient of efficient values indicate the EMD-SVR model shows good model performances and provides an effective way for the short-term prediction of nonlinear and non-stationary waves. Ibarra-Berastegi et al. (2015) analyzed the performance of three types of statistical models and a well-known physics-based model for forecasting the wave energy flux. Three techniques are used: analogues, random forests (a machine learning algorithm) and a combination of the two. The numerical model applied is the Wave Model

(WAM). Ibarra-Berastegi et al. (2015) found that over horizons between 3 and 16–19 h at locations near the coast, the random forests models outperform the others, including WAM. These models exploit the inherent predictability associated with the strong autocorrelation present in ocean energy values.

In recent years, Bayesian optimization (BO) has emerged as a practical tool for high-quality parameter selection in prediction systems. Cornejo-Bueno et al. (2017) showed that BO can be used to obtain the optimal parameters of a prediction system for problems related to ocean wave features prediction. They proposed the Bayesian optimization of a hybrid Grouping Genetic Algorithm for attribute selection combined with an Extreme Learning Machine (GGA-ELM) approach for prediction. The system used data from neighbor stations in order to predict the significant wave height and the wave energy flux at a goal marine structure facility, which was tested in a real problem involving buoys data in the Western coast of the USA, improving the performance of the GGA-ELM without a BO approach. Harpham et al. (2011) outlined an application of the Bayesian statistical methodology which combines ensemble of multiple predictions and new sources of observational data such as GNSS reflectometry and FerryBoxes. The method of Harpham et al. (2011) modifies the probabilities of ensemble wave forecasts based on recent past performance of individual members against a set of observations from various data source types. Each data source is harvested and mapped against a set of spatio-temporal feature types and then used to post-process ensemble model output.

Precise prediction of wave heights is still an evading problem whether it is done using physics based modeling or by extensively used data driven technique of Artificial Neural Network (ANN). A numerous of recent papers have presented encouraging results using ANN, especially when combined with traditional numerical wave models. Campos and Guedes Soares (2016) developed and evaluated hybrid models using statistical tools to reduce the bias of significant wave heights. The "hybrid model" consists of two models working together: (1) numerical wave model (in this case, WAM) and (2) Artificial Neural Network and linear regression. The numerical model predicts the wave heights while the target of the statistical model was used to predict the residue (difference of measurement minus model); finally combined to provide a final accurate estimation at the Brazilian coast. The model using linear regression proved to be efficient in reducing bias, but not the scatter index (SI) or the root mean square error (RMSE). The neural network model presented the best results, especially with 16 to 32 neurons at the intermediate layer. The final bias was reduced from 0.13 to 0.06 meters and SI from 0.12 to 0.03.

In recent years, machine learning approaches are being widely used for the prediction of wave heights. However, these approaches involve batch learning algorithms that are not well-equipped to address the demands of continuously changing data stream. Kumar et al. (2017) conducted a study to predict the daily wave heights in different geographical regions using sequential learning algorithms, namely the Minimal Resource Allocation Network (MRAN) and the Growing and Pruning Radial Basis Function (GAP-RBF) network. They compared the performance of MRAN and GAP-RBF with Support Vector Regression (SVR) and Extreme Learning Machine (ELM). Results of Kumar et al. (2017) showed that the MRAN and GAP-RBF outperform the SVR and ELM with minimal network resources, in the daily wave height prediction, and also predict the significant wave heights accurately. Kumar et al. (2017) concluded that MRAN outperforms GAP-RBF with minimal architecture.

Berbić et al. (2017) applied neural networks and support vector machine for significant wave height prediction for the following 0.5—5.5 hours, using information from 3 or more time points. In the first stage, predictions were made by varying the quantity of significant wave heights from previous time points and various ways of using data are discussed. Afterwards, the influence of wind was taken into account. Predictions of were made using two machine learning methods — artificial neural networks (ANN) and support vector machine (SVM). Sánchez et al. (2017) presented a mathematical model that uses artificial neural networks for

the assessment of the wave energy potential of sites, based on data recorded by wave monitoring instrumentation. The performance of the neural network model was compared to that of the Nearshore Wave Prediction System (NWPS), which combines SWAN, WAVEWATCH III and other numerical models. The performance of the neural network trained with the 23 years' hindcast was satisfactory; better than the NWPS in terms of relative bias but worse in terms of scatter index. Therefore, Sánchez et al. (2017) concluded that neural networks can make an optimal use of the data produced by wave monitoring instrumentation and are useful to characterize the wave energy resource of a coastal site. In Dixit and Londhe (2016), Neuro Wavelet Technique (NWT) was used specifically to explore the possibility of prediction of extreme events for five major hurricanes Katrina 2005, Dean 2007, Gustav 2008, Ike 2008, Irene 2011 at four locations (NDBC wave buoys stations) in the Gulf of Mexico. Neuro Wavelet Technique was employed by combining Discrete Wavelet Transform and Artificial Neural Networks. To develop these Neuro wavelet models to forecast the waves with lead times of 12 hr to 36 hr in advance, previously measured significant wave heights at same locations were used. From the results Dixit and Londhe (2016) concluded that the Neuro Wavelet Technique can be employed to solve the ever eluding problem of accurate forecasting of the extreme events.

Lo et al. (2015) developed artificial neural network (ANN)-based models for forecasting precipitation, in which the training parameters were adjusted using a parameter automatic calibration (PAC) approach. A classical ANN-based model, the multilayer perceptron (MLP) neural network, was used to verify the utility of the proposed ANN–PAC approach. The traditional multiple linear regression model was selected as the benchmark for comparing the accuracy of the ANN–PAC model. In addition, two MLP ANN models based on a trial-and-error calibration method were constructed by manually tuning the parameters. Lo et al. (2015) found that the results yielded by the ANN–PAC model were more reliable than those yielded by the manually tuning and traditional regression models. In addition, the computing efficiency of the ANN–PAC model decreased with an increase in the number of increments within the parameter ranges because of the considerably increased computational time, whereas the prediction errors decreased because of the model's increased capability of identifying optimal solutions. Kumar et al. (2017) proposed the use of an ensemble of Extreme Learning Machine (Ens-ELM) to predict the daily wave height, exploring the randomness of initialization in ELM to obtain better generalization performance. For each sample in the data set, the output of the ELM with the least mean square for each sample in the data set is reported as its output. The Ens-ELM network is trained using the past wave data and the measured atmospheric conditions obtained in these stations between Jan 1, 2011 and Dec 31, 2014 and is tested with data in these stations between Jan 1, 2015 and Aug 30, 2015. In this study, the performance of Ens-ELM is evaluated in comparison with ELM, Online Sequential ELM (OS-ELM), and Support Vector Regression (SVR). From this study, Kumar et al. (2017) infer that the Ens-ELM outperforms ELM, OS-ELM and SVR in the daily wave height prediction.

Durán-Rosal et al. (2017) presented a methodology for the detection and prediction of Segments containing very high significant wave height (SSWH) values in oceans. A genetic algorithm (GA) combined with a likelihood-based local search is proposed for the first stage (detection), and the second stage (prediction) is tackled by an Artificial Neural Network (ANN) trained with a Multiobjective Evolutionary Algorithm (MOEA). Given the unbalanced nature of the dataset, the MOEA is specifically designed to obtain a balance between global accuracy and individual sensitivities for both classes. The results of Durán-Rosal et al. (2017) showed that the GA is able to group segments of significant wave heights in a specific cluster of segments and that the MOEA obtains ANN models able to perform an acceptable prediction of these SSWH.

Various methods are typically used to estimate the characteristics of nearshore wave breaking, mostly based on empirical, analytical and numerical techniques. Kouvaras and Dhanak (2017)

extended the approach of Deo et al. (2001) approach, using neural networks, to predict other characteristics of wave breaking, including the type of wave breaking, and the position of breaking over a fringing reef, as well as the associated wave setup, and the rate of dissipation of wave energy. The corresponding neural network models for wave setup within the surf zone and the difference in energy flux between the incident and broken wave have success rates of approximately 89% and 94% respectively. Kouvaras and Dhanak (2017) argue that the method may be extended to provide predictive models for consideration of a range of natural coastal conditions, random waves, and various bottom profiles and complex geometry, based on training and testing of the models using representative field and laboratory observational data, in support of accurate prediction of near-shore wave phenomena.

Krasnopolsky et al. (2016) introduced a neural network (NN) technique to fill gaps in satellite data, linking satellite-derived fields of interest with other satellites and in situ physical observations. They proved that NN technique provides an accurate and computationally cheap method for filling in gaps in satellite ocean color observation fields and time series.

10.   CONCLUSIONS

10.1   Summary

To take-away from this report is that while much progress is being made, the committee has several concerns:

- Operating in polar and other regions due to lack of knowledge / data and large uncertainty / increased risk.

- The effect of climate change on waves and met-ocean phenomenon, including ice, and associated effect on structures.

- The uncertainty in climate change models and the uncertainty in environmental prediction models. This uncertainty stems from the lack of uncertainty quantification.

10.2   Recommendations

The committee would like to make the following recommendations:

- For continued advancement all environmental time series data should be saved in its unfiltered form for others to use – develop standard big data format and meta data requirement.

- There is a need for improved uncertainty quantification methods, and these methods should be utilized by the community.

- With the increased use of data analytics and higher fidelity numerical tools there is a need for more computing resources to be available to the community.

- ISSC should include computer science/numerical methods experts on this committee.

- Other ISSC committees should start to consider the effect of climate change on their areas. The Environment committee should increase its interaction with other committees with respect to climate change.

- With the increasing activity in Polar Regions, there is a need for a polar sea state definition for design. Data to generate the definitions is needed.

- The ISSC should continue to encourage sharing of environmental information to improve forecasts as public service

- Identify fixed test sites in the ocean for developing benchmark data sets.

- Continue working with the ITTC to develop uncertainty quantification procedures and encourage them to include longer term environmental uncertainty quantification.

- There is a need for in situ measurements in extreme conditions, particularly coupled air/waves/ocean interactions and fluxes

10.3   *Advances*

The committee was encouraged by the progress and activity in the field, including new facilities, new techniques, and new models. These include:

- University of Miami Surge-Structure-Atmosphere-Interaction Tank (SUSTAIN).

- The utilization of big data analytics / machine intelligence.

- The use of existing fixed test sites (wave energy test sites and wind farms etc.) in the ocean for developing benchmark data sets.

- The advent and increased use of undersea gliders, wave gliders, wave riders, small buoys, UAVs and UUVs in gathering oceanographic data which could lead to more data becoming available.

- Comprehensive inter-calibrated and validated satellite metocean database for the full period of satellite observations (University of Melbourne)

REFERENCES

Aarnes, O. J., Abdalla, S., Bidlot, J. R., & Breivik, Ø. (2015). Marine wind and wave height trends at different ERA-Interim forecast ranges. Journal of Climate, 28(2), 819-837.

Aarnes, O. J., M. Reistad, O. Breivik, E. Bitner-Gregersen, L. Ingolf Eide, O. Gramstad, A. K. Magnusson, B. Natvig, and E. Vanem (2017). Projected changes in significant wave height toward the end of the 21st century: Northeast Atlantic, J. Geophys. Res. Oceans, 122, 3394−3403, doi:10.1002/2016JC012521.

Abdel-Moati, H. et al. (2017). Near field ice detection using infrared based optical imaging technology. Opt. and Laser Technol.

Aberg, S. Rychlik, I. Leadbetter, R. (2008). Palm distributions of wave characteristics in encountered seas, Annals of Appl. Prob., Vol 18 (3), pp. 1059-1084.

Adcock, T. A. A. & Taylor, P. H. (2014). The Physics of Anomalous ('Rogue') Ocean Waves. Reports on Progress in Physics, 77, 105901-105901.

Aijaz, S., Ghantous, M., Babanin, A.V., I. Thomas, Ginis, B., and Wake, G. (2017). Non-breaking wave-induced mixing in upper-ocean during tropical cyclones using coupled hurricane-ocean-wave modelling. Journal of Geophysical Research Oceans, 122, 3939–3963, doi:10.1002/2016JC012219

Aijaz, S., Rogers, W.E., and Babanin, A.V. (2016). Wave spectral response to sudden changes in wind direction in finite-depth waters. Ocean Modelling, 103, 98-117

Akpınar, A., Bingölbali, B., Van Vledder, G.Ph., (2016). Wind and wave characteristics in the Black Sea based on the SWAN wave model forced with the CFSR winds. Ocean Engineering 126, 276–298.

Alford, L., Lyzenga, D., Nwogu, O., Beck, R., Johnson, J., Zundel, A., Andrews, M., Coller, J., Katz, E., McKelvey, C., O'Brien, A., Smith, G., and Wijesundara, S., (2016). Performance Evaluation of a Multi-Ship System for Environmental and Ship Motion Forecasting, Proc. 31st Symp. on Naval Hydrodynamics, 11-16 Sep, Monterey, CA.

Almar, R., Larnier, S., Castelle, B., Scott, T. & Floc'h, F. (2016). On the use of the Radon transform to estimate longshore currents from video imagery. Coastal Engineering, 2016, 114: 301-308.

Alpers W., A. Mouche, J. Horstmann, A. Y. Ivanov., V. S. Barabanov (2015). Application of a new algorithm using Doppler information to retrieve complex wind fields over the Black Sea from ENVISAT SAR images. Int. Journal of Remote Sensing, 36(3), 863-881.

Alvise, B., Francesco, B., Filippo, B., Sandro, C., Mauro, S., (2017). Space-time extreme wind waves: Analysis and prediction of shape and height. Ocean Modelling 113, 201–216.

Amrutha, M.M., Kumar, V.S., (2015). Short-term statistics of waves measured off Ratnagiri, eastern Arabian Sea. Applied Ocean Research 53, 218–227.

Amrutha, M.M., Kumar, V.S., Sandhya, K.G., Nair, T.M.B., Rathod, J.L., (2016). Wave hindcast studies using SWAN nested in WAVEWATCH III - comparison with measured nearshore buoy data off Karwar, eastern Arabian Sea. Ocean Engineering 119, 114–124.

Antão, E.M., Guedes Soares, C., (2016). Approximation of the joint probability density of wave steepness and height with a bivariate gamma distribution. Ocean Eng. 126, 402–410.

Appendini, C.M., Camacho-Magaña, V., Breña-Naranjo, J.A., (2016). ALTWAVE: Toolbox for use of satellite L2P altimeter data for wave model validation. Advances in Space Research 57, 1426–1439.

Ardhuin F, Gille ST, Menemenlis D, Rocha CB, Rascle N, Chapron B, Gula J, Molemaker J (2016). Small-scale open ocean currents have large effects on wind wave heights. J Geophys Res 122, DOI 10.1002/2016JC012413

Ardhuin, F. J. Stopa, B. Chapron, F. Collard, M. Smith, J. Thomson, M. Doble, B. Blomquist, Collins III, C.O., and Wadhams, P. (2017). Measuring ocean waves in sea ice using SAR imagery: A quasi-deterministic approach evaluated with Sentinel-1 and in situ data. Remote Sensing of Environment, 189, 211–222

Ashton, I.G.C., Johanning, L. (2015). On errors in low frequency wave measurements from wave buoys. Ocean Engineering 95 11–22.

Azariadis, P., (2017). On Using Density Maps for the Calculation of Ship Routes, Evolving Systems : An Interdisciplinary J. for Adv. Sc. and Techn., 8(2), pp. 135–145. doi: 10.1007/s12530-016-9155-7.

Babanin, A.V. (2012). Swell attenuation due to wave-induced turbulence. Proceedings of the ASME 2012 31st International Conference on Ocean, Offshore and Arctic Engineering OMAE2012, July 1-6, 2012, Rio de Janeiro, Brazil, ISBN 978-0-7918-4489-2, 5p

Babanin, A.V. (2017). Similarity theory for turbulence, induced by orbital motion of surface water waves. Procedia IUTAM, 20, 99-102

Babanin, A.V., (2011). Breaking and Dissipation of Ocean Surface Waves. Book, Cambridge University Press, 480p

Babanin, A.V., and McConochie, J. (2013) Wind measurements near the surface of waves. Proceedings of the ASME 2013 32nd International Conference on Ocean, Offshore and Arctic Engineering OMAE2013, June 9-14, 2013, Nantes, France, 6p

Babanin, A.V., Onorato, M., and Qiao, F. (2012). Surface waves and wave-coupled effects in lower atmosphere and upper ocean. Journal of Geophysical Research, 117, doi:10.1029/2012JC007932, 10p.

Babanin, A.V., van der Westhuysen, A., Chalikov, D., and Rogers, W.E. (2017). Advanced wave modelling including wave-current interaction. In "The Sea: The Science of Ocean Prediction, Eds. Nadia Pinardi, Pierre F.J. Lermusiaux, Kenneth H. Brink and Ruth Preller", Journal of Marine Research, 75, 239–262

Bae D M, Prabowo A R, Cao B, et al. (2016). Numerical simulation for the collision between side structure and level ice in event of side impact scenario[J]. Latin American Journal of Solids and Structures, 2016, 13(16): 2991-3004.

Barnard, P.L., Short, A.D., Harley, M.D., Splinter, K.D., Vitousek, S., Turner, I.L., Allan, J., Banno, M., Bryan, K.R., Doria, A., Hansen, J.E., Kato, S., Kuriyama, Y., Randall-Goodwin, E., Ruggiero, P., Walker, I.J., Heathfield, D.K., (2015). Coastal vulnerability across the Pacific dominated by El Niño/Southern Oscillation. Nature Geoscience, v.8, pp. 801-807.

Barthelemy, X., Banner, M., Peirson, W., Fedele, F., Allis, M. & Dias, F. (2015). On the Local Properties of Highly Nonlinear Unsteady Gravity Water Waves. Part 2. Dynamics and onset of Breaking. arXiv Preprint arXiv:1508.06002.

Bateman, W. J. D., Swan, C. & Taylor, P. H. (2003). On the Calculation of the Water Particle Kinematics Arising in a Directionally Spread Wavefield. J. Comput. Phys., 186, 70-92.

Benetazzo, A., Ardhuin, F., Bergamasco, F., Cavaleri, L., Guimarães, P. V., Schwendeman, M., Sclavo, M., Thomson, J. & Torsello, A. (2017). On the Shape and Likelihood of Oceanic Rogue Waves. Scientific Reports, 7, 8276.

Benetazzo, A., Barbariol, F., Bergamasco, F., Torsello, A., Carniel, S. & Sclavo, M. (2015). Observation of Extreme Sea Waves in a Space–Time Ensemble. Journal of Physical Oceanography, 45, 2261-2275.

Benilov, A. Y., (2012). On the turbulence generated by the potential surface waves. J. Geophys. Res. (Oceans), 117, doi:10.1029/2012JC007948

Bennett, V. C. & Mulligan, R. P. (2017). Evaluation of surface wind fields for prediction of directional ocean wave spectra during Hurricane Sandy. Coastal Eng., 2017, 125: 1-15.

Bennetts, L.G., Alberello, A., Meylan, M.H., Cavaliere, C., Babanin, A.V., and Toffoli, A. (2015) An idealised experimental model of ocean surface wave transmission by an ice floe. Ocean Modelling, 96, 85-92, http://dx.doi.org/10.1016/j.ocemod.2015.03.001

Bentamy A., Grodsky, S. A., Elyouncha, A., Chapron, B., Desbiolle, F. (2016). Homogenization of Scatterometer Wind Retrievals, Int. J. Climatol. doi:10.1002/joc.

Bento, A.R., Gonçalves, M., Campos, R.M., Guedes Soares, C., (2016). Comparison Between Two Forecast Systems Implemented with WAM and WAVEWATCH 3 for the North Atlantic. Proceedings of the 35th International Conference on Ocean, Offshore and Arctic Engineering - OMAE2016. June 19-24, 2016, Busan, South Korea.

Berbić, J., Ocvirk, E., Carević, D., Lončar, G., (2017). Application of neural networks and support vector machine for significant wave height prediction. Oceanologia 59, 331-349.

Bergsma, J. et al. (2014). On the Measurement of Submersion Ice Resistance of Ships, Using Artificial Ice. In: International Ocean and Polar Engineering Conference. Busan, Korea: International Society of Offshore and Polar Engineers, pp. 1125-1131.

Bernier, N.B., Alves, J.-H.G.M., Tolman, H., Chawla, A., Peel, S., Pouliot, B., Bélanger, J.-M., Pellerin, P., Lépine, M., Roch, M., (2015). Operational Wave Prediction System at Environment Canada: Going Global to Improve Regional Forecast Skill. Wea. Forecasting.

Beyá, J., Álvarez, M., Gallardo, A., Hidalgo, H., Winckler, P., (2017). Generation and validation of the Chilean Wave Atlas database. Ocean Modelling 116, 16–32.

Bitner-Gregersen E. (2015). Joint met-ocean description for design and operations of marine structures, Applied Ocean Research, Vol.51, pp.279-292.

Bitner-Gregersen, E (2017). Rethinking rogue waves, DnVGL Feature, DNVGL.

Bitner-Gregersen, E. and Gramstad, O., (2015). Rogue Waves: impact on ships and offshore structures, DNV-GL Strategic Research and Innovation, Position Paper 05-2015.

Bitner-Gregersen, E.M., (2017). Wind and Wave Climate in Open Sea and Coastal Waters. Proceedings of the ASME 2017 36th International Conference on Ocean, Offshore and Arctic Engineering OMAE2017.

Bitner-Gregersen, E.M., and Toffoli, A. (2015). Wave steepness and rogue waves in the changing climate in the North Atlantic, Proceeding of the ASME 2015 34th International Conference on Ocean, Offshore and Arctic Engineering, St. John's, Newfoundland, Canada.

Bitner-Gregersen, E.M., Guedes Soares, C., and Vantorre, M. (2016). Adverse weather conditions for ship maneuverability, Transport. Research Procedia, Vol.14, pp.1631-1640.

Bouvy A., Henn, R. and Hensse, J. (2009). Acoustic wave height measurements in a towing facility, Proc. 1st Int. Conf. on Adv. Model Meas. Techn. for the EU Maritime Ind. (AMT '09), 1 - 2 Sep, Nantes, France.

Breivik, O. , Bidlot, J.-R., and Janssen, P.A.E.M. (2016). A Stokes drift approximation based on the Phillips spectrum. Ocean Modelling, 100, 49–56

Breivik, Ø., Allen, A. A. (2008). An operational search and rescue model for the Norwegian Sea and the North Sea, Journal of Marine Systems, Vol 69(1-2), pp. 99-113.

Breivik, Ø., Allen, A. A., Maisondieu, C., Roth, J-C., (2011). Wind-induced drift of objects at sea: The Leeway field method. Applied Ocean Research, Vol 33, pp. 100-109.

Brumer, S.E., Zappa, C.J., Brooks, I.M., Tamura, H., Brown, S.M., Blomquist, B.W., Fairall, C.W. And Cifuentes –Lorenzen, A. (2017). Whitecap Coverage Dependence on Wind and Wave Statistics as Observed during SO GasEx and HiWinGS. Journal of Physical Oceanography, 47, 2211-2235

Caires, S., Groeneweg, J., van Nieuwkoop, J. (2016). Lifting of time-and space-evolving winds for the determination of extreme hydraulic conditions. Coastal Engineering, 2016, 116: 152-169.

Calini, A., Schober, C.M., (2017). Characterizing JONSWAP rogue waves and their statistics via inverse spectral data. Wave Motion 71, 15–17.

Cambazoglu, M. K., Blain, C. A., Smith, T. A., Linzell, R. S. (2016). Relationships between wind predictions and model resolution over coastal regions. Ocean Engineering, 2016, 112: 97-116.

Campbell, A. J., Bechle, A. J., and Wu, C. H. (2014). Observations of surface waves interacting with ice using stereo imaging, J. Geophys. Res. Oceans, 119, 3266–3284, doi:10.1002/2014JC009894.

Campos, R.M., Guedes Soares, C., (2016). An hybrid model to forecast significant wave heights. In: Guedes Soares, C., Garbatov, Y., Sutulo, S., Santos, T.A. (Eds.), Maritime Technology and Engineering. Taylor and Francis Group, CRC Press, London, pp. 473–479, ISBN 978-1-138-03000-8, DOI: 10.1201/b21890-138.

Campos, R.M., Guedes Soares, C., (2016). Assessment of three wind reanalyses in the North Atlantic Ocean. Journal of Operational Oceanography, v. 10, 30–44.

Campos, R.M., Guedes Soares, C., (2016). Comparison and assessment of three wave hindcasts in the North Atlantic Ocean. Journal of Operational Oceanography, v. 9, 26-44.

Campos, R.M., Guedes Soares, C., (2016). Comparisons of HIPOCAS and ERA Wind and Wave Reanalyses in the North Atlantic Ocean. Ocean Engineering, v. 112, 320–334.

Campos, R.M., Guedes Soares, C., (2016). Estimating Extreme Waves in Brazil Using Regional Frequency Analysis. Proceedings of the 35th International Conference on Ocean, Offshore and Arctic Engineering - OMAE2016. June 19-24, 2016, Busan, South Korea.

Candella, R.N., (2015). Rogue waves off the south/southeastern Brazilian coast. Nat Hazards.

Castro-Santos, L. & Diaz-Casas, V. (2015). Economic influence of location in floating offshore wind farms. Ocean Engineering, 2015, 107: 13-22.

Chabchoub, A. & Grimshaw, R. (2016). the Hydrodynamic Nonlinear Schrödinger Equation: Space and Time. Fluids, 1, 23.

Chabchoub, A. (2016). Tracking Breather Dynamics in Irregular Sea State Conditions. Physical Review Letters, 117, 144103.

Chabchoub, A., Hoffmann, N. P. and Akhmediev, N., (2011). Rogue wave observation in a water wave tank, Physical Review Letter, Vol. 106, 204502.

Chabchoub, A., Hoffmann, N., Branger, H., Kharif, C., & Akhmediev N., (2013). Experiments on wind-perturbed rogue wave hydrodynamics using the Peregrine breather model, Physics of Fluids, Vol 25, 101704 (2013); doi: http://dx.doi.org/10.1063/1.4824706.

Chabchoub, A., Kibler, B., Finot, C., Millot, G., Onorato, M., Dudley, J. M. & Babanin, A. V. (2015). The Nonlinear Schrödinger Equation and the Propagation of Weakly Nonlinear Waves in Optical Fibers and on the Water Surface. Annals of Physics, 361, 490-500.

Chalikov, D. V. (2016). Numerical Modeling of Sea Waves, Springer international Publishing.

Chalikov, D., & Bulgakov, K. (2017). Estimation of wave height probability based on the statistics of significant wave height. J. Ocean Eng. Mar. Energy, DOI 10.1007/s40722-017-0093-7, 7p.

Chander, S. et al. (2015). Hydrodynamic Study of Submerged Ice Collisions. In: Int. Conf. on Offshore Mechanics and Arctic Engineering. St. John's, Newfoundland: ASME.

Chang K.Y., He S.S., Chou C.C., Kao S.L. and Chiou A.S., (2015). Route Planning and Cost Analysis for Travelling through the Arctic Northeast Passage Using Public 3d Gis, Int. J. of Geographical Inform. Sc., 29(8), pp. 1375–1393.

Chen, C., Shiotani, S. & Sasa, K. (2015). Effect of ocean currents on ship navigation in the east China sea. Ocean Engineering, 2015, 104: 283-293.

Chen, H. & Christensen, E.D. (2017). Development of a numerical model for fluid-structure interaction analysis of flow through and around an aquaculture net cage. Ocean Engineering, 2017, 142: 597-615.

Chen, S.S., Curcic, M., (2016). Ocean surface waves in Hurricane Ike (2008) & Superstorm Sandy (2012): Coupled model predictions & observations. Ocean Modelling 103, 161–176.

Chen, Y. L., Zhan, J. P., Wu, J., Wu, J. (2017). A fully-activated flapping foil in wind gust: Energy harvesting performance investigation. Ocean Engineering, 2017, 138: 112-122.

Chen, Z. B., He, Y. J., Zhang, B., Qiu, Z. F. (2015). Determination of nearshore sea surface wind vector from marine X-band radar images. Ocean Engineering, 2015, 96: 79-85.

Chendi Wang, Jianfang Fei, Juli Ding, Ruiqing Hu, Xiaogang Huang, Xiaoping Cheng. (2017). Development of a new significant wave height and dominant wave period parameterization scheme. Ocean Engineering, volume 135, 2017, pages 170-182.

Choi, J., Kirby, J. T., Yoon, S. B. (2015). Boussinesq modeling of longshore currents in the SandyDuck experiment under directional random wave conditions. Coastal Engineering, 2015, 101: 17-34.

Christou, M. & Ewans, K. (2014). Field Measurements of Rogue Water Waves. J. Phys. Oceanogr., 44, 2317-2335.

Clauss, G., Kosleck, S., and Testa, D., (2009). Critical Situations of Vessel Operations in Short Crested Seas – Forecast and Decision Support System, Int. Conf. on Offshore Mech. and Arctic Eng. (OMAE), May 31-Jun 5, Honolulu, Hawaii, USA.

Clauss, G.F., (2002). Dramas of the sea: episodic waves and their impact on offshore structures, Applied Ocean Research, Vol. 24, pp. 147–161.

Collins, C. O., Rogers, W. E., Marchenko, A., and Babanin, A. V. (2015). In situ measurements of an energetic wave event in the Arctic marginal ice zone, Geophys. Res. Lett. pp. 1–8.

Collins, O. C. I., Rogers, W. E. and Lund, B. (2016). An investigation into the dispersion of ocean surface waves in sea ice, Ocean Dynamics , doi:10.1007/ s10236-016-1021-4.

Cooley, S. and Pavelsky, T. (2016). Spatial and temporal patterns in Arctic river ice breakup revealed by automated ice detection from MODIS imagery. Remote Sensing of Environment, 175, pp. 310-322.

Cornejo-Bueno,L., Garrido-Merchán, E.C., Hernández-Lobato, D., Salcedo-Sanz, S., (2017). Bayesian Optimization of a Hybrid System for Robust Ocean Wave Features Prediction. Neurocomputing (2017), doi: 10.1016/j.neucom.2017.09.025.

Cox, C. S., Zhang, X. and Duda, T. F. (2017). Suppressing breakers with polar oil films: Using an epic sea rescue to model wave energy budgets. Geophys. Res. Lett., 44, 1414–1421, doi:10.1002/2016GL071505.

Craig, W. & Sulem, C. (1993). Numerical Simulation of Gravity Waves. J. Comput. Phys., 108, 73-83.

D'Asaro, E.A., Thomson, J,. Shcherbina, A.Y., Harcourt, R.R., Cronin, M.F., Hemer, M.A., and Fox-Kemper, B. (2014). Quantifying upper ocean turbulence driven by surface waves. GEOPHYSICAL RESEARCH LETTERS, 41, 102–107, doi:10.1002/2013GL058193

Dabbi, E.P., Haigh, I.D., Lambkin, D., Hernon, J., Williams, J.J., Nicholls, R.J., (2015). Beyond significant wave height: A new approach for validating spectral wave models. Coastal Engineering 100, 11–25.

Dai, J. (2016). Numerical simulation for dynamic positioning in pack ice. MEng. Memorial University of Newfoundland.

Daley, C. et al. (2014). GPU-Event-Mechanics Evaluation of Ice Impact Load Statistics. In: Arctic Technology Conference. Houston, Texas: Offshore Technology Conference.

Day, S., Clelland, D. and Valentine, G. (2011). Development of a low-cost laser wave measurement system, Proc. 2nd Int. Conf. on Advanced Model Measurement Techn. for the Maritime Ind, (AMT'11), 4 – 6 Apr, Newcastle upon Tyne, UK.

De Garcia, L., Osawa, N., Tamaru, H., Fukasawa, T., (2016). A study on the influence of ship weather routing in Fatigue Life prediction of ship structure, JASNAOE Annual Autum Meeting, 2016, JASNAOE

Deng Y., Yang, J., Tian, X., Li, X., Xiao, L., (2016). An experimental study on deterministic freak waves: generation, propagation and local energy, Ocean Engineering 118 (2016) 83-92.

Deng Y., Yang, J., Zhao, W., Li, X., Xiao, L., (2016). Freak wave forces on a vertical cylider, Coastal Engineering 114 (2016) 9-18

Deng, Y., Yang, J., Tian, X. and Li, X., (2015). Experimental investigation on rogue waves and their impacts on a vertical cylinder using the Peregrine Breather model, Ships and Offshore Structures, Vol. 11, pp. 757-765.

Deo, M. C., Jha, A., Chaphekar, A. S., Ravikant, K., (2001). Neural networks for wave forecasting. Ocean Engineering, vol. 28, no. 7, p. 889–898

Desbiolles Fabien, Bentamy Abderrahim, Blanke Bruno, Roy Claude, Mestas-Nunez Alberto M., Grodsky Semyon A., Herbette Steven, Cambon Gildas, Maes Christophe (2017). Two Decades [1992-2012] of Surface Wind Analyses based on Satellite Scatterometer Observations. Journal Of Marine Systems , 168, 38-56 .

Dixit, P., Londhe, S., (2016). Prediction of extreme wave heights using neuro wavelet technique. Applied Ocean Research 58, 241–252.

Dobrynin, M. et al. (2015). Prediction of Arctic Sea Ice for Ship Routing: Forecast Experiment and Ship Cruise. In: Arctic Technology Conference. Copenhagen, Denmark: Offshore Technology Conference.

Dommermuth, D. G. & Yue, D. K. P. (1987). A High-Order Spectral Method For the Study of Nonlinear Gravity Waves. J. Fluid Mech., 184, 267-288.

Donelan, M. A. & Magnusson, A.-K. (2017). The Making of the Andrea Wave and Other Rogues. Scientific Reports, 7, 44124.

Dong, Y., Frangopol, D.M., Sabatino, S., (2016), A decision support system for mission based ship routing considering multiple performance criteria, Reliability engineering and system safety 150 (2016) 190-201.

Drago, M., Mattioli, M., and Quondamatteo, F. (2015). MetOcean design criteria for deep water offshore systems. Proceedings of the ASME 2015 34th International Conference on Ocean, Offshore and Arctic Engineering, May 31-June 5, 2015, St. John's, Newfoundland, Canada.

Drost, E.J.F., Lowe, R.J., Ivey, G.N., Jones, N.L., Péquignet, C.A., (2017). The effects of tropical cyclone characteristics on the surface wave fields in Australia's North West region. Continental Shelf Research 139, 35–53.

Duan, W Y., Han, Y., Huang, L.M., Zhao, B.B., Wang, M.H., (2016). A hybrid EMD-SVR model for the short term prediction of significant wave height, Ocean Engineering 124 (2016) 54-73.

Ducrozet, G. & Gouin, M. (2017). Influence of Varying Bathymetry in Rogue Wave Occurrence Within Unidirectional and Directional Sea-States. Journal of Ocean Engineering and Marine Energy.

Ducrozet, G., Bonnefoy, F., Le Touzé, D. & Ferrant, P. (2012). A Modified High-Order Spectral Method for Wavemaker Modeling in a Numerical Wave Tank. European Journal of Mechanics - B/Fluids, 34, 19-34.

Ducrozet, G., Bonnefoy, F., Le Touzé, D. & Ferrant, P. (2016). Hos-Ocean: Open-Source Solver for Nonlinear Waves in Open Ocean Based on High-Order Spectral Method. Computer Physics Communications, 203, 245-254.

Düll, W.-P., Schneider, G. & Wayne, C. E. (2016). Justification of the Nonlinear Schrödinger Equation for the Evolution of Gravity Driven 2d Surface Water Waves in a Canal of Finite Depth. Archive for Rational Mechanics and Analysis, 220, 543-602.

Durán-Rosal, A.M., Fernández, J.C., Gutiérrez, P.A., Hervás-Martínez, C., (2017). Detection and prediction of segments containing extreme significant wave heights. Ocean Engineering 142, 268–279.

Durrant, T., Greenslade, D., Hemer, M., & Trenham, C. (2014). A global wave hindcast focussed on the Central and South Pacific (Vol. 40, No. 9, pp. 1917-1941).

Duz, B., Bunnik, T., Kapsenberg, G. & Vaz, G., (2016). Numerical simulation of nonlinear free surface water waves - coupling of a potential flow solver to a URANS/VoF code, Proc. 35th Int. Conf. on Ocean, Offshore and Arctic Eng, OMAE2016, Jun 19-24, Busan, Korea

Duz, B., Lindeboom, R., Scharnke, J., Helder, J. and Bandringa H. (2016). Comparison of Breaking Wave Kinematics from Numerical Simulations with PIV Measurements, 36th Int. Conf. on Ocean, Offshore & Arctic Eng. OMAE2017, Jun 25-30, Trondheim, Norway.

Emanuel, K. (2017). A fast intensity simulator for tropical cyclone risk analysis. Natural Hazards, 2017, 88(2): 779-796.

Erceg, S., Ehlers, S., Ellingsen, I., Slagstad, D., von Bock und Polach, R., and Erikstad, S.O., (2013). Ship Performance Assessment for Arctic Transport Routes, Int. Conf. on Offshore Mech. and Arctic Eng. (OMAE), June 9-14, Nantes, France.

Fan, Y., Rogers, W.E., (2016). Drag coefficient comparisons between observed and model simulated directional wave spectra under hurricane conditions. Ocean Modelling 102, 1–13.

Fazelpour, A. et al. (2016). Infrared Image Analysis for Estimation of Ice Load on Structures. In: Arctic Technology Conference. St. John's, Newfoundland: Offshore Technology Conference.

Fedele, F. (2015). On the Kurtosis of Deep-Water Gravity Waves. Journal of Fluid Mechanics, 782, 25-36.

Fedele, F. (2016). Are Rogue Waves Really Unexpected? Journal of Physical Oceanography, 46, 1495-1508.

Fedele, F., Benetazzo A., Gallego G., Shih P.C., Yezzi A., Barbariol F. and Ardhuin F. (2013). Space–time measurements of oceanic sea states. Ocean Modelling, 70, p.103-115

Fedele, F., Brennan, J., Ponce De León, S., Dudley, J. & Dias, F. (2016). Real World Ocean Rogue Waves Explained Without the Modulational Instability. Scientific Reports, 6, 27715.

Fenoglio-Marc, L., Dinardo, S., Scharroo, R., Roland, A., Sikiric, M.D., Lucas, B., Becker, M., Benveniste, J., Weiss, R., (2015). The German Bight: A validation of CryoSat-2 altimeter data in SAR mode. Advances in Space Research 55, 2641–2656.

Fernández, H., Sriram, V., Schimmels, S. and Oumeraci, H., (2014). Extreme wave generation using self-correcting method-Revisited, Coastal Engineering, Vol. 93, pp. 15-31.

Filatov, S.V., Parfenyev, V.M., Vergeles, S.S., Brazhnikov, M.Yu., Levchenko, A.A. and Lebedev, V. V. (2016). Nonlinear Generation of Vorticity by Surface Waves. Phys. Rev. Lett., 115, 054501, 5p

Fissel, D. B. et al. (2015). The Distribution of Massive Ice Features by Ice Types from Multi-Year Upward Looking Sonar Ice Draft Measurements. In: Arctic Technology Conference. Copenhagen, Denmark: Offshore Technology Conference.

Fore, A. G., Stiles, B. W., Chau, A. H., Williams, B., Dunbar, R. S., & Rodriguez, E. (2014). Point-wise wind retrieval and ambiguity removal improvements for the QuikSCAT

climatological data set. Geoscience and Remote Sensing, IEEE Transactions on, 52(1), 51-59.

Fossen, T. I. & Lekkas, A. M. (2017). Direct and indirect adaptive integral line of sight path following controllers for marine craft exposed to ocean currents. International Journal of Adaptive Control and Signal Processing, 2017, 31(4): 445-463.

ftp://ftp.ifremer.fr/ifremer/cersat/products/swath/altimeters/waves/documentation/publications/Sepulveda_etal_2015.pdf

Gemmrich, J. & Thomson, J. (2017). Observations of the Shape and Group Dynamics of Rogue Waves. Geophysical Research Letters, 44, 1823-1830.

Ghorbani, M.A., Asadi, H., Makarynskyy, O., Makarynska, D., Yaseen, Z.M., (2017). Augmented chaos-multiple linear regression approach for prediction of wave parameters. Engineering Science and Technology, an International Journal 20, 1180–1191.

Girolamo, P.D., Di Risio, M., Beltrami, G.M., Bellotti, G., Pasquali, D., (2017). The use of wave forecasts for maritime activities safety assessment. Applied Ocean Research 62, 18–26

Giske, F.-I.G., Leira, B.J., Øiseth, O., (2017). Efficient computation of cross-spectral densities in the stochastic modelling of waves and wave loads. Applied Ocean Research 62, 70–88.

Godoi, V.A., Bryan, K.R., Stephens, S.A., Gorman, R.M., (2017). Extreme waves in New Zealand waters. Ocean Modelling 117, 97–110.

Gomit, G., Calluaud, D., Chatellier, L., David, L. & Fréchou, D. (2013). Optical measurements of free surface for the analysis of ship waves in towing tank, Proc. 3rd Int. Conf. on Advanced Model Meas. Techn. for the Maritime Ind, (AMT'13), Sep, Gdansk, Poland.

Gouin, M., Ducrozet, G. & Ferrant, P. (2016). Development and Validation of a Non-Linear Spectral Model for Water Waves over Variable Depth. European Journal of Mechanics - B/Fluids, 57, 115-128.

Gouin, M., Ducrozet, G. & Ferrant, P. (2017). Propagation of 3d Nonlinear Waves over an Elliptical Mound with a High-Order Spectral Method. European Journal of Mechanics - B/Fluids, 63, 9-24.

Gramstad, O. & Trulsen, K. (2007). Influence of Crest and Group Length on the Occurrence of Freak Waves. J. Fluid Mech., 582, 463-472.

Gramstad, O. (2017). Modulational Instability in Jonswap Sea States Using the Alber Equation. ASME 2017 36th International Conference on Ocean, Offshore and Arctic Engineering. Trondheim, Norway.

Gramstad, O., and Babanin, A.V. (2016). The generalized kinetic equation as a model for the nonlinear transfer in third generation wave models. Ocean Dynamics, 66, 509-526, doi:10.1007/s10236-016-0940-4

Gramstad, O., Bitner-Gregersen, E. and Vanem E. (2017). Projected changes in the occurrence of extreme and rogue waves in future climate in the North Atlantic , Proc. 36th Int. Conf. on Ocean, Offshore and Arctic Eng., OMAE2017, June 25-30, Trondheim, Norway.

Grin, R., Dallinga, R., and Boelen, P., (2016). Voyage Simulations Techniques as Design Tool for Ferries, Proc. RINA Conf. Design & Operations of Ferries & Ro-Pax Vessels, May 25-26, London, UK.

Guo, A, Fang, Q., Li, H., (2015). Analitical solution of hurricane wave force acting on submerged bridge decks, Ocean Engineering 108 (2015) 519-528.

Guo, B., Bitner-Gregersen, E.M., Sun, H., and Helmers, J.B. (2016). Statistics analysis of ship response in extreme seas, Ocean engineering, Vol. (119), pp.154-164.

Hagen, Ø., Grue, I.H., Birknes-Berg, J., Lian, G., Bruserud, K., (2017). Analysis of Short-Term and Long-Term wave statistics by time domain simulations statistics. Proceedings of the ASME 2017 36th Int. Conference on Ocean, Offshore & Arctic Engineering OMAE2017.

Hao Qin, Wenyonng Tang, Hongxiang Xue, Zhe Hu, JIngting Guo. (2017). Numerical study of wave impact on the deck-house caused by freak waves. Ocean Engineering, volume 133, 2017, pages 151-169.

Hara, T., and Sullivan, P.P. (2015). Wave boundary layer turbulence over surface waves in a strongly forced condition, J. Phys. Oceanogr., 45, 868–883

Harpham, Q., Tozer, N., Cleverley, P., Wyncoll, D., Cresswell, D., (2016). A Bayesian method for improving probabilistic wave forecasts by weighting ensemble members. Environmental Modelling & Software 84, 482-493.

Hashim, R., Roy, C., Motamedi, S., Shamshirband, S., Petković, D., (2016). Selection of climatic parameters affecting wave height prediction using an enhanced Takagi-Sugeno-based fuzzy methodology. Renewable and Sustainable Energy Reviews 60, 246–257.

Hendricks, S. et al. (2014). Sea Ice Thickness Surveying with Airborne Electromagnetics - Grounded Ridges and Ice Shear Zones near Barrow, Alaska. In: Arctic Technology Conference. Houston, Texas: Offshore Technology Conference.

Hennig, J., Scharnke, J., Schmittner, C.E. and Berg J. van den (2015). ShorT-CresT: Directional wave measurements at MARIN, Proc. 34th Int. Conf. on Ocean, Offshore and Arctic Eng., OMAE2015, May 31-June 5, St. John's, Newfoundland, Canada.

Hennig, J., Scharnke, J., Swan, C., Hagen, O., Ewans, K., Tromans, P. and Forristall, G., (2015). Effect of short-crestedness on extreme wave impacts – A summary of findings from the Joint Industry Project 'ShorTCresT', Proc. 34th Int. Conf. on Ocean, Offshore and Arctic Eng. (OMAE). ASME Paper OMAE2015-41167.

Hisette, Q. et al. (2017). Discrete Element Simulation of Ship Breaking Through Ice Ridges. In: International Ocean and Polar Engineering Conference. San Francisco, California: International Society of Offshore and Polar Engineers, pp. 1401-1409.

Hithin, N.K., Kumar, V.S., Shanas, P.R., (2015). Trends of wave height and period in the Central Arabian Sea from 1996 to 2012: A study based on satellite altimeter data. Ocean Engineering 108, 416–425.

Holub, C. et al. (2017). Ice Drift Tracking Using Photogrammetric Methods on Radar Data. In: International Ocean and Polar Engineering Conference. San Francisco, California: International Society of Offshore and Polar Engineers, pp. 1338-1342.

Hoque, Md.A., Perrie,W., Solomon, S.M., (2017). Evaluation of two spectral wave models for wave hindcasting in the Mackenzie Delta. Applied Ocean Research 62, 169–180.

Hosking, J.R.M., Wallis, J. R. (1997). Regional Frequency Analysis – An Approach Based on L-Moments. Cambridge University Press, Cambridge, UK.

Hu J, Zhou L. (2015). Experimental and numerical study on ice resistance for icebreaking vessels[J]. International Journal of Naval Architecture and Ocean Engineering, 2015, 7(3): 626-639.

Hu S. S., Wang Y., Liu Z. S., Wang H. Y. (2016). Exploration of measurement principle of a three-dimensional current sensor for measuring the upwelling. Ocean Engineering, 2016,127: 48-57.

Huisman M, Janßen C F, Rung T, et al. (2016). Numerical Simulation of Ship-Ice Interactions with Physics Engines under Consideration of Ice Breaking[C]//The 26th International Ocean and Polar Engineering Conference. International Society of Offshore and Polar Engineers, 2016.

Iafrati, A., Babanin, A.V. and Onorato, M. (2014). Modelling of ocean-atmosphere interaction phenomena during the breaking of modulated wave trains. Journal of Computational Physics, 271, 151-171

Ibarra-Berastegi, G., Saénz, J., Esnaola, G., Ezcurra, A., Ulazia, A., (2015). Short-term forecasting of the wave energy flux: Analogues, random forests, and physics-based models. Ocean Engineering 104, 530–539.

IPCC, (2014): Climate Change 2014: Synthesis Report. Contribution of Working Groups I, II and III to the Fifth Assessment Report of the Intergovernmental Panel on Climate Change [Core Writing Team, R.K. Pachauri and L.A. Meyer (eds.)]. IPCC, Geneva, Switzerland, 151 pp.

ISO (2008). Guidance for Uncertainties in Measurement (GUM), JCGM100.

Iyerusalimskiy, A., Choi J., Park G., Kim Y., Yu, H. (2011). The interim results of the long-term ice loads monitoring on the large Arctic tanker, Proc. of the Int. Conf. on Port and Ocean Eng. under Arctic Conditions (POAC11), Montreal, Canada.

Jane, R., Valle, L.D., Simmonds, D., Raby, A., (2016). A copula-based approach for the estimation of wave height records through spatial correlation. Coastal Eng. 117, 1–18.

Jeans, G., Xiao, W., Osborne, A. R., Jackson, C. R. & Mitchell, D. A. (2017). The Application of Nonlinear Fourier Analysis to Soliton Quantification for Offshore Engineering. 36th Int. Conference on Ocean, Offshore & Arctic Engineering (OMAE). Trondheim, Norway.

Jiang, H., Babanin, A.V., and Chen, G. (2016). Event-based validation of swell arrival time. Journal of Physical Oceanography, 46, 3563-3569

Jiang, H., Babanin, A.V., Liu, Q., Stopa, J.E., Chapron, B., Chen, G., (2017). Can contemporary satellites estimate swell dissipation rate? Remote Sensing of Environment 201, 24–33.

Karvonen, J. et al. (2016). Improving Sea Ice Information and Weather Forecasting for Operational Purposes. In: International Ocean and Polar Engineering Conference. Rhodes, Greece: International Society of Offshore and Polar Engineers, pp. 1163-1166.

Kerkeni, S. et al. (2014). DYPIC Project: Technological and Scientific Progress Opening New Perspectives. In: Arctic Technology Conference. Houston, Texas: Offshore Technology Conference.

Kim, B. and Kim, T. (2017). Monte Carlo Simulation for Offshore Transportation, Ocean Eng., Vol 129, pp. 177–190. doi: 10.1016/j.oceaneng.2016.11.007.

Kim, B. and Kim, T-W., (2017). Weather routing for offshore transportation using genetic algorithm, Appl Ocean Res., Vol 63, Pp. 262 – 275.

Kim, H. et al. (2016). Characterization of Full Scale Operational Ice Pressures and Hull Response on a Large Arctic Tanker. In: Arctic Technology Conference. St. John's, Newfoundland: Offshore Technology Conference.

Kim, J., Pedersen, G. K., Løvholt, F. & Leveque, R. J. (2017). A Boussinesq Type Extension of the Geoclaw Model - A Study of Wave Breaking Phenomena Applying Dispersive Long Wave Models. Coastal Engineering, 122, 75-86.

Kim, Y. and Hermansky, G., (2014). Uncertainties in seakeeping analysis and related loads and response procedures, Ocean Engineering 86 68–81.

Kirby, J. T. (2016). Boussinesq Models and their Application to Coastal Processes across a Wide Range of Scales. J. of Waterway, Port, Coastal, & Ocean Eng., 142, 03116005.

Klebert, P., Patursson, Ø., Endresen, P. C., Rundtop, P., Birkevold, J., Rasmussen, H. W. (2015). Three-dimensional deformation of a large circular flexible sea cage in high currents: Field experiment and modeling. Ocean Engineering, 2015, 104: 511-520.

Klein, M., Clauss, G. F., Rajendran, S., Guedes Soares, C. & Onorato, M. (2016). Peregrine Breathers as Design Waves for Wave-Structure Interaction. Ocean Eng., 128, 199-212.

Kohout, A. L., Williams, M. J. M., Toyota, T., Lieser, J. and Hutchings, J. (2016). In situ observations of wave-induced sea ice breakup, Deep-Sea Research Part II: Topical Studies in Oceanography , 131 , 22–27, doi:10.1016/ j.dsr2.2015.06.010.

Kouvaras, N., Dhanak, M.R., (2017). Prediction of characteristics of wave breaking in shallow water using neural network techniques. Proceedings of the ASME 2017 36th International Conference on Ocean, Offshore and Arctic Engineering OMAE2017.

Krasnopolsky, V., Nadiga, S., Mehra, A., Bayler, E., Behringer, D., (2016). Neural Networks Technique for Filling Gaps in Satellite Measurements: Application to Ocean Color Observations. Computational Intelligence & Neuroscience, Vol. 2016, Article ID 6156513, 9 pages.

Kumar, N.K., Savitha, R., Al Mamun, A., (2017). Ocean wave height prediction using ensemble of Extreme Learning Machine. Neurocomputing 0 0 0, 1–9.

Kumar, N.K., Savitha, R., Al Mamun, A., (2017). Regional ocean wave height prediction using sequential learning neural networks. Ocean Engineering 129, 605–612.

Kumar, P., Min, S.-K. , Weller, E., Lee, H., Wang, X.L., (2016). Influence of Climate Variability on Extreme Ocean Surface Wave Heights Assessed from ERA-Interim and ERA-20C. Journal of Climate, v.29, 00. 4031-4046.

Kumar, U.M., Swain, D., Sasamal, S.K., Reddy, N.N., Ramanjappa, T., (2015). Validation of SARAL/AltiKa significant wave height and wind speed observations over the North Indian Ocean. Journal of Atmospheric and Solar-Terrestrial Physics 135, 174–180.

Kurtz, N. T. and Markus, T. (2012). Satellite observations of Antarctic sea ice thickness and volume. J. Geophys. Res., 117, 2012. doi: 10.1029/2012JC008141

Laface, V., Arena, F., (2016). A new equivalent exponential storm model for long-term statistics of ocean waves. Coastal Engineering 116, 133–151.

Laface, V., Arena, F., Kougioumtzoglou, I.A., Santos, K.R.M., (2017). Joint Time-Frequency analysis of small scale ocean storms via the harmonic wavelet transform. Proceedings of the ASME 2017 36th Int. Conf. on Ocean, Offshore and Arctic Engineering OMAE2017.

Laface, V., Arena, F., Maisondieu, C., Romolo, A., (2017). On Long Term statistics of ocean storms starting from partitioned sea states. Proceedings of the ASME 2017 36th International Conference on Ocean, Offshore and Arctic Engineering OMAE2017.

Lakshmi, D. D., Murty, P. L. N., Bhaskaran, P. K., Sahoo, B., Kumar, T. S., Shenoi, S. S. C., Srikanth, A. S. (2017). Performance of WRF-ARW winds on computed storm surge using hydodynamic model for Phailin and Hudhud cyclones. Ocean Eng., 2017, 131: 135-148.

Lamas, F., Ramirez, M. A. & Fernandes, A. C. (2017). Yaw galloping of a TLWP Platform under high speed currents by analytical methods and its comparison with experimental results. Proc. of the OMEA 2017 Conference, 25-30 June 2017 Trondheim, Norway.

Larson, E., Simonsen, M., and Mao, W. (2015). DIRECT Optimization Algorithm in Weather Routing of Ships, Proc. 25th Int. Offshore and Polar Eng. Conf. (ISOPE), June 21-26, Kona, Hawaii, USA.

Lavidas, G., Venugopal, V., Friedrich, D., (2017). Sensitivity of a numerical wave model on wind re-analysis datasets. Dynamics of Atmospheres and Oceans 77, 1–16.

Leadbetter, M.R., Rychlik, I., Stambaugh, K., (2011). Estimating Dynamic Stability Event Probabilities from Simulation and Wave Modeling Methods, 12th Int. Ship Stability Workshop, Washington DC, USA.

Lee, H.S., (2015). Evaluation of WAVEWATCH III performance with wind input and dissipation source terms using wave buoy measurements for October 2006 along the east Korean coast in the East Sea. Ocean Engineering 100, 67–82.

Lee, T., Kim, H. Chung, H., Bang, Y., Myung, H., (2015). Energy efficient path planning for a marine surface vehicle considering heading angle, Ocean Engineering 107 (2015) 118-131

Lenain, L. & Melville W.K. (2014). Autonomous surface vehicle measurements of the ocean's response to Tropical Cyclone Freda. J. Atmos. Oceanic Technol., 31, p.2169–2190

Li, J.-G., Saulter,A. (2012). Assessment of the updated Envisat ASAR ocean surface wave spectra with buoy and altimeter data. Remote Sensing of Environment 126, 72–83.

Li, N., Cheung, K.F., Stopa, J.E., Hsiao, F., Chen, Y.-L., Vega, L., Cross, P., (2016). Thirty-four years of Hawaii wave hindcast from downscaling of climate forecast system reanalysis. Ocean Modelling 100, 78–95.

Lin, Y-H., Fang, M-C. and Yeung, R.W., (2013). The optimization of ship weather-routing algorithm based on the composite influence of multi-dynamic elements, Appl. Ocean Res, Vol 43, pp. 184 – 194.

Lindeboom, R.C.J. and Scharnke, J., (2016). Determination of wave kinematics in breaking waves making use of Particle Image Velocimetry, NATO Specialists Meeting "Progress and Challenges in Validation Testing for Comp. Fluid Dyn.", 26 - 28 Sep, Avila, Spain.

Liu, D.Y. Ma, Y.X., Dong, G.H. and Perlin, M., (2016). Detuning and wave breaking during nonlinear surface wave focusing, Ocean Engineering, Vol. 113, pp. 215-223.

Liu, K., Chen, Q. & Kaihatu, J. M. (2016). Modeling Wind Effects on Shallow Water Waves. Journal of Waterway, Port, Coastal, and Ocean Engineering, 142, 04015012.

Liu, Q., Babanin, A., Fan, Y., Zieger, S., Guan, C., Moon, I.-J., (2017). Numerical simulations of ocean surface waves under hurricane conditions: Assessment of existing model performance. Ocean Modelling 118, 73–93.

Liu, Q., Babanin, A.V., Zieger, S., Young, I.R., and Guan, C. (2016). Wind and wave climate in the Arctic Ocean as observed by altimeters. Journal of Climate, 29, 7957-7975

Liu, Q., Lewis, T., Zhang, Y., Sheng, W., (2015). Performance assessment of wave measurements of wave buoys. International Journal of Marine Energy 12, 63–76.

Liu, S. H., Zhang, Q. S., Zhao, X., Zhang, X. Y., Li, S. H., Jing, J. E. (2017). Study of an expendable current profiler detection method. Ocean Engineering, 2017, 132: 40-44.

Lo, D.-C., Wei, C.-C., Tsai, E.-P., (2015). Parameter Automatic Calibration Approach for Neural-Network-Based Cyclonic Precipitation Forecast Models. Water 2015, 7, 3963-3977.

Loyd's Register Marine, (2015). Wind-powered shipping: A review of the commercial, regulatory and technical factors affecting uptake of wind-assisted propulsion, Southampton: Lloyd's Register Group Limited.

Lu, L-F., Sasa, K., Sasaki, W., Terada, D., Kano, T. and Mizojiri, T., (2017). Rough wave simulation and validation using onboard ship motion data in the Southern Hemisphere to enhance ship weather routing, Ocean Engineering, Vol 144, pp. 61 – 77

Lu, R. ; Ringsberg, J. ; Mao, W. (2017). Wind-assisted propulsion for shipping: status and perspectives, Proceedings of the International Conference on Ships and Offshore Structures (ICSOS 2017) in Shenzhen, China, September 11-13, 2017. p. 561-571.

Lu, W. et al. (2016). A Shipborne Measurement System to Acquire Sea Ice Thickness and Concentration at Engineering Scale. In: Arctic Technology Conference. St. John's, Newfoundland: Offshore Technology Conference.

Lu, X. et al. (2017). Observations of Arctic snow and sea ice cover from CALIOP lidar measurements. Remote Sensing of Environment, 194, pp. 248-263.

Lubbad, R. et al. (2016). Oden Arctic Technology Research Cruise 2015. In: Arctic Technology Conference. St. John's, Newfoundland: Offshore Technology Conference.

Lucas, C., Guedes Soares, C., (2015). On the modelling of swell spectra. Ocean Engineering 108, 749–759. Ocean Engineering 108, 749–759.

Lucas, C., Muraleedharan, G., Guedes Soares, C., (2017). Regional frequency analysis of extreme waves in a coastal area. Coastal Engineering 126, 81–95.

Ma, Y., Dong, G., Perlin, M., Liu, S., Zang, J. and Sun, Y., (2009). Higher-harmonic 29 focused-wave forces on a vertical cylinder, Ocean Engineering, Vol. 36, pp. 595-604.

Mao, W. ; Rychlik, I. (2017). Estimation of Weibull distribution for wind speeds along ship routes. Journal of Engineering for the Maritime Environment. 231 (2) p. 464-480.

Mao, W. and Rychlik, I. (2016). Estimation of Weibull distribution for wind speeds along ship routes, Proceedings of the Institution of Mechanical Engineers, Part M: Journal of Engineering for the Maritime Environment, DOI: 1475090216653495.

Mao, W., Li, Z., Ringsberg, J.W., and Rychlik, I. (2012). Application of a ship-routing fatigue model to case studies of 2800 TEU and 4400 TEU container vessels. Journal of Engineering for the Maritime Environment. Vol.226(3), pp.222–234.

Mao, W., Ringsberg, J., and Rychlik, I. (2010b). Development of a fatigue model useful in ship routing design, J. of Ship Research, Vol 54(4), pp. 281-293

Mao, W., Rychlik, I., and Storhaug, G. (2010a). Safety index of fatigue failure for ship structure details, J. of Ship Research, Vol 54(3), pp. 197-208

Marchenko, A.V., Gorbatsky, V.V. and Turnbull, I.D. (2015). Characteristics of under-ice ocean currents measured during wave propagation events in the Barents Sea. Proc. of the 23nd International Conference on Port and Ocean Engineering under Arctic Conditions June 14-18, 2015 Trondheim, Norway, 11p

Martínez-Asensio, A., Marcos, M., Tsimplis, M.N., Jordà, G., Feng, X., Gomis, D., (2016). On the ability of statistical wind-wave models to capture the variability and long-term trends of the North Atlantic winter wave climate. Ocean Modelling 103, 177–189.

Mayerle, R., Narayanan, R., Etri, T., Wahab, A.K.A. (2015). A case study of sediment transport in the Paranagua Estuary Complex in Brazil. Ocean Engineering, 2015, 106: 161-174.

McGonigal, D., Hagen, D. and Guzman, L., (2011). Extreme Ice Features Distribution in the Canadian Arctic, Proc. Int. Conf. on Port and Ocean Eng. under Arctic Conditions (POAC11), Montreal, Canada.

Memos, C. D., Klonaris, G. T. & Chondros, M. K. (2016). On Higher-Order Boussinesq-Type Wave Models. J. of Waterway, Port, Coastal, and Ocean Engineering, 142, 04015011.

MEPC 71/5/13 (2017). Progress and present status of the draft revised Guidelines for determining minimum propulsion power to maintain the manoeuvrability of ships in adverse conditions. Submitted by Denmark, Germany, Japan, Spain and IACS to IMO, 2017.

MEPC 71/INF.28 (2017). Draft revised Guidelines for determining minimum propulsion power to maintain the manoeuvrability of ships in adverse conditions. Submitted by Denmark, Germany, Japan, Spain and IACS to IMO, 2017.

MEPC 71/INF.29 (2017). Supplementary information on the draft revised Guidelines for determining minimum propulsion power to maintain the manoeuvrability of ships in adverse conditions. Submitted by Denmark, Germany, Japan and Spain to IMO, 2017.

Metrikin I, Kerkeni S, Jochmann P, et al. (2015). Experimental and numerical investigation of dynamic positioning in level ice[J]. Journal of Offshore Mechanics and Arctic Engineering, 2015, 137(3): 031501.

Michael Banks, Nagi Abdussanmie, (2017). The response of a semisubmersible model under focused wave groups: Experimental investigation, Journal of Ocean Engineering and Science, 2017.

Mierke D, Janßen C, Rung T. (2015). GPU-accelerated large-eddy simulation of ship-ice interactions[C]//Proc. 6th Int. Conf. on Comp. Methods in Marine Engng. 2015: 229-240.

Minnick, L., Bassler, C., Perceival, S. and Hanyok, L., (2010). Large-scale wave kinematics measurements of regular waves and large-amplitude wave groups, Proc. 29th Int. Conf. on Ocean, Offshore and Arctic Eng. (OMAE). ASME Paper OMAE 2010-20240.

Minoura, M (2016). Stochastic sea state model based on Fourier series expansion, Proceeding of 26th ISOPE, Rhodes, Greece

Mintu, S. et al. (2016). State-of-the-Art Review of Research on Ice Accretion Measurements and Modelling. In: Arctic Technology Conference. St. John's, Newfoundland: Offshore Technology Conference. .

Montes-Iturrizaga, R. and Heredia-Zavoni, E. (2016). Reliability analysis of mooring lines using copulas to model statisticaldependence of environmental variables Applied Ocean Research, Vol.59, pp.564-576.

Montiel, F., Squire, V.A. and Bennetts, L.G. (2016). Attenuation and directional spreading of ocean wave spectra in the marginal ice zone. J. Fluid Mech., 790, 492-522.

Mori, N., Onorato, M., and Janssen, P.A.E.M., (2011). On the Estimation of the Kurtosis in Directional Sea States for Freak Wave Forecasting, J. of Physical Oceanography, Vol 41, pp. 1484-1497.

Mosig, J. E. M., Montiel, F., and Squire, V. A. (2015). Comparison of viscoelastic-type models for ocean wave attenuation in ice-covered seas, Journal of Geophysical Research: Oceans , pp. 1–17, doi:10.1002/ 2015JC010700

Mudge, T.D., Fissel, D.B., de Saavedra Álvarez, M. M. and Marko, J.R. (2011). Investigations of Variability for Ship Navigation through the Northwest Passage, 1982-2010, Proc. Int. Conf. on Port and Ocean Eng. under Arctic Conditions (POAC11), Montreal, Canada.

Muraleedharan, G., Lucas, C., Guedes Soares, C., (2016). Regression quantile models for estimating trends in extreme significant wave heights. Ocean Engineering 118, 204–215.

Muraleedharan, G., Lucas, C., Martins, D., Guedes Soares, C., Kurup, P.G., (2015). On the distribution of significant wave height and associated peak periods. Coastal Engineering 103, 42–51.

Murray Rudman, Paul W. Cleary. (2016). The influence of mooring system in rogue wave impact on an offshore platform. Ocean Engineering, volume 115, 2016, pages 168-181.

Murty, P.L.N., Sandhya, K.G., Bhaskaran, Prasad K., Jose, F., Gayathri, R., Balakrishnan Nair, T.M., Kumar, T.S., Shenoi, S.S.C. (2014). A coupled hydrodynamic modeling system for PHAILIN cyclone in the Bay of Bengal. Coastal Engineering, vol. 93, 2014, pages 71-81.

Naaijen, P., van Dijk, R.R.T., Huijsmans, R.H.M. and El-Mouhandiz, A.A., (2009). Real time estimation of ship motions in short crested seas, Proc. 28th Int. Conf. on Ocean, Offshore and Arctic Engineering (OMAE). ASME Paper OMAE2009-79366.

Nagi Abdussamie, Yuriy Drobyshevski, Roberto Ojeda, Giles Thomas, Walid Amin. (2017). Experimental investigation of wave-in-deck impact events on a TLP model. Ocean Engineering, volume 142, 2017, pages 541-562.

Nam, J.-H., Park, I., Lee, H.J., Kwon, M.O., Choi, K. and Seo, Y.-K. (2013). Simulation of Optimal Arctic Routes Using a Numerical Sea Ice Model Based on an Ice-Coupled Ocean Circulation Method, Int. J. of Naval Arch. and Ocean Eng., Vol 5(2), pp. 210–226. doi: 10.2478/IJNAOE-2013-0128.

Nayak, S., Panchang, V., (2015). A Note on Short-term Wave Height Statistics. Aquatic Procedia 4, 274 – 280. International Conference on Water Resources, Coastal and Ocean Engineering (ICWRCOE 2015).

Nelissen, D. Traut, M., Köhler, J., Mao, W., Faber, J. and Ahdour S. (2016). Study on the analysis of market potentials and market barriers for wind propulsion technologies for ships. European Commission, DG Climate Action, 2016. 128 p.

Neville, M. A. et al. (2016). Physical Ice Management Operations - Field Trials and Numerical Modeling. In: Arctic Technology Conference. St. John's, Newfoundland: Offshore Technology Conference.

Niclasen, B.A., Simonsen, K., (2007). Note on wave parameters from moored wave buoys. Applied Ocean Research 29, 231–238.

Nielsen, U.D. and Jensen, J.J., (2011). A novel approach for navigational guidance of ships using onboard monitoring systems. Ocean Eng., Vol 38, pp. 444 - 455.

Nielsen, U.D., Jensen, J.J., Petersen, P.T. and Ito, Y., (2011), Onboard monitoring of fatigue damage rates in the hull, Marine Structures, Vol 24 (2), pp. 182 - 206.

Nikishova, A., Kalyuzhnaya, A., Boukhanovsky, A., Hoekstra, A., (2017). Uncertainty quantification and sensitivity analysis applied to the wind wave model SWAN. Environmental Modelling & Software 95, 344-357.

Nørgaard, J.Q.H., Andersen, T.L., (2016). Can the Rayleigh distribution be used to determine extreme wave heights in non-breaking swell conditions? Coastal Engineering 111, 50–59.

Nose, T., Babanin, A.V., and Ewans, K. (2016). Directional analysis and potential for spectral modelling of infragravity waves. Proceedings of the ASME 2016 35th International Conference on Ocean, Offshore and Arctic Engineering OMAE2016, June 19-24, 2016, Busan, South Korea, 11p

Noshokaty, S., (2017). Shipping Optimisation Systems (SOS): Tramp Optimisation Perspective, J. of Shipping and Trade, Vol 2(1), pp. 1–36. doi: 10.1186/s41072-017-0021-y.

Ogeman, V., Mao, W. and Ringsbergs, J. W. (2013). Comparison of computational methods for evaluation of wave-load-induced fatigue damage accumulation in ship structure details, Proc. 5th Int. Conf. on Comp. Methods in Marine Eng. (MARINE 2013), May 29-31, Hamburg, Germany.

Onorato, M. & Suret, P. (2016). Twenty Years of Progresses in Oceanic Rogue Waves: the Role Played By Weakly Nonlinear Models. Natural Hazards, 84, 541-548.

Onorato, M., Cavaleri, L., Fouques, S., Gramstad, O., Janssen, P. A. E. M., Monbaliu, J., Osborne, A. R., Pakozdi, C., Serio, M., Stansberg, C. T., Toffoli, A. & Trulsen, K. (2009).

Statistical Properties of Mechanically Generated Surface Gravity Waves: A Laboratory Experiment in a Three-Dimensional Wave Basin. J. Fluid Mech., 627, 235-257.

Onorato, M., Osborne, A. R. & Serio, M. (2006). Modulational Instability in Crossing Sea States: A Possible Mechanism for the formation of Freak Waves. Phys. Rev. Lett., 96, 014503.

Onorato, M., Proment, D., Clauss, G. & Klein, M. (2013). Rogue Waves: From Nonlinear Schrödinger Breather Solutions To Sea-Keeping Test. Plos one, 8, E54629.

Orimolade, A.K., Haver, S., and Gudmestad, O.T. (2016). Estimation of extreme significant wave heights and the associated uncertainties: A case study using NORA10 hindcast data for the Barents Sea, Marine Structures, Vol.49, pp.1-17.

Osborne, A. (2010). Non-Linear Ocean Waves and the Inverse Scattering Transform, Academic Press.

Osborne, A. R. & Leon, S. P. D. (2017). Properties of Rogue Waves and the Shape of the Ocean Wave Power Spectrum. ASME (2017) 36th international Conference on Ocean, offshore and Arctic Engineering (OMAE). Trondheim, Norway.

Pan, S., Fan, Y., Chen, J., Kao, C., (2016). Optimization of multi-model ensemble forecasting of typhoon waves. Water Science and Engineering, 9(1):52-57.

Pan, Z. Y., Vada, T., Finne, S., Nestegård, A., Hoff, J. R., Hermundstad, E. M. & Stansberg, C. T. (2016). Benchmark Study of Numerical Approaches for Wave-Current Interaction Problem of Offshore Floaters. Proceedings of the OMEA 2016 Conference, 19-24 June 2016 Busan, South Korea.

Park, J., and Kim, N. (2015). Two-phase approach to optimal weather routing using geometric programming, J. of Marine Sc. and Techn., 20, pp. 679 - 688.

Parker, K., Hill, D.F., (2017). Evaluation of bias correction methods for wave modeling output. Ocean Modelling 110, 52–65.

Perelman, O., Wu, C.H., Boucheron, R. and Fréchou, D. (2011). 3D wave fields measurements techniques in model basin: Application on ship wave measurement, Proc. 2nd Int. Conf. on Advanced Model Measurement Techn. for the Maritime Ind, (AMT'11), 4 – 6 Apr, Newcastle upon Tyne, UK.

Perez, J., Menendez, M., Losada, I.J. GOW2: (2017). A global wave hindcast for coastal applications. Coastal Engineering, volume 124, 2017, pages 1-11.

Peric, R., Hoffmann, N. & Chabchoub, A. (2014). Initial Wave Breaking Dynamics of Peregrine-Type Rogue Waves: A Numerical and Experimental Study.

Pezzutto,P., Saulter, A., Cavaleri, L., Bunney, C., Marcucci, F., Torrisi, L., Sebastianelli, S., (2016). Performance comparison of meso-scale ensemble wave forecasting systems for Mediterranean sea states. Ocean Modelling 104, 171–186.

Pillai, A. C., Chick, J., Khorasanchi, M., Barbouchi, S., Johanning, L. (2017). Application of an offshore wind farm layout optimization methodology at Middelgrunden wind farm. Ocean Engineering, 2017, 139: 287-297.

Podgorski, K., Rychlik, I., (2016). Spatial size of waves. Marine Structures 50, 55-71.

Poli, P., Hersbach, H., Dee, D.P., Berrisford, P., Simmons, A.J., Vitart, F., Laloyaux, P., Tan, D.G.H., Peubey, C., Thepaut, J.-N., Tr´emolet, Y., Holm, E.V., Bonavita, M., Isaken, L., Fisher, M., (2016), ERA-20C: An Atmospheric Reanalysis of the Twentieth Century. Journal of Climate, 29, 4083-4097.

Portilla, J., Caicedo, A.L., P.adilla-Hernández, R., Cavaleri, L., (2015). Spectral wave conditions in the Colombian Pacific Ocean. Ocean Modelling 92, 149–168.

Portilla-Yandún, J., Cavaleri, L., Van Vledder, G.Ph., (2015). Wave spectra partitioning and long term statistical distribution. Ocean Modelling 96, 148–160.

Qiao, F, Yuan, Y., Deng, J,. Dai, D. and Song, Z. (2016). Wave–turbulence interaction-induced vertical mixing and its effects in ocean and climate models. Phil. Trans. R. Soc. A, 374: 20150201, http://dx.doi.org/10.1098/rsta.2015.0201

Qin, H., Tang, W., Hu, Z. & Guo, J. (2017a). Structural Response of Deck Structures on the Green Water Event Caused By Freak Waves. Journal of Fluids and Structures, 68, 322-338.

Qin, H., Tang, W., Xue, H., Hu, Z. & Guo, J. (2017b). Numerical Study of Wave Impact on the Deck-House Caused By Freak Waves. Ocean Engineering, 133, 151-169.

Qiu, W., Roussset, J.M. & Rodriguez, C., (2017). Benchmark Studies on Two-Body Interactions in Waves: Model Tests & Uncertainty Analysis, Joint ITTC-ISSC Workshop, Wuxi, 2017.

Qiu, W., Sales, J.J., Lee, D., Lie, H., Magarovskii, V., Mikami, T., Rousset, J.M., Sphaier, S., and Wang, X., (2014). Uncertainties related to Predictions of Loads and Responses for Ocean and Offshore Structures, Ocean Engineering, Vol. 86, pp. 58-67.

Queffeulou, P., Croizé-Fillon, D., (2017). Global altimeter SWH data set. Laboratoire d'Océanographie Physique et Spatiale IFREMER. Report available at ftp://ftp.ifremer.fr/ifremer/cersat/products/swath/altimeters/waves/documentation/altimeter_wave_merge__11.4.pdf

Rae J G L, Hewitt H T, Keen A B, et al. (2015). Development of global sea ice 6.0 CICE configuration for the Met Office Global Coupled Model[J]. Geoscientific Model Development Discussions (Online), 2015, 8(3).

Rapizo, H., Babanin, A.V., Provis, D., and Rogers, W.E. (2017). Current-induced dissipation in spectral wave models, Journal of Geophysical Research Oceans. 122, 2205–2225, doi:10.1002/2016JC012367

Rapizo, H., Waseda, T., Babanin, A.V. and Toffoli, A. (2016). Laboratory experiments on the effects of a variable current field on the spectral geometry of water waves. Journal of Physical Oceanography, 46, 2695-2717

Rapp, R.J. and Melville, W.K., (1990). Laboratory measurements of deep-water breaking waves, Phil. Trans. of the Royal Soc., Series A, Vol. 331, pp. 735-800.

Reichl, B. G., Wang, D., Hara, T., Ginis, I. and Kukulka, T. (2016). Langmuir turbulence parameterisation in tropical cyclone conditions. J. Phys. Oceanogr., 46, 863–886, doi:10.1175/JPO-D-15-0106.1.

Reimer, N., and Duong, Q.T (2013). Prediction of Travelling Time and Exhaust Gas Emission of Ships on the Northern Sea Route, Int. Conf. on Offshore Mech. and Arctic Eng. (OMAE), June 9-14, Nantes, France.

Reineman, D.R., Thomas, L.N., Caldwell, M.R., (2017). Using local knowledge to project sea level rise impacts on wave resources in California. Ocean & Coastal Management, 138, 181-191.

Reite, K., Ladstein, J., and Haugen, J. (2017). Data-driven Real-time Decision Support and its Application to Hybrid Propulsion Systems, OMAE2016-61031, Int. Conf. on Offshore Mech. and Arctic Eng. (OMAE), June 25-30, Trondheim, Norway.

Residori, S., onorato, M., Bortolozzo, U. & Arecchi, F. T. (2017). Rogue Waves: A Unique Approach to Multidisciplinary Physics. Contemporary Physics, 58, 53-69.

Resio, D.T., Vincent, L., Ardag, D., (2016). Characteristics of directional wave spectra and implications for detailed-balance wave modeling. Ocean Modelling 103, 38–52.

Resolution MEPC.232(65), (2013). Interim guidelines for determining minimum propulsion power to maintain the manoeuvrability in adverse conditions. IMO, 2013.

Richon, J. B., Reeves, M., Darquier M. and Fréchou D. (2009). Development of a Laser Gauge for Dynamic Wave Height Measurements in the B600 Towing Tank. Proc. 1st Int. Conf. on Advanced Model Measurement Techn. (AMT '09), 1 - 2 Sep, Nantes France.

Robertson, B., Jin, Y., Bailey, H., Buckham, B., (2017). Calibrating wave resource assessments through application of the triple collocation technique. Renewable Energy 114, 166-179.

Rogers, W. E., Thomson, J., Shen, H. H., Doble, M. J., Wadhams, P., and Cheng, S. (2016). Dissipation of wind waves by pancake and frazil ice in the autumn beaufort sea. Journal of Geophysical Research: Oceans, 121 (11), 7991–8007

Rogers, W.E., Babanin, A.V., and Wang, D.W. (2012). Observation-consistent input and whitecapping-dissipation in a model for wind-generated surface waves: Description and simple calculations. Journal of Atmospheric and Oceanic Technology, 29(9), 1329-1346

Rousset C, Vancoppenolle M, Madec G, et al. (2015). The Louvain-La-Neuve sea ice model LIM3. 6: global and regional capabilities[J]. Geoscientific Model Development, 2015, 8(10): 2991-3005.

Rueda, A., Vitousek, S., Camus, P., Tomás, A., Espejo, A., Losada, I.J., Barnard, P.L., Erikson, L.H., Ruggiero, P., Reguero, B.G., Mendez, F.J., (2017). A global classification of coastal flood hazard climates associated with large-scale oceanographic forcing. Scientific Reports | 7: 5038 | DOI:10.1038/s41598-017-05090-w.

Rychlik, I. (2015). Spatio-temporal model for wind speed variability. Annales de l'ISUP, Vol. 59, pp. 25-55.

Saket, A., Peirson, W. L., Banner, M. L., Barthelemy, X. & Allis, M. J. (2016). On the Threshold for Wave Breaking of Two-Dimensional Deep Water Wave Groups in the Absence and Presence of Wind. Journal of Fluid Mechanics, 811, 642-658.

Salmon, J.E., Holthuijsen, L.H., Zijlema, M., van Vledder, G.Ph., and Pietrzak, J.D. (2015). Scaling depth-induced wave-breaking in two-dimensional spectral wave models. Ocean Modelling 87 (2015) 30–47

Samiksha, S.V., Polnikov, V.G., Vethamony, P., Rashmi, R., Pogarsk, F., Sudheesh, K., (2015). Verification of model wave heights with long-term moored buoy data: Application to wave field over the Indian Ocean. Ocean Engineering 104, 469–479.

Sánchez, A.S., Rodrigues, D.A., Fontes, R.M., Martins, M.F., Kalid, R.A., Torres, E.A., (2017). Wave resource characterization through in-situ measurement followed by artificial neural networks' modeling. Renewable Energy, doi: 10.1016/j.renene.2017.09.032 .

Sandhya, K G., Remya, P.G., Balakrishnan Nair, T.M., Arun, N., (2016), On the co-existence of high energy low frequency waves and locally generated cyclone waves off the Indian east coast, Ocean Engineering 111 (2016) 148-154.

Sartini, L., Besio, G., Cassola, F., (2017). Spatio-temporal modelling of extreme wave heights in the Mediterranean Sea. Ocean Modelling 117, 52–69.

Sartini, L., Mentaschi, L., Besio, G., (2015). Comparing different extreme wave analysis models for wave climate assessment along the Italian coast. Coastal Eng., 100, 37–47.

Sasa, K. (2017). Optimal Routing of Short-Distance Ferry from the Evaluation of Mooring Criteria, Int. Conf. on Offshore Mech. & Arctic Eng. (OMAE), June 25-30, Trondheim, Norway.

Sayeed, T. et al. (2017). A review of iceberg and bergy bit hydrodynamic interaction with offshore structures. Cold Regions Science and Technology, 135, pp. 34-50.

Sayeed, T. M. et al. (2015). Experimental Investigation of Ice Mass Hydrodynamic Interaction with Offshore Structure in Close Proximity. In: International Conference on Offshore Mechanics and Arctic Engineering. St. John's, Newfoundland: ASME.

Scanlon, B., O. Breivik, J. –R. Bidlot, P.A. Janssen, E. M., Callaghan, A.H., Ward, B. (2016). Modeling Whitecap Fraction with a Wave Model. Journal of Physical Oceanograpy, 46, 887-894

Schmittner, C., Brouwer, J. and Henning, J., (2014). Application of focusing wave groups in model testing practice, In: Proc. of the 33rd Int. Conf. on Ocean, Offshore and Arctic Eng. (OMAE). ASME Paper OMAE2014-23949.

Scibilia, F. et al. (2014). Full-Scale Trials and Numerical Modeling of Sea Ice Management in the Greenland Sea. In: Arctic Technology Conference. Houston, Texas: Offshore Technology Conference.

Scott, T., Austin, M., Masselink, G. & Russell, P. (2016) Dynamics of rip currents associated with groynes—field measurements, modelling and implications for beach safety. Coastal Engineering, 2016, 107: 53-69.

Seemanth, M., Bhowmick, S.A., Kumar, R., Sharma, R., (2016). Sensitivity analysis of dissipation parameterizations in a third-generation spectral wave model, WAVEWATCH III for Indian Ocean. Ocean Engineering 124, 252–273.

Seiffert, B. & Ducrozet, G. (2016). Deep Water Wave-Breaking in a High-Order Spectral Model. 31th Intl Workshop on Water Waves and Floating Bodies. Plymouth, United States.

Seiffert, B. & Ducrozet, G. (2017). A Comparative Study of Wave Breaking Models in a High-Order Spectral Model. the ASME 2017 36th international Conference on Ocean, offshore and Arctic Engineering (OMAE). Trondheim, Norway.

Sepulveda, H.H., Queffeulou, P., Ardhuin, F., (2015). Assessment of SARAL AltiKa wave height measurements relative to buoy, Jason-2 and Cryosat-2 data. Marine Geodesy, 38 (S1),449-465, doi: 10.1080/01490419.2014.1000470. Report available at

Seyffert, H.C., Kim, D.-H., Troesch, A.W., (2016). Rare wave groups. Ocean Engineering 122, 241–252.

Shanas, P.R., Aboobacker, V.M., Albarakati, A.M.A., Zubier, K.M. (2017). Superimposed wind-waves in the Red Sea. Ocean Engineering, volume 138, 2017, pages 9-22.

Shu L, Liang J, Hu Q, et al. (2017). Study on small wind turbine icing and its performance[J]. Cold Regions Science and Technology, 2017, 134: 11-19.

Shu Q, Song Z, Qiao F. (2015). Assessment of sea ice simulations in the CMIP5 models[J]. The Cryosphere, 2015, 9(1): 399-409.

Shun-qi Pan, Yang-ming Fan, Jia-ming Chen, Chia-chuen Kao (2016). Optimization of multi-model ensemble forecasting of typhoon waves. Water Science and Engineering, volume 9, issue 1, 2016, pages 52-57.

Siadatmousavi, S.M., Jose, F., Silva, G.M., (2016). Sensitivity of a third generation wave model to wind and boundary condition sources and model physics: A case study from the South Atlantic Ocean off Brazil coast. Computers & Geosciences 90, 57–65.

Simonsen, H.M.; Larsson, E. ; Mao, W., and Ringsberg, J.W. (2015). State-of-the-art within ship weather routing, Proceedings of the ASME Thirty-fourth International Conference on Ocean, Offshore and Arctic Engineering (OMAE2015) in St John's, Newfoundland and Labrador, Canada, May 31-June 5, 2015.. p. 11(pp.).

Skoglund, L., Kuttenkeuler, J., Rosen, A., Ovegard, E., (2015). A comparative study of deterministic and esemble weather forecasts for weather routing, Journal of Marine Science Technology (2015) 29:429-441

Smith, G., Babanin, A.V., Riedel, P., Young, I.R., Oliver, S., and Hubbert, G. (2011). Introduction of a new friction routine into the SWAN model that evaluates roughness due to bedform and sediment size changes. Coastal Engineering, 58, 317-326

Smith, R.K., and Montgomery, M.T. (2014). On the existence of the logarithmic surface layer in the inner core of hurricanes. Q. J. R. Meteorol. Soc., 140, 72–81, DOI:10.1002/qj.2121

Song M, Kim E, Amdahl J (2015). Fluid-structure-interaction analysis of an ice block-structure collision[C]//Proceedings of the International Conference on Port and Ocean Engineering Under Arctic Conditions. 2015.

Staneva, S., Alari, V., Breivik, Ø, Bidlot, J.-R. & Mogensen, K. (2016). Effects of wave-induced forcing on a circulation model of the North Sea. Ocean Dynamics, DOI 10.1007/s10236-016-1009-0

Stansberg, C.T., Frechou, D., Henn, R., Hennig, J., Bouvy, A., Borleteau, J-P., Ollivier M. and Ran, H. (2009). 3D Structures in wave elevation patterns, Proc. 1st Int. Conf. on Adv. Model Meas. Techn. for the EU Maritime Ind. (AMT '09), 1 - 2 Sep, Nantes, France.

Stansberg, C.T., Frechou, D., Henn, R., Hennig, J., Bouvy, A., Borleteau, J-P., Ollivier M. and Ran, H. (2011). Investigation of techniques for 3d wave surface measurements and analysis, Proc. 2nd Int. Conf. on Adv. Model Meas. Techn. for the Maritime Ind., (AMT'11), 4 – 6 Apr, Newcastle upon Tyne, UK.

Stefanakos, C. (2016). Fuzzy time series forecasting of nonstationary wind and wave data. Ocean Engineering, 2016, 121: 1-12.

Stefanakos, C.N., Vanem, E., (2017). Climatic forecasting of wind and waves using fuzzy inference systems. Proceedings of the ASME 2017 36th International Conference on Ocean, Offshore and Arctic Engineering OMAE2017.

Stoney, L., Walsh, K., Babanin, A.V., Ghantous, M., Govekar, P. and Young, I.R. (2017). Simulated ocean response to tropical cyclones: The effect of a novel parameterization of mixing from unbroken surface waves. Journal of Advances in Modeling Earth Systems, 9, doi:10.1002/2016MS000878, 22p

Stopa, J.E., Ardhuin, F., Babanin, A., Ziege, S., (2016). Comparison and validation of physical wave parameterizations in spectral wave models. Ocean Modelling 103, 2–17.

Stroeve J, Notz D. (2015). Insights on past and future sea-ice evolution from combining observations and models[J]. Global and Planetary Change, 2015, 135: 119-132.

Struthi, C., Sriram. V. (2017). Wave impact load on jacket structure in intermediate water depth. Ocean Engineering, volume 140, 2017, pages 183-194.

Stuckey, P. et al. (2016). Modelling Iceberg-Topsides Impacts Using High Resolution Iceberg Profiles. In: Arctic Technology Conference. St. John's, Newfoundland: Offshore Technology Conference.

Sulis, A., Cozza, R., Annis, A., (2017). Extreme wave analysis methods in the gulf of Cagliari (South Sardinia,Italy). Ocean & Coastal Management 140, 79-87.

Suzuki, N., and Fox-Kemper B. (2016). Understanding Stokes forces in the wave-averaged equations, J. Geophys. Res. Oceans, 121, 3579–3596, doi:10.1002/2015JC011566

Tagliaferri, F., Viola, I. M., Flay, R. G. J., (2015). Wind direction forecasting with artificial neural networks and support vector machines. Ocean Engineering, 97, pp.65-73.

Takagi, K., Hamamichi, S., Wada, R., Sakurai, Y., (2017). Prediction of wave time-history using multipoint measurements. Ocean Engineering 140, 412–418.

Tamaru, H. (2016) About the Optimum Route by the Weather Routing, JASNAOE Annual Autum Meeting, 2016, JASNAOE.

Thomson, J., and Rogers, W. E. (2014). Swell and sea in the emerging Arctic Ocean, Geophysical Research Letters , 41 (9), 3136–3140, doi:10.1002/ 2014GL059983

Thomson, J., Squire, V., Ackley, S., Roger,s E., Babanin, A., Guest, P., Maksym, T., Wadhams, P., Stammerjohn, S., Fairall, C., Persson, O., Doble, M., Graber, H., Shen H., Gemmrich, J., Lehner, S., Holt, B., Williams, T., Meylan, M., and Bidlot, J. (2013). Sea State and Boundary Layer Physics of the Emerging Arctic Ocean. Science Plan. Technical Report, APL-UW TR1306, Applied Physical Laboratory, University of Washington, 58p

Toffoli, A., Bennetts, L.G., Meylan, M.H., Cavaliere, C., Alberello, A., Elsnab, J. and Monty, J.P. (2015). Sea ice floes dissipate the energy of steep ocean waves, Geophys. Res. Lett., 42, doi:10.1002/2015GL065937

Toffoli, A., Bitner-Gregersen, E. M., Osborne, A. R., Serio, M., Monbaliu, J. and Onorato, M. (2011). Extreme Waves in Random Crossing Seas: Laboratory Experiments and Numerical Simulations, Geophysical Research Letters, Vol 38, doi: 10.1029/2011.

Tolman H.L., Banner M.L., Kaihatu J.M., (2013). The NOPP operational wave model improvement project. Ocean Modelling, 70, 2–10

Troitskaya, Y., Kandaurov, A., Ermakova, O., Kozlov, D., Sergeev, D. and Zilitinkevich, S. (2017) Bag-breakup fragmentation as the dominant mechanism of sea-spray production in high winds. Nature, 7, 1614, DOI:10.1038/s41598-017-01673-9

Troitskaya, Y., Ezhova, E., Soustova, I. and Zilitinkevich, S. (2016). On the effect of sea spray on the aerodynamic surface drag under severe winds. Ocean Dynamics, 66, 659–669

Trulsen, K. (2017). Rogue Waves in the Ocean, the Role of Modulational Instability, and Abrupt Changes of Environmental Conditions That Can Provoke Non Equilibrium Wave Dynamics. In: Velarde, M. G., Tarakanov, R. Y. & Marchenko, A. V. (Eds.) the Ocean in Motion- Circulation, Waves, Polar Oceanography Springer-Verlag.

Trulsen, K., Nieto Borge, J. C., Gramstad, O., Aouf, L. & Lefèvre, J. M. (2015). Crossing Sea
         State and Rogue Wave Probability during the Prestige Accident. Journal of Geophysical
         Research: Oceans, 120, 7113-7136.
Tsai. W.-T., S.-M. Chen, G.-H. Lu, (2015). Numerical Evidence of Turbulence Generated by
         Nonbreaking Surface Waves. J. Phys. Oceanogr., 45, 174-180
Tsou, M C (2016), Multi target collision avoidance route planning under an ECDIS framework,
         Ocean engineering 121 (2016) 268-278
Turnbull, I. et al. (2015). Operational iceberg drift forecasting in Northwest Greenland. Cold
         Regions Science and Technology, 110, pp. 1-18.
Turnbull, I. et al. (2016). Empirical Prediction of Sea Ice Surface Temperature from Surface
         Meteorological Parameters in Pistolet Bay Northern Newfoundland. In: Arctic
         Technology Conference. St. John's, Newfoundland: Offshore Technology Conference.
Uiboupin, R. & Laanemets, J. (2015). Upwelling parameters from bias-corrected composite
         satellite SST maps in the Gulf of Finland (Baltic Sea). IEEE Geoscience & Remote
         Sensing Letters, 2015, 12(3): 592-596.
Ulbrich, U., Leckebusch, G.C., Pinto, J.G., (2009). Extra-tropical cyclones in the present and
         future climate: a review. Theor Appl Climatol , 96, 117–131.
Umesh, P. A., Bhaskaran, P. K., Sandhya, K. G., Nair, T. B (2017). An assessment on the
         impact of wind forcing on simulation and validation of wave spectra at coastal
         Puducherry, east coast of India. Ocean Engineering, 2017, 139: 14-32.
Utne, I., Sørensen, A., and Schjølberg, I., (2017). Risk Management of Autonomous Marine
         Systems and Operations, Int. Conf. on Offshore Mech. and Arctic Eng. (OMAE), June 25-
         30, Trondheim, Norway.
Vanem, E. (2016). Joint statistical models for significant wave height and wave period in a
         changing climate, Marine Structures, Vol.49, pp.180-205.
Vanem, E., (2017). A regional extreme value analysis of ocean waves in a changing climate.
         Ocean Engineering 144, 277–295.
Vanem, E., and Bitner-Gregersen, E.M. (2015). Alternative Environmental Contours for Marine
         Structural Design—A Comparison Study. Journal of Offshore Mechanics and Arctic
         Engineering, Vol.137, 051601-1.
Varlas, G., Katsafados, P., Papadopoulos, A., Korres, G., (2017). Implementation of a two-way
         coupled atmosphere-ocean wave modeling system for assessing air-sea interaction over
         the Mediterranean Sea. Atmospheric Research xxx, xxx–xxx.
Veltcheva, A., Guedes Soares, C., (2016). Analysis of wave groups by wave envelope-phase
         and the Hilbert Huang transform methods. Applied Ocean Research 60, 176–184.
Veltcheva, A., Guedes Soares, C., (2016). Nonlinearity of abnormal waves by the Hilbert–
         Huang Transform method. Ocean Engineering 115, 30–38.
Vettor, R and Soares, C G (2016). Development of a ship weather routing system, Ocean
         Engineering 123 (2016) 1-14
Victor A. Godoi, Karin R. Bryan, Scott A. Stephens, Richard M. Gorman. (2017). Extreme
         waves in New Zealand waters. Ocean Modelling, 2017.
Walsh, K.J.E., Govekar, P., Babanin, A.V., Ghantous, M., Spence, P., and Scoccimarro, E.
         (2017). The effect on simulated ocean climate of a parameterization of unbroken wave-
         induced mixing incorporated into the k-epsilon mixing scheme. Journal of Advances in
         Modeling Earth Systems, 9, 735-758, doi:10.1002/2016MS000707
Wang, C., Zhang, H., Feng, K. R., Li, Q. W. (2017). A simple gradient wind field model for
         translating tropical cyclones. Natural Hazards, 2017, 88(1): 651-658.
Wang, H., Mao, W., and Eriksson, L. (2017). Benchmark study of five optimization algorithm
         for weather routing, Proceedings of the ASME 2017 36th Int. Conference on Ocean,
         Offshore and Arctic Engineering, OMAE2017, June 25 - 30, 2017, Trondheim, Norway.
Wang, J. et al. (2016). Ice Model Tests for Dynamic Positioning Vessel in Managed Ice. In:
         Arctic Technology Conf.. St. John's, Newfoundland: Offshore Technology Conference.

Wang, L., Liang, B., Li, H., (2017). A new non-parametric correction model and its applications to hindcasting wave data. Ocean Engineering 132, 11–24.

Wang, S., Zhang, H. D. & Guedes Soares, C. (2016). Slamming Occurrence for A Chemical Tanker Advancing in Extreme Waves Modelled With the Nonlinear Schrödinger Equation. Ocean Engineering, 119, 135-142.

Wang, X. X., Wan, R., Zhao, F. F., Huang, L. Y., Sun, P. & Tang, Y. L. (2016). Comparative study of dynamics of gravity cages with different meshes in waves and current. Proceedings of the OMEA 2016 Conference, 19-24 June 2016 Busan, South Korea.

Wang, Y. & Zou, Z. L. (2015). An experimental and numerical study of bimodal velocity profile of longshore currents over mild-slope barred beaches. Ocean Engineering, 2015, 106: 415-423.

Wang, Y. et al. (2015). A Method of Above-water Iceberg 3D Modelling Using Surface Imaging. In: International Ocean and Polar Engineering Conference. Kona, Big Island, Hawaii: International Society of Offshore and Polar Engineers, pp. 1706-1712.

Waseda, T., Hallerstig, M., Ozaki, K. & Tomita, H. (2011). Enhanced Freak Wave Occurrence With Narrow Directional Spectrum in the North Sea. Geophysical Research Letters, 38, N/A-N/A.

WAVEWATCH III® Development Group, The 2016 User manual and system documentation of WAVEWATCH III® version 5.16. Tech. Note 329, NOAA/NWS/NCEP/MMAB, College Park, MD, USA, 326p

Way, B., Khan, F., and Veitch, B., (2015). The Northern Sea Route vs. the Suez Canal Route – an Economic Analysis Incorporating Probabilistic Simulation Optimization of Vessel Speed, Int. Conf. on Offshore Mech. and Arctic Eng. (OMAE), May 31-June 5, St. John's, Canada.

Weisse R., Bisling P., Gaslikova L., Geyer B., Groll N., Hortamani M., Matthias V., Maneke M., Meinke I., Meyer E.M., Schwichtenberg F., Stempinski F., Wiese F. and Wöckner-Kluwe K. (2015). Climate services for marine applications in Europe, Earth Perspectives Vol.2(3), DOI 10.1186/s40322-015-0029-0.

Wen, X., and Mobbs, S. (2014). Numerical Simulations of Laminar Air–Water Flow of a Non-linear ProgressiveWave at Low Wind Speed. Boundary-Layer Meteorol., 150, 381–398

Wen, X., and Mobbs, S. (2015). Numerical Simulations of Air–Water Flow of a Non-linear Progressive Wave in an Opposing Wind. Boundary-Layer Meteorol., 156, 91–112

West, B. J., Brueckner, K. A., Janda, R. S., Milder, D. M. & Milton, R. L. (1987). A New Numerical Method for Surface Hydrodynamics. J. Geophys. Res., 92, 11803-11824.

Wijaya, A. P. (2017). Dynamic averaging method to detect sea surface current from radar images. Proc. of the OMAE 2017 Conference, 25-30 June 2017 Trondheim, Norway.

Wimmer, W., Challenor, P., Retzler, C., (2016). Extreme wave heights in the North Atlantic from Altimeter Data. Renewable Energy 31, 241–248.

Xiao, D., Fang, F., Pain, C. C. & Navon, I. M. (2017). Towards non-intrusive reduced order 3D free surface flow modelling. Ocean Engineering, 2017, 140: 155-168.

Xiao, W., Liu, Y., Wu, G. & Yue, D. K. P. (2013). Rogue Wave Occurrence and Dynamics By Direct Simulations of Nonlinear Wave-Field Evolution. J. Fluid Mech., 720, 357-392.

Xie, Z., (2016). Numerical modelling of wind effects on breaking waves in the surf zone. Ocean Dynamics, 67, 1251–1261

Xu, H. H. & Lin, P. Z. (2017). A new two-step projection method in an ISPH model for free surface flow computations. Coastal Engineering, 2017, 127: 68-79.

Yaakob, O., Hashim, F.E., Omar, K.M., Md Din, A.H., Koh, K.K., (2016). Satellite-based wave data and wave energy resource assessment for South China Sea. Renewable Energy 88, 359-371.

Yablonsky, R. M., Ginis, I., Thomas, B., Tallapragada, V., Sheinin, D. and Bernardet, L. (2015). Description and analysis of the ocean component of NOAA's operational

hurricane weather research and forecasting (HWRF) model. J. Atmos. Oceanic Technol., 32, 144–163

Yang, C.-S. and Ouchi, K. (2017). Application of Velocity Bunching Model to Estimate Wave Height of Ocean Waves Using Multiple Synthetic Aperture Radar Data, J. of Coastal Res, Vol 79(Sp1), pp. 94–98. doi: 10.2112/SI79-020.1.

Yang, D., Pettersen, B., Xiong, Y. L. (2016). Interactions between two flat plates at different positions in a current. Ocean Engineering, 2016, 119: 75-85.

Yang, L., Zhou, X., Mertikas, S.P., Zhu, L., Yang, L., Lei, N., (2017). First calibration results of Jason-2 and SARAL/AltiKa satellite altimeters from the Qianli Yan permanent Cal/Val facilities, China. Advances in Space Research 59, 2831–2842.

Yang, Y., Irish, J. L., Socolofsky, S. A. (2015). Numerical investigation of wave-induced flow in mound–channel wetland systems. Coastal Engineering, 2015, 102: 1-12.

Yim, S. C., Osborne, A. R. & Mohtat, A. (2017). Nonlinear Ocean Wave Models and Laboratory Simulation of High Seastates and Rogue Waves. ASME 2017 36th Int. Conference on Ocean, offshore and Arctic Engineering. Trondheim, Norway.

Yin, K., Xu, S., Huang, W., Xie, Y. (2017). Effects of sea level rise and typhoon intensity on storm surge and waves in Pearl River Estuary. Ocean Engineering, volume 136, 2017, pages 80-93.

Younan, A. et al. (2016). Overview of the 2012 Iceberg Profiling Program. In: Arctic Technology Conference. St. John's, Newfoundland: Offshore Technology Conference.

Young, I.R., Babanin, A.V., and Zieger, S. (2011a). Response to Comment on "Global trends in wind speed and wave height". Science, 334, 166-167

Young, I.R., Babanin, A.V., and Zieger, S. (2013). The decay rate of ocean swell observed by altimeter. Journal of Physical Oceanography, 43, 2322-2333

Young, I.R., Sanina, E., and Babanin, A.V. (2017). Calibration and cross-validation of a global wind and wave database of Altimeter, Radiometer and Scatterometer measurements. J. of Atmospheric and Oceanic Technology, 34, 1285-1306, doi:10.1175/JTECH-D-16-0145

Young, I.R., Vinoth, J., (2013). An "extended fetch" model for the spatial distribution of tropical cyclone wind–waves as observed by altimeter. Ocean Engineering 70, 14–24.

Young, I.R., Zieger, S., and Babanin, A.V. (2011b). Global trends in wind speed and wave height. Science, 332, 451-455

Yu B, Karr D G, Song H, et al. (2016). A surface ice module for wind turbine dynamic response simulation using FAST[J]. Journal of Offshore Mechanics and Arctic Engineering, 2016, 138(5): 051501.

Zakharov, V. E. (1968). Stability of Periodic Waves of Finite Amplitude on the Surface of a Deep Fluid. Journal of Applied Mechanics and Technical Physics, 9, 190-194.

Zambon, J. B., He, R., and Warner, J. C. (2014). Investigation of hurricane Ivan using the coupled ocean-atmosphere-wave-sediment transport (COAWST) model, Ocean Dyn., 64, 1535–1554, doi:10.1007/s10236-014-0777-7.

Zhang, H.Q., Nie B.C. (2016). Modelling windwave driven by typhoon Chan-Hom (201509) in the East China Sea. Theoretical & Applied Mechanics Letters, volume 6, 2016, pages 297-301.

Zhang, Q., Zhou, X. L. & Wang, J. H. (2017). Numerical investigation of local scour around three adjacent piles with different arrangements under current. Ocean Engineering, 2017, 142: 625-638.

Zhantao Zhuo, Shinji Sato (2015). Characteristics of wave grouping and freak wave observed by two typhoons. Procedia Engineering, volume 116, 2015, pages 277-284.

Zhao, X., and Shen, H. (2016). A diffusion approximation for ocean wave scatterings by randomly distributed ice floes. Ocean Modelling, 107, 21–27

Zhe Hu, Hongxiang Xue, Wenyong Tang, Xiaoying Zhang. (2015). A combined wave-dam-breaking model for rogue wave overtopping. Ocean Engineering, volume 104, 2015, pages 77-88.

Zhe Hu, Wenyong Tang, Hongxinag Xue, Xiaoying Zhang, Kunpeng Wang. (2017). Numerical Study of rogue wave overtopping with a fully-coupled fluid-structure interaction model. Ocean Engineering, volume 137, 2017, pages 48-58.

Zheng, J., Sang S., Wang J., Zhou C., Zhao H. (2017). Numerical simulation of typhoon-induced storm surge along Jiangsu coast, Part I: Analysis of tropical cyclone. Water Science and Engineering, volume 10, issue 1, 2017, pages 2-7.

Zhilin Sun, Senjun Huang, Hui NIe, Jiange Jiao, Saihua Huang, Lili Zhu, Dan Xu. (2015). Risk analysis of seawall overflowed by storm surge during super typhoon. Ocean Engineering, volume 107, 2015, pages 178-185.

Zhou, C., Zheng, J., Zhang, J., Fu, X., (2017). Study on the extreme high water levels and wave heights of different return periods in Laizhou Bay, China. Proceedings of the ASME 2017 36th International Conference on Ocean, Offshore and Arctic Engineering OMAE2017.

Zhou, M. et al. (2014) Working towards seafloor and underwater iceberg mapping with a Slocum glider. In: Autonomous Underwater Vehicles (AUV). Oxford, Mississippi: IEEE.

Zhou, Q. and Peng, H. (2014) Numerical Simulation of a Dynamically Controlled Ship in Level Ice. International Journal of Offshore and Polar Engineering, 24(3), pp. 184-191.

Zhu, N., Kim, Y., Kim, K.-H., Shin, B.-S., (2016). Change detection of ocean wave characteristics. Expert Systems With Applications 51, 245–258.

Zhuo, Z., Sato, S., (2015). Characteristics of Wave Grouping and Freak Wave Observed by Two Typhoons. Procedia Engineering 116, 277 – 284. 8th International Conference on Asian and Pacific Coasts (APAC 2015).

Zieger, S., Babanin, A.V., Rogers, W.E., and Young, I.R. (2015). Observations-based input and dissipation terms for WAVEWATCH III. Ocean Modelling, 96(1), 2-25, http://dx.doi.org/10.1016/j.ocemod.2015.07.014